Lectures outline

1- end of gaseous detectors (MPGD part)

2- trigger example with gaseous detector

3- Calorimeter detectors *(one word about neutron interaction)*

4- trigger with calorimeter det. (and MM gaseous detector)

5- magnets (briefly)

Thanks to Laurent Serin (LAL) for the calorimetry part.

Calorimeter detectors
Energy measurements

Outline

1- Calorimeter definition & history, illustration with some major physics results

2- Electromagnetic interaction and shower development

3- Electromagnetic calorimeters technologies

4- e/γ reconstruction, calibration and performance

4- Hadronic shower development

5- Hadronic calorimeters technologies

6- Jets reconstruction calibration and performance

7- Missing transverse energy measurement

8- Conclusion

Slides categories

** For information*
*** Useful to know*
**** Needs to know*

Calorimetry definition

History of calorimeters

Illustration with some major physics results

Calorimetry definition

- Experimental technique used in Nuclear Physics, Particle Physics and Astroparticle to detect a particle and measure some of its properties based on total or partial absorption of the particle in a fiducial volume

- Destructive process :
  Particle is absorbed in the medium or exit it quite modified

- Particle energy is converted in a detectable signal.

- Key element of any High Energy Physics (HEP) experiment

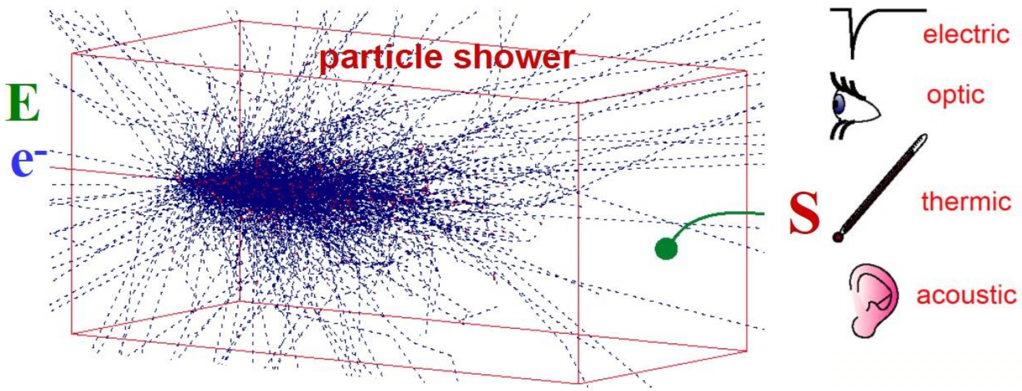

***

Calorimeters needed for HEP

Sensitive **to all charged and neutrals** particles in final state
Good resolution at high energy, and **"sizeable" detectors**

Analyse magnétique

$$\frac{\sigma(p)}{p} = ap \oplus b$$

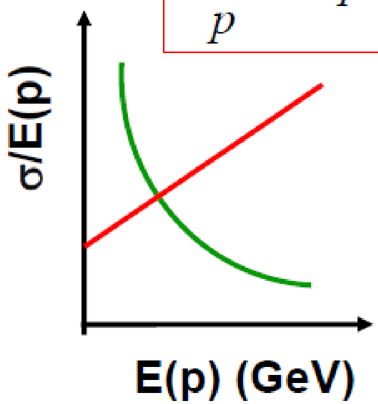

$$\frac{\sigma(E)}{E} \approx \frac{a}{\sqrt{E}}$$

Calorimètre

ATLAS : calo $\sigma(E)/E \sim \frac{10\%}{\sqrt{E}} \oplus 0.7\ \%$

tracking $\sigma(p)\,/\,p \sim\ 5.10^{-4}\, p \oplus 1\%$

At 40 GeV for electrons similar energy resolution

Calorimeter shower depth ~ ln E/E_c almost energy independent
→ Calorimeter can be compact detector

Magnetic spectrometer :

$$\sigma(p)\,/\,p \sim\ p/(BL^2)$$

→ Detector size has to grow quadratically to maintain resolution

Calorimeter can also provide:
- Position/angular measurement
- Time measurement
- **Trigger**
- Particle identification (e, γ, π, μ, h…)

***

Calorimeter History (1)

Calorimetry (calor = heat in latin) is originally a concept used in thermodynamics/chemistry :

- Isolated box with a substance to study
- Exchange of heat measured by temperature variation
- 1 calorie = 4.185 Joule = 2.6 10^{7} TeV

→increases by 1 °C in normal condition 1g of water

1 GeV induces a $\Delta T \sim 4.10^{-14}$ K in 1 liter of water

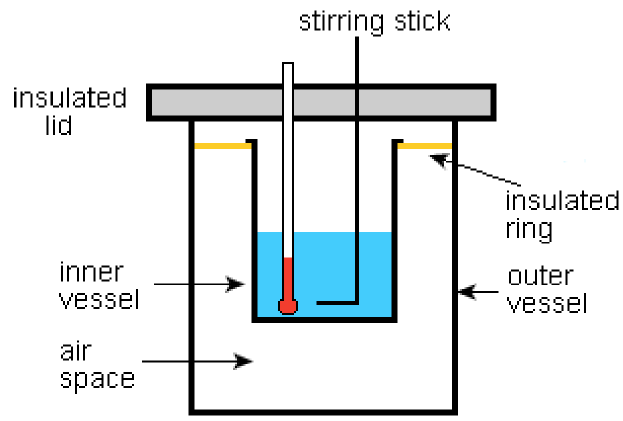

First use in 1878 (Langley) to measure electromagnetic radiation from sun :

- 2 platinum strips, one isolated from radiation, and the second receiving the radiation connected to a Wheaston bridge
- measure Energy/Temperature through resistance change

→30 % accuracy measurement :1.77 kW/m^2 instead of 1.38kW/m^2

Orthmann & Meitner (1930) : differential calorimeter used to measure mean energy of electrons in ^{210}B beta decay : E=0.33 MeV @ 6 %

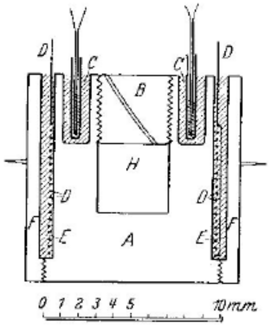

Fig. 1.
Längsschnitt durch ein Kalorimetergefäß.
Woodsches Metall.

→ Such calorimeters still used in the field, named " Bolometers", used in dark matter experiments (Edelweiss, CDMS….) or Cosmic Microwave Background (Planck) (see M. Charles' lesson)

*

Interlude : cryogenic μcalorimeter

Definitely best energy resolution for very low energy but not the subject of this lesson

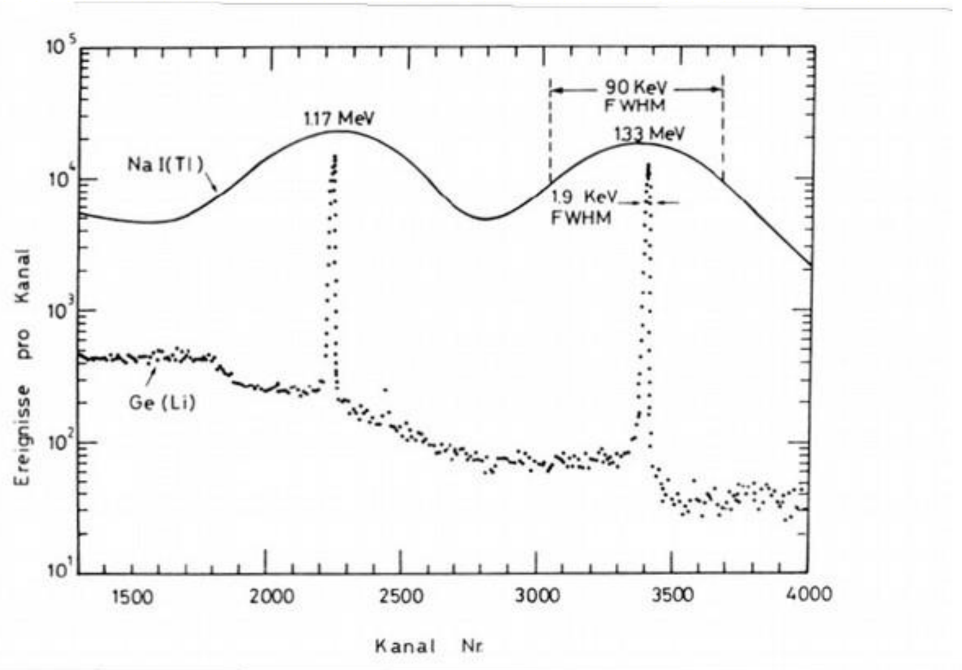

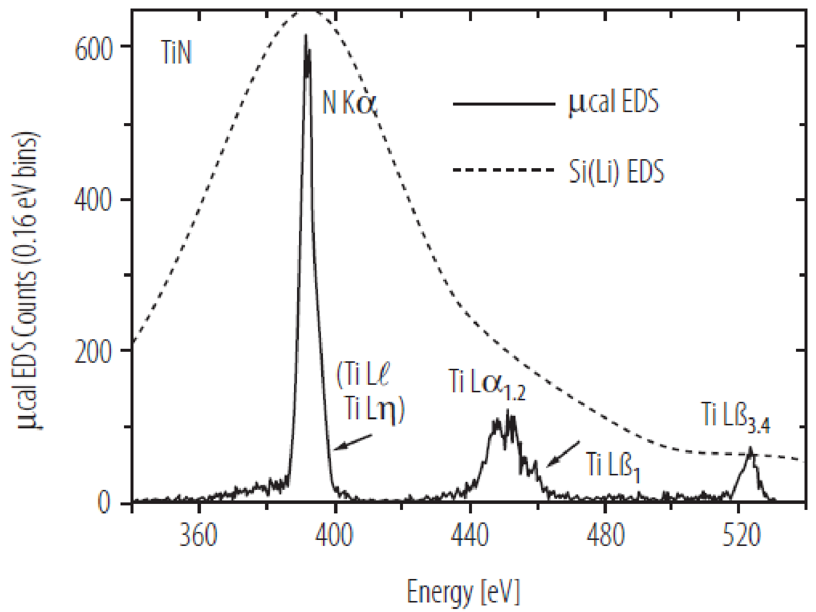

At **100 MeV**, solid state (Si, Ge) detectors have ~25/30 better resolution than scintillators

At few **hundred eV,** cryogenic bolometer can have 50 better resolution
Ok for event energy measurement but not individual particle energy measurement

*

Calorimeter History (2)

First HEP sampling calorimeter in 1953
for High Energy cosmic ray particle E > 10^{14} eV

Sandwich of ionization chambers and scintillation counters interleaved with iron :
-visible energy extracted from numbers of secondary particle (n(x)) and energy loss ionisation and scintillation Counters ($E_{visible} = dE/dx \int n(x).dx$)
- Fraction of the visible energy lost in absorbers plate

→ **Need to be calibrated with particle of known energy, not yet available at accelerators**

- 60-70' accelerators became main facilities for particle physics :
  - Need to measure also neutral particles (π^0, γ, neutrons…)
  - Charged particle accurately measured with large spectrometers detectors : 10m arms for electrons from J/Ψ

→ Plenty of calorimeters development/technologies

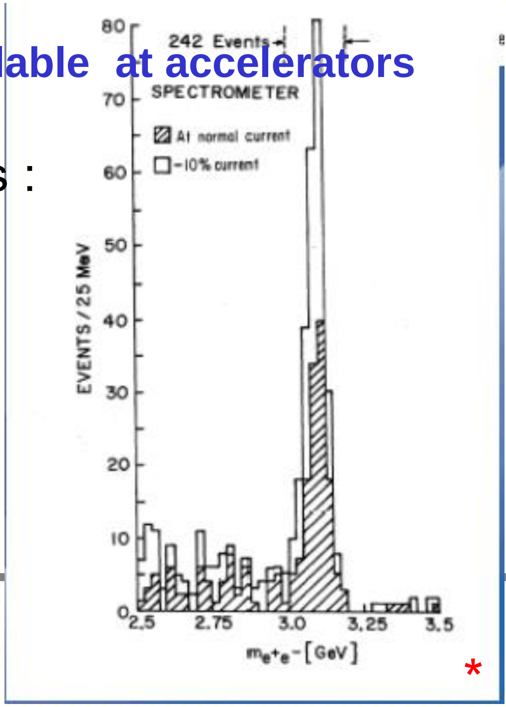

*

Classification of calorimeters

Per particle type

Electromagnetic calorimeters :

$e^{+/-}$, γ and π^0

Hadron calorimeters :

Charged and neutral hadrons, jets

Per construction technique

Full absorption detector, active medium for energy degradation and signal generation

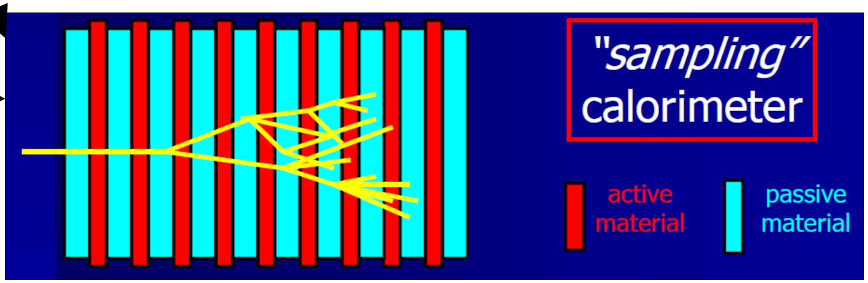

Alternate layers of absorbers to degrade particle energy and active medium to provide detectable signal

***

Classification of calorimeters

By signal detection technology

Homogeneous Calorimeters
- Scintillation/ Crystal
- Semiconductor
- Cherenkov
- Ionization (Noble Liquids)

Sampling Calorimeters
- Scintillation
- Gas
- Solid State
- Liquids
- *Common Absorbers:* *Pb, Fe, Cu, U* , W

Existing Electromagnetic Calorimeters

Technology/Experiment	Depth	Resolution	Year
NaI(Tl) (Crystal Ball)	$20X_0$	$2.7\%/E^{1/4}$	1983
$Bi_4Ge_3O_{12}$ (BGO) (L3)	$22X_0$	$2\%/\sqrt{E} \oplus 0.7\%$	1993
CsI (KTeV)	$27X_0$	$2\%/\sqrt{E} \oplus 0.45\%$	1996
CsI(Tl) (BaBar)	$16–18X_0$	$2.3\%/E^{1/4} \oplus 1.4\%$	1999
CsI(Tl) (BELLE)	$16X_0$	1.7% for $E_\gamma > 3.5$ GeV	1998
$PbWO_4$ (PWO) (CMS)	$25X_0$	$3\%/\sqrt{E} \oplus 0.5\% \oplus 0.2/E$	1997
Lead glass (OPAL)	$20.5X_0$	$5\%/\sqrt{E}$	1990
Liquid Kr (NA48)	$27X_0$	$3.2\%/\sqrt{E} \oplus 0.42\% \oplus 0.09/E$	1998
Scintillator/depleted U (ZEUS)	$20–30X_0$	$18\%/\sqrt{E}$	1988
Scintillator/Pb (CDF)	$18X_0$	$13.5\%/\sqrt{E}$	1988
Scintillator fiber/Pb spaghetti (KLOE)	$15X_0$	$5.7\%/\sqrt{E} \oplus 0.6\%$	1995
Liquid Ar/Pb (NA31)	$27X_0$	$7.5\%/\sqrt{E} \oplus 0.5\% \oplus 0.1/E$	1988
Liquid Ar/Pb (SLD)	$21X_0$	$8\%/\sqrt{E}$	1993
Liquid Ar/Pb (H1)	$20–30X_0$	$12\%/\sqrt{E} \oplus 1\%$	1998
Liquid Ar/depl. U (DØ)	$20.5X_0$	$16\%/\sqrt{E} \oplus 0.3\% \oplus 0.3/E$	1993
Liquid Ar/Pb accordion (ATLAS)	$25X_0$	$10\%/\sqrt{E} \oplus 0.4\% \oplus 0.3/E$	1996

**

Example of calorimeters

Fixed target calorimeters : NA5 at CERN (1978) QCD measurements
One of the first segmented calorimeter

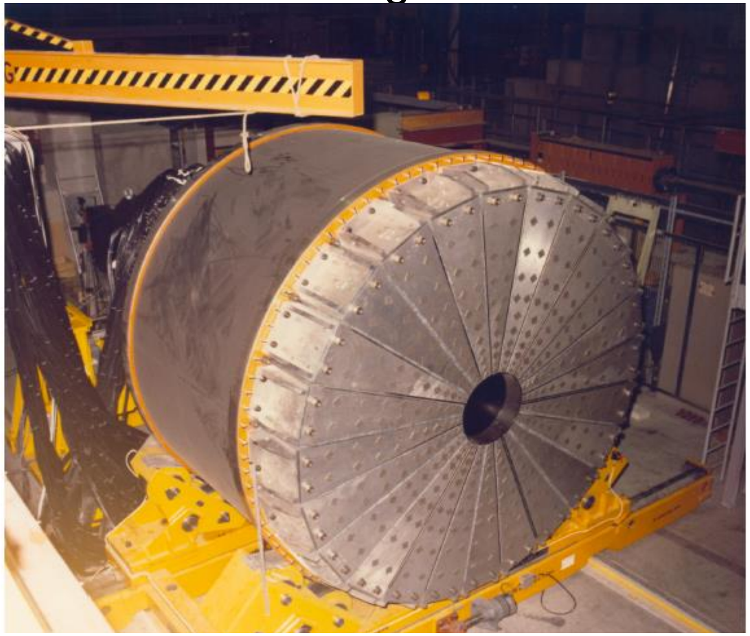

24 (φ) x 10 (θ) cells
EM section : Scintillator/Pb
Had section :Scintillator/Fe
using two different Wave Length Shifter (WLS)

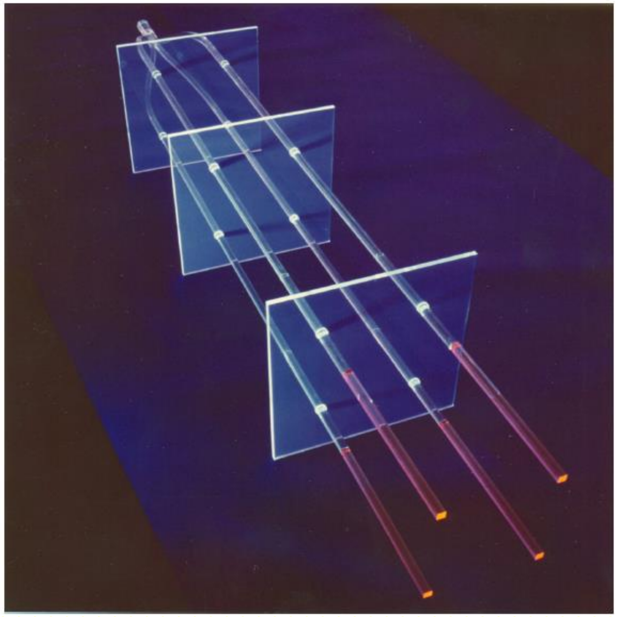

Main idea : guide the light of both section in single rod read by two PM behind yellow (EM) and green (Had) filters

*

Example of calorimeters

Fixed target calorimeters : CP violation in K decays experiment : NA31 / NA48 / KTeV

→ Need to measure accurately $K_L \rightarrow \pi^0\pi^0 \rightarrow 4\gamma$ $(Br(K_L \rightarrow 3\pi^0)/(Br(K_L \rightarrow 2\pi^0) \sim 300$

→ Shower separation + invariant mass : fine granularity and energy resolution

→ Homogeneous calorimeters

KTeV 3100 pure CsI crystals

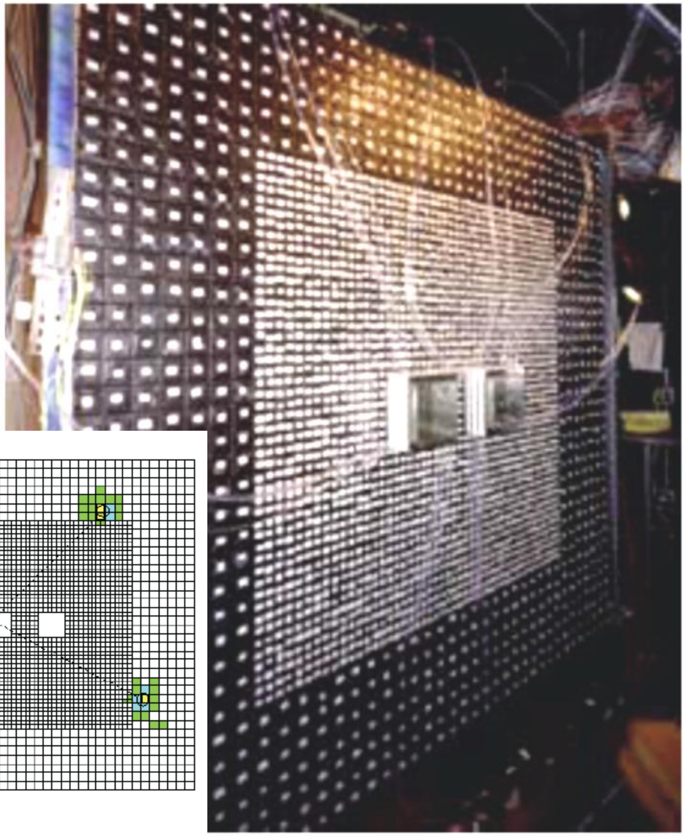

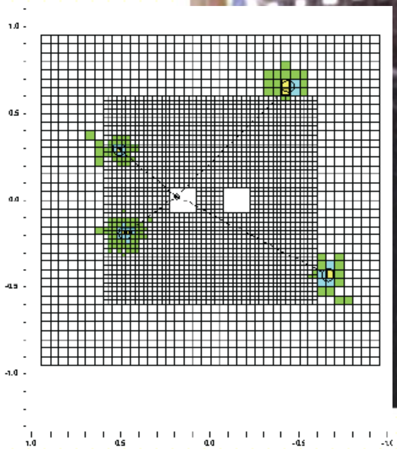

Liquid Krypton calorimeters,
still in used in K experiments at CERN

*

LHC calorimeters

LHC electromagnetic calorimeters, two different approaches

ATLAS : Liquid Argon / Lead sampling electromagnetic calorimeter

CMS : Homogeneous calorimeter $PbWO_4$ crystals

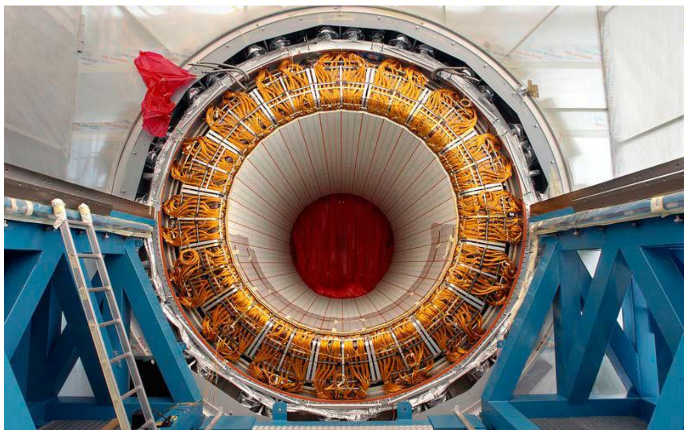

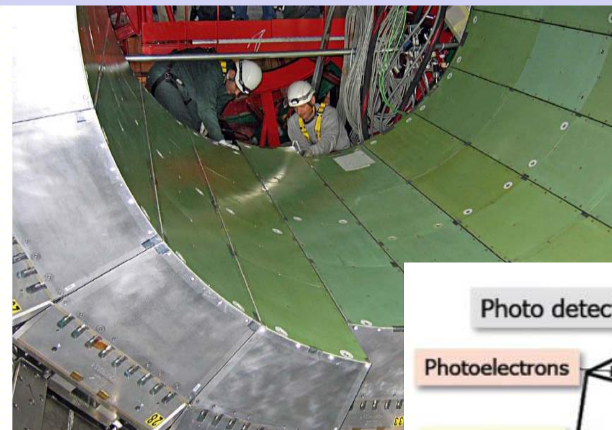

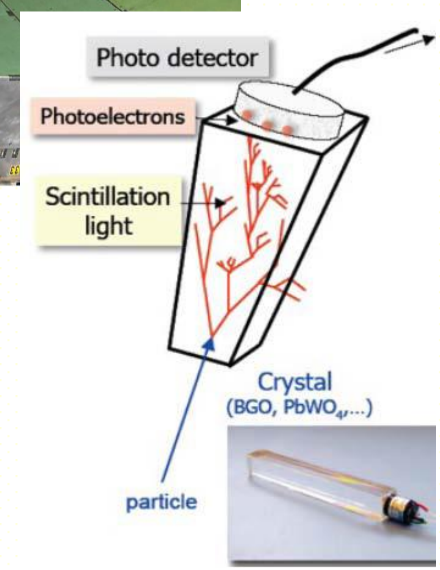

Key detector of Higgs discovery

ATLAS calorimeter better than CMS or CMS better than ATLAS ?

**

H→γγ in ATLAS and CMS

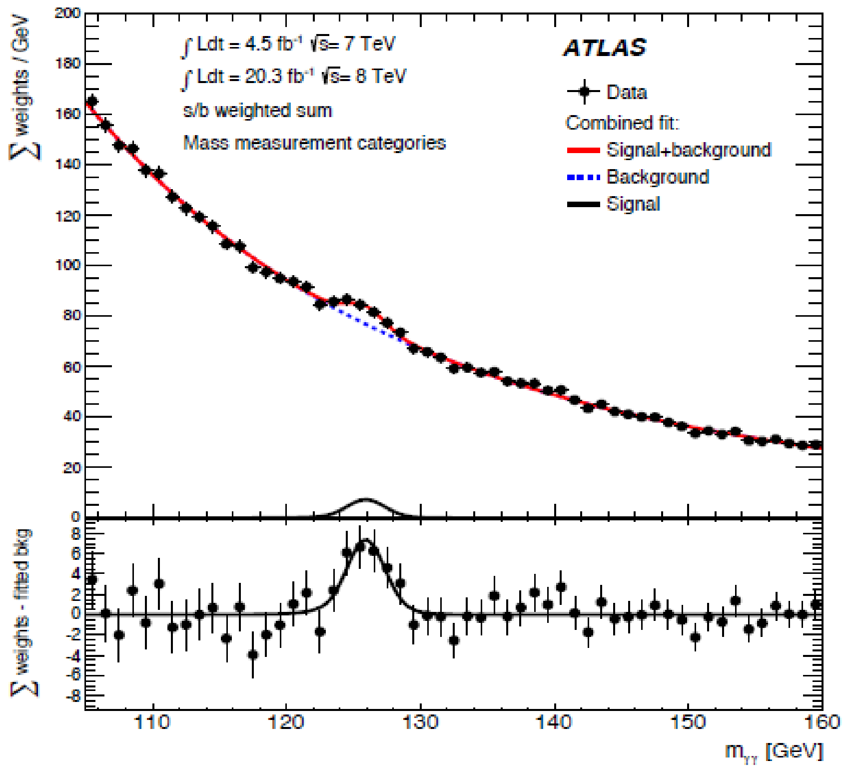

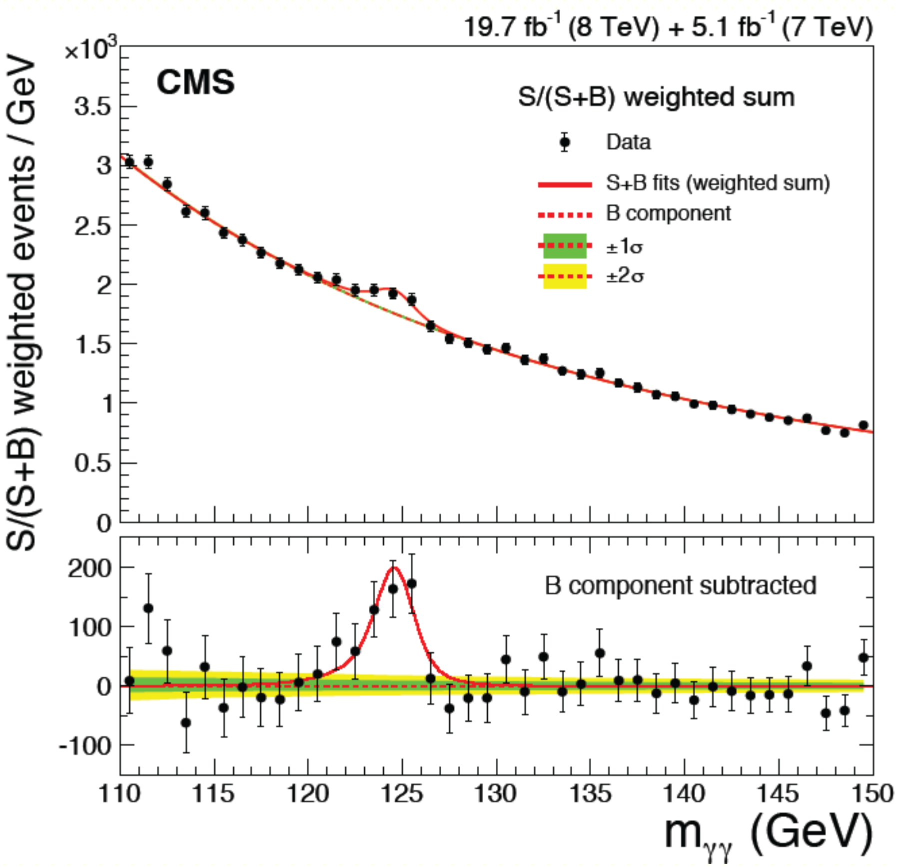

Quite a similar result with different detectors (similar $S/\sqrt{B}$, scales as $1/\sigma_{(masse)}$)
CMS : Energy resolution
ATLAS : Granularity (jet rejection) and angular resolution

$$m_{\gamma\gamma} = 2\, E_1\, E_2\, (1-\cos(\theta))$$

$$\frac{\Delta m_{\gamma\gamma}}{m_{\gamma\gamma}} = \frac{1}{2}\left(\frac{\Delta E_1}{E_1} \oplus \frac{\Delta E_2}{E_2} \oplus \frac{\Delta\theta_{\gamma\gamma}}{\tan(\theta_{\gamma\gamma}/2)}\right)$$

**

Electromagnetic interaction and shower development

e+/e- interaction in matter

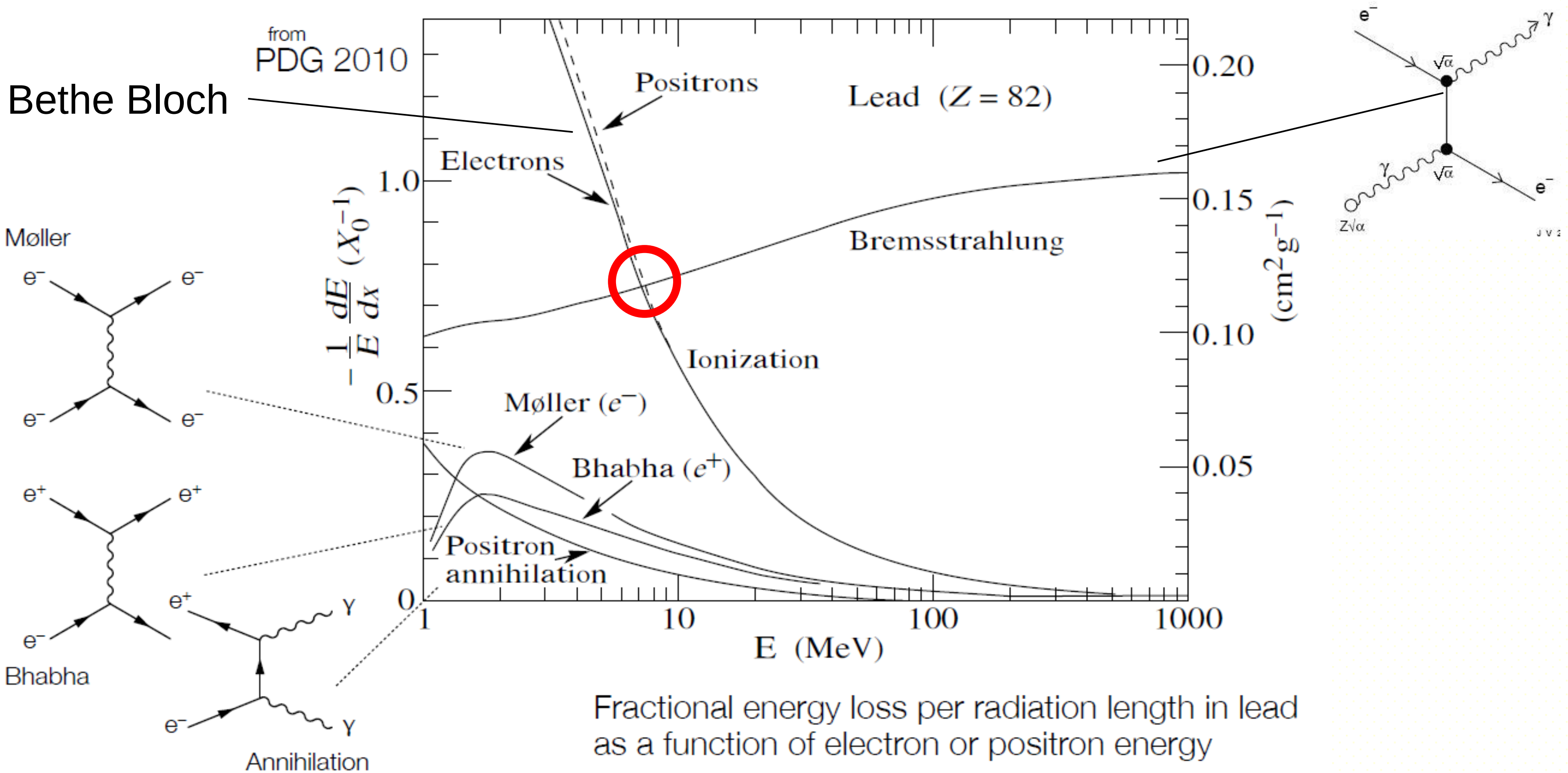

Fractional energy loss per radiation length in lead as a function of electron or positron energy

Critical energy E_c : defined by $(dE/dX)_{ion} = (dE/dx)_{brem}$

Radiation length : mean distance after which an electron has lost by radiation all but a fraction 1/e of its initial energy X_0 (E(after 1 X_0) =E(initial)/e)

***

Summary for e+/e-

1) Above critical energy Ec (~a few MeV) fractional energy loss dominated by bremsstrahlung, below dominated by ionization/excitation

2) Energy loss by ionisation almost independent of incident energy, by radiation linear with energy

3) $\varepsilon_0 = 610\ \mathrm{MeV}/(Z+1.24).$ $$X_0 = \frac{716.4\,\mathrm{g.cm^{-2}}\,A}{Z(Z+1)\ln(187/\sqrt{Z})}$$

High Z material provide low critical energy and small radiation length (compact detector)

(You should divide by the density ρ to have X_0 in cm)

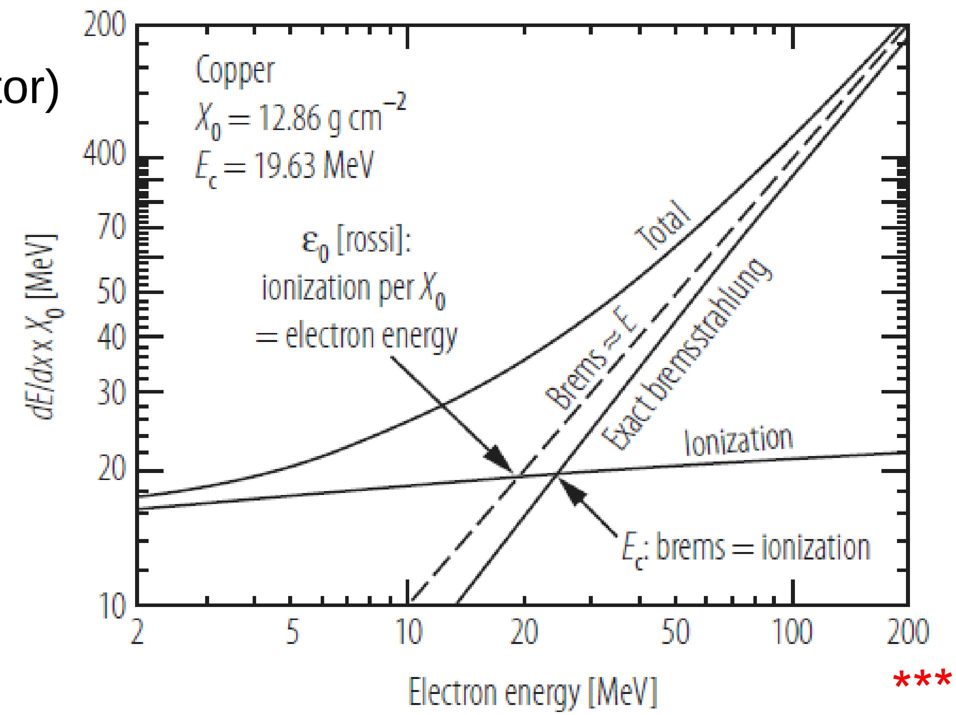

***

Photon interaction in matter

Pair creation

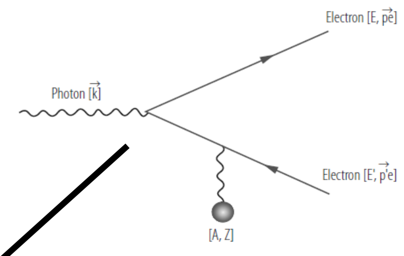

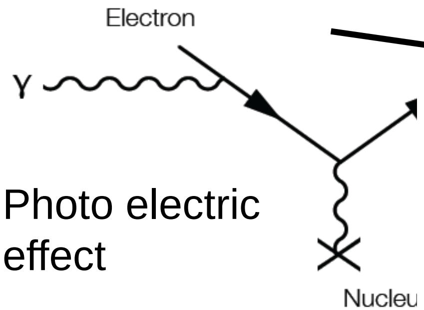

Photo electric effect

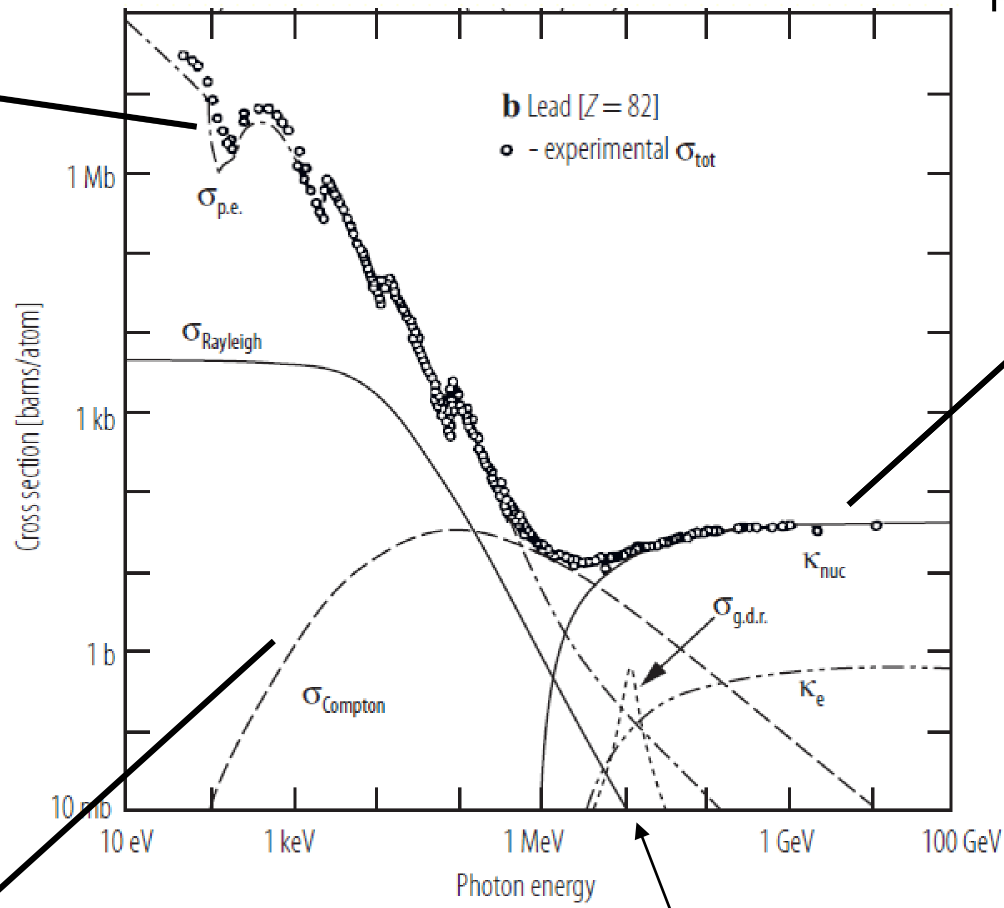

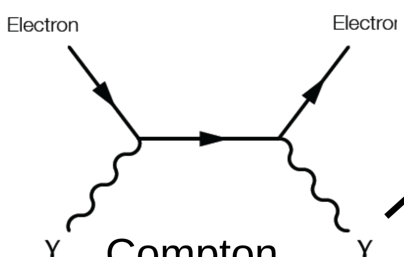

Compton scattering

***

Photon interaction in matter

Pair creation

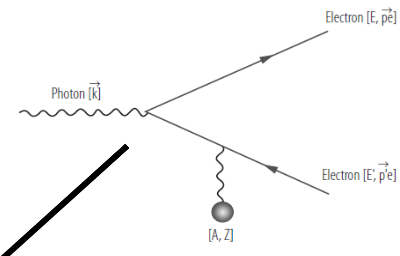

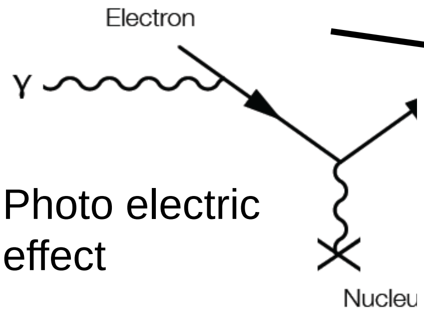

Photo electric effect

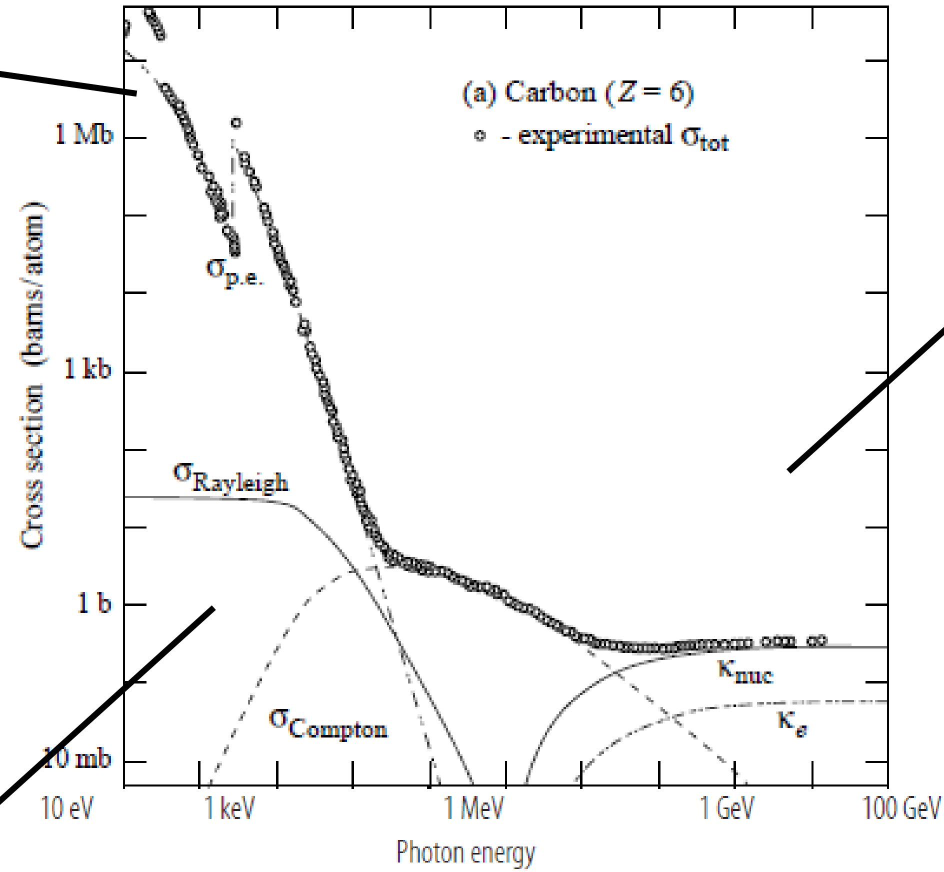

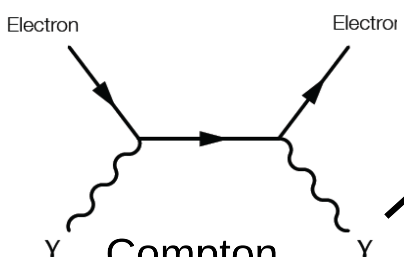

Compton scattering

Summary for γ

1) Above a few $m_e c^2$, photon interaction is dominated by pair production.
Cross section is constant with energy (similar fractional energy loss in brem)
Probability that a high energy photon is not converted into e+e- pair after 9/7 X_0 is 1/e (37 %)

$$\sigma = 7/9\, A/(X_0 N_A).$$

2) At intermediate energy (keV→GeV), Compton scattering contribution
For high Z, max of cross section ~ pair creation cross-section
For small Z, max of cross section > pair creation cross-section

3) Low energy photon (< MeV) is dominated by photo-electric effect
Z^5 dependence of cross-section.
In low Z material, photon can show large mean free path length …. and escape detection.

***

A simplified EM shower model

EM shower model :

- After 1 X_0 , $e^{+/-} \rightarrow e^{+/-}\gamma$ and $\gamma \rightarrow$ e+ e- with proba 100 %
- Equal energy split
- Cascade stops when electron/positron reaches ε (~critical energy)

1) What is the number of particles after n X_0 N(n) =

2) What is the charged particle energy after n X_0 E(n) =

3) The cascade process stops when $E=\varepsilon$ (E_c) at n_{max} =
   What is the total number of particles at n_{max} N_{max} =

4) By defining s_0 as the track length of electrons below the critical energy, compute the total track length T of all charged particles T =
   (neglect 1 wrt 2**nmax)

Conclude about the energy resolution if you measure T ?

**

Simplified EM shower model

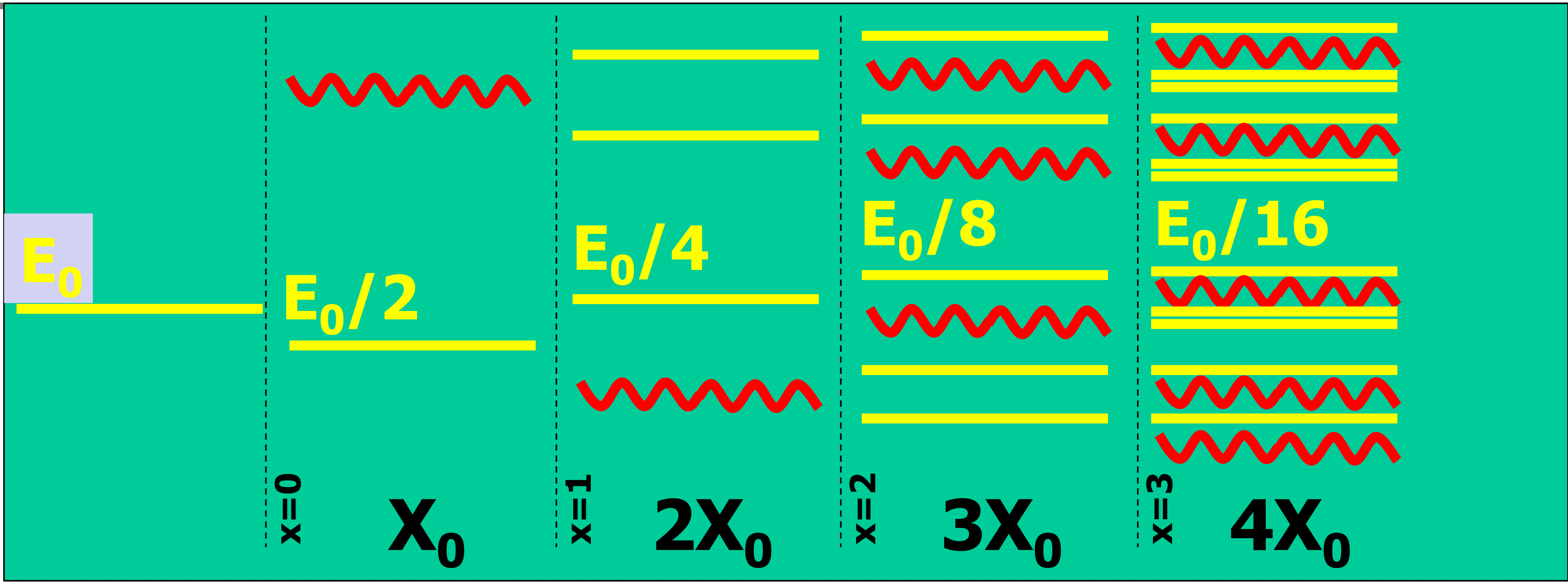

*

EM shower versus Had. shower in air

Electromagnetic shower

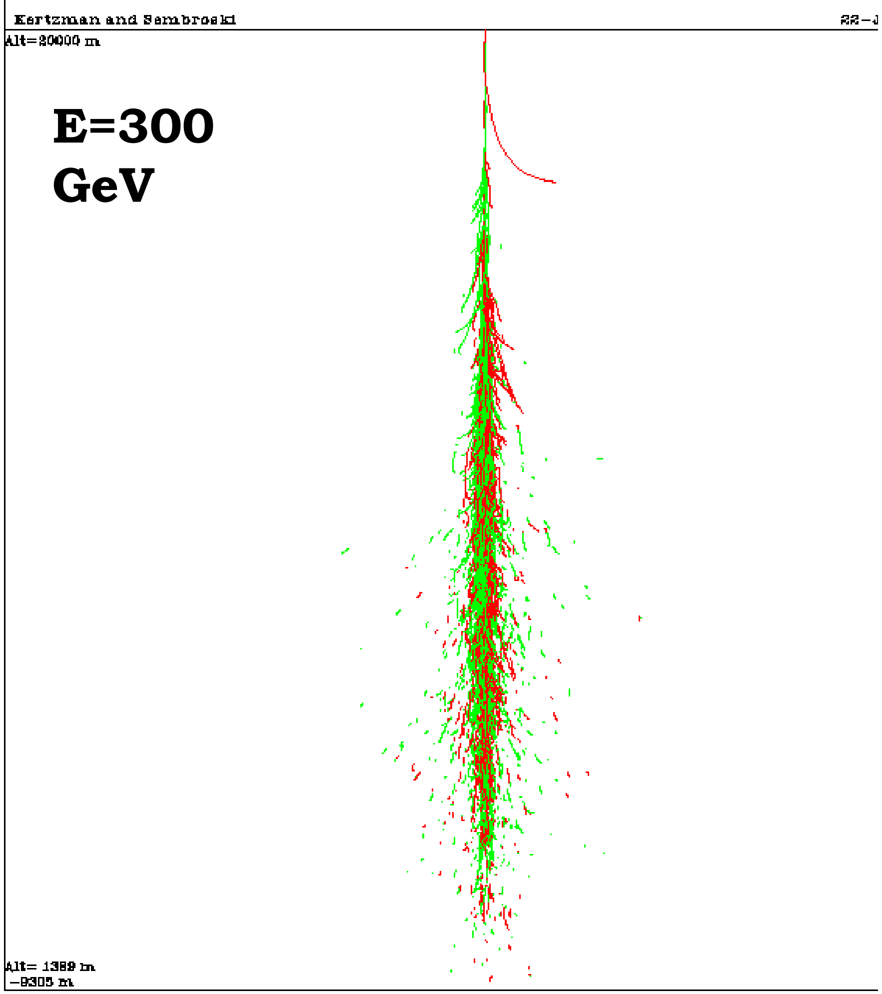

Hadronic shower

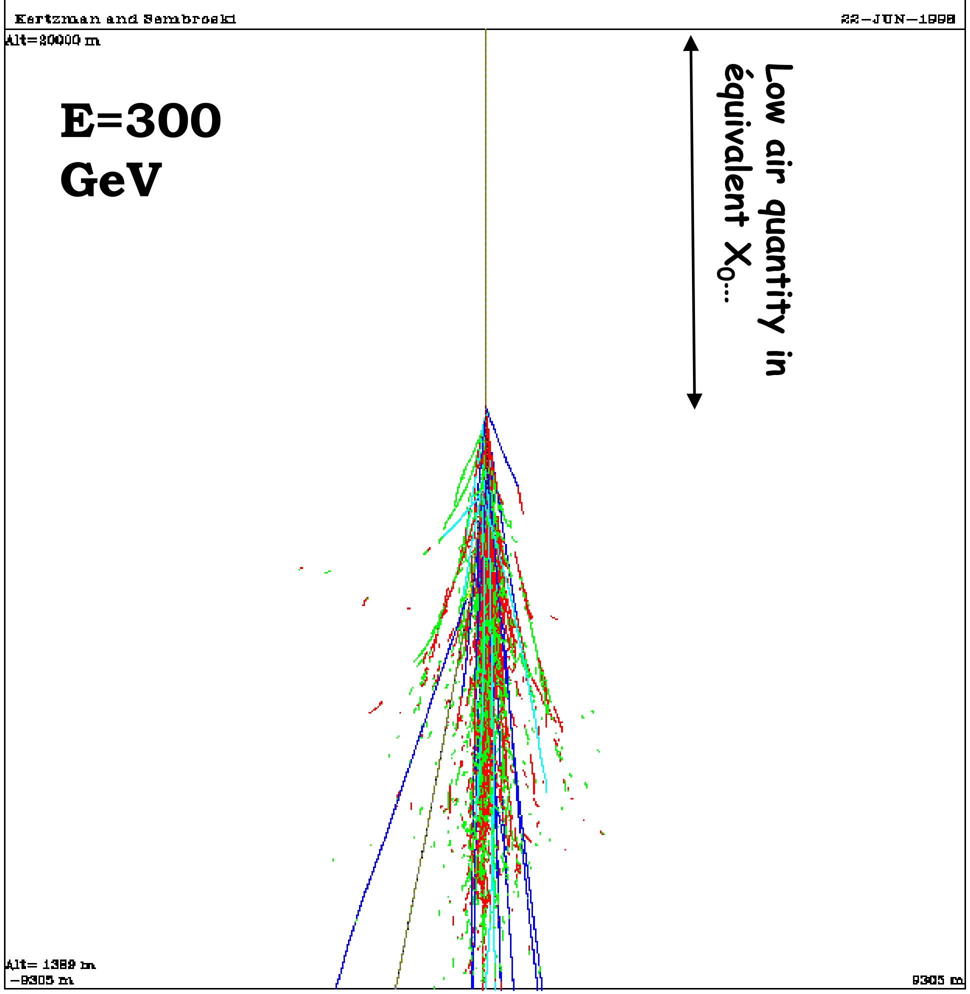

Total amount of air at sea level ~$23.X_0$

Implication : the hadronic showers

In an hadronic shower, there will be production of many π, K and neutrons. $\pi 0$ will give an EM component (from 15 to 20% of initial E), some of the π et K at low energies will give – by decay - μ, ν. Neutrons are difficult to detect (neutral, heavy part.) and will escape. This gives with neutrino the invisible energy of the shower.

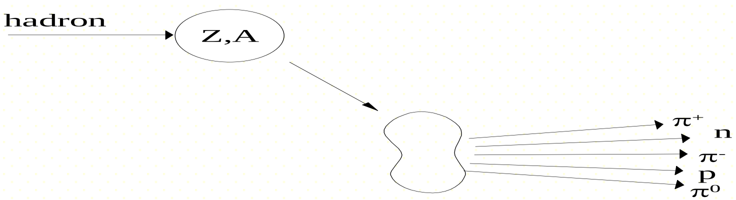

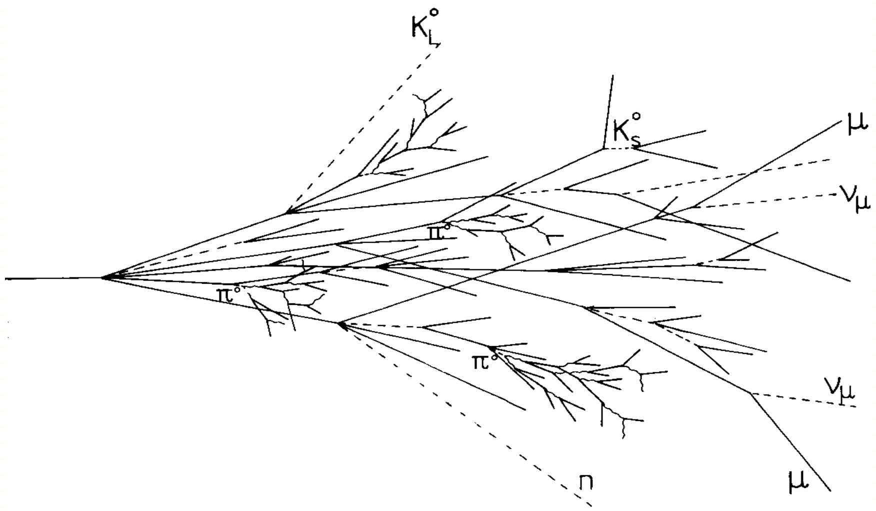

Multiplicity varies with E $\propto \ln(E)$
=> Quick development of the shower

$$\sigma_{inel} \approx \sigma_0 A^{0.7} \quad \sigma_0 \approx 35\,mb$$

~ independant of the energie above 1 GeV for p, π, K…

$$n(\pi^0) \approx \ln E(GeV) - 4.6$$

example 100 GeV: $n(\pi 0) \approx 18$

Remarq : energy profil deposition are different between EM and Had. showers : higher multiplicity for hadronic interaction at the begining of the shower development.

secondaries : $p_t \approx 0.35\ GeV/c$

How the hadronic shower is produced ?

Secondary particules production in hadronic showers are coming from "spallation" :

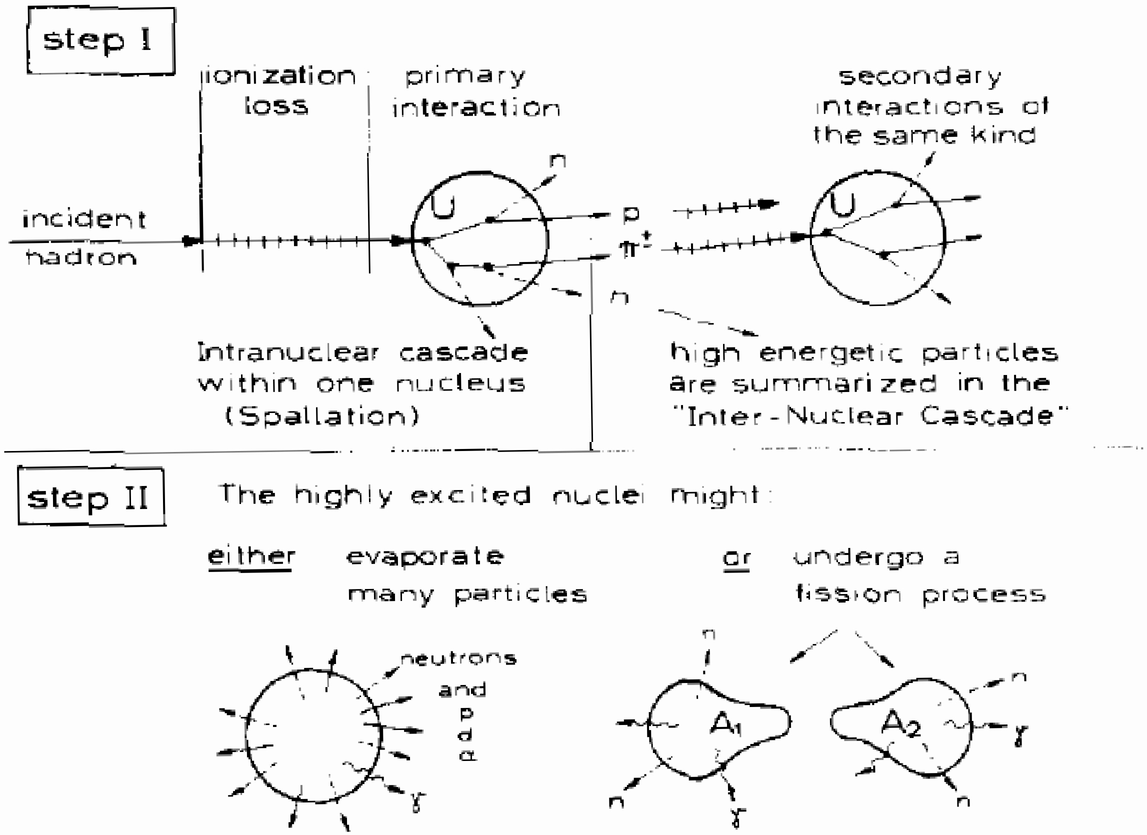

Fig. 6. Step I: Development of an "internuclear cascade". From one nucleus an intranuclear cascade releases a few high energetic spallation products, which are able to iniciate further intranuclear cascade processes. Step II: The highly excited nuclei remaining from each intranuclear cascade deexcite.

H.Bruckmann et al., NIM-A263(1988) 136

Longitudinal shower development (1)

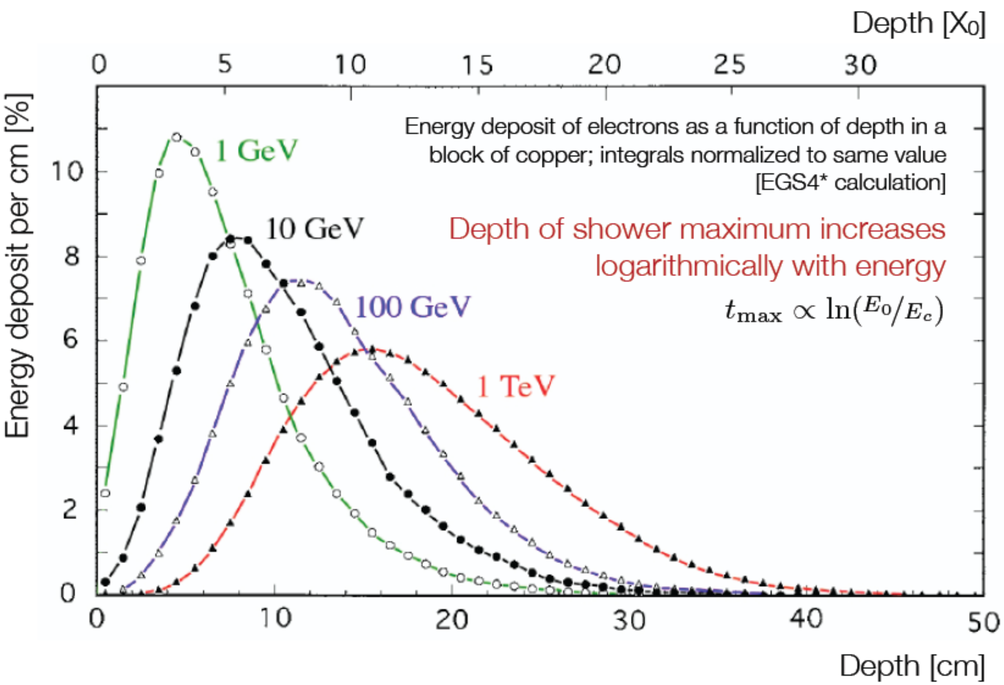

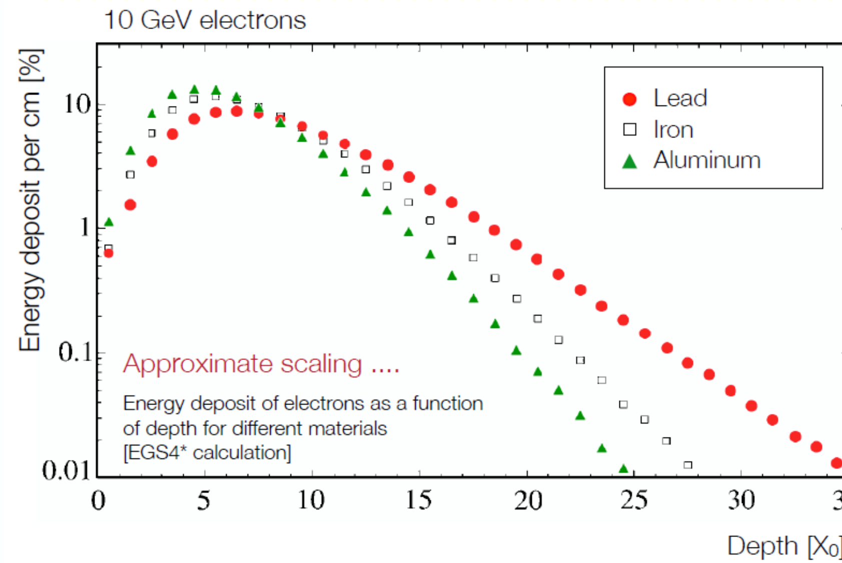

Longitudinal profile well described by

$$\frac{\mathrm{d}E}{\mathrm{d}t} = E_0 b \frac{(bt)^{a-1}\,\mathrm{e}^{-bt}}{\Gamma(a)} \;,$$

$$t_{max} = \frac{a-1}{b} = \ln\left(\frac{E_0}{E_c}\right) + C_{\gamma e}$$

-0.5 for e+/-
+0.5 for γ

ε (Pb) = 7 MeV, ε(Al) = 39 MeV

Shower starts early in low Z material
(tmax dependence with E_c)
[$dE/dx * X_0 \sim Z \times 1/Z^2 = 1/Z$]
Not true when looking at depth in cm !
Radiation length Al : 89 mm, Pb 5.6 mm

***

Longitudinal shower development (2)

Higher penetration power of photons

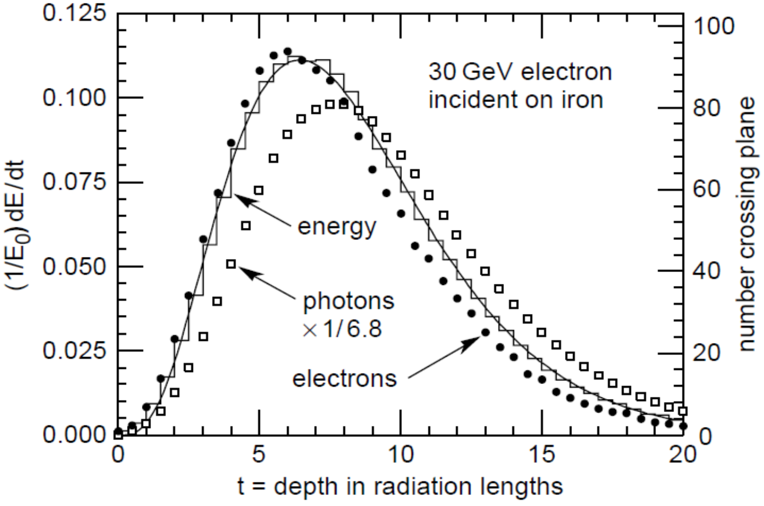

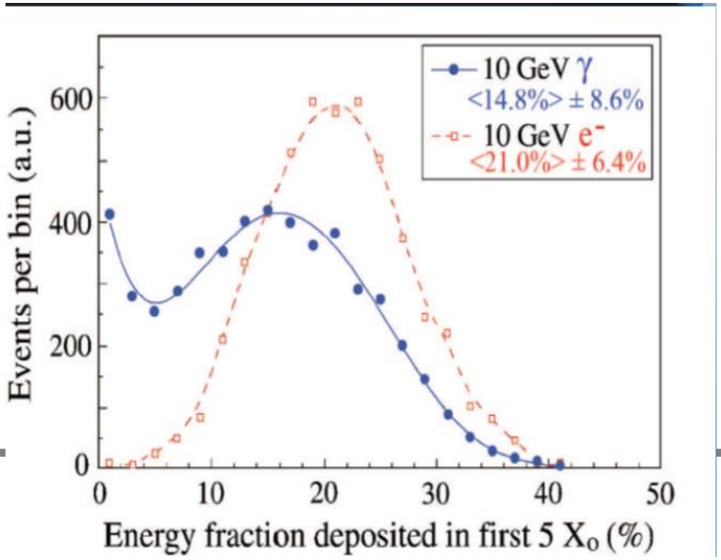

Fraction of energy deposited by e- and e+

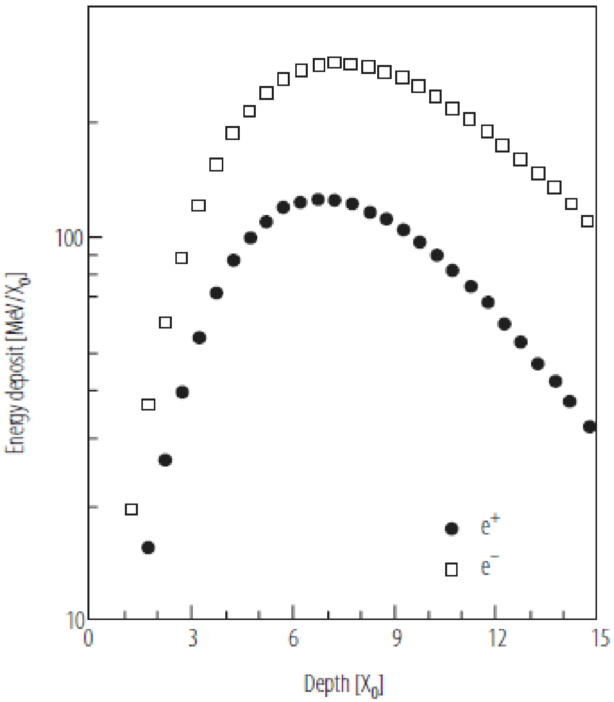

75 % deposited by e-, 25 % by e+
Why ?

***

Shower containment

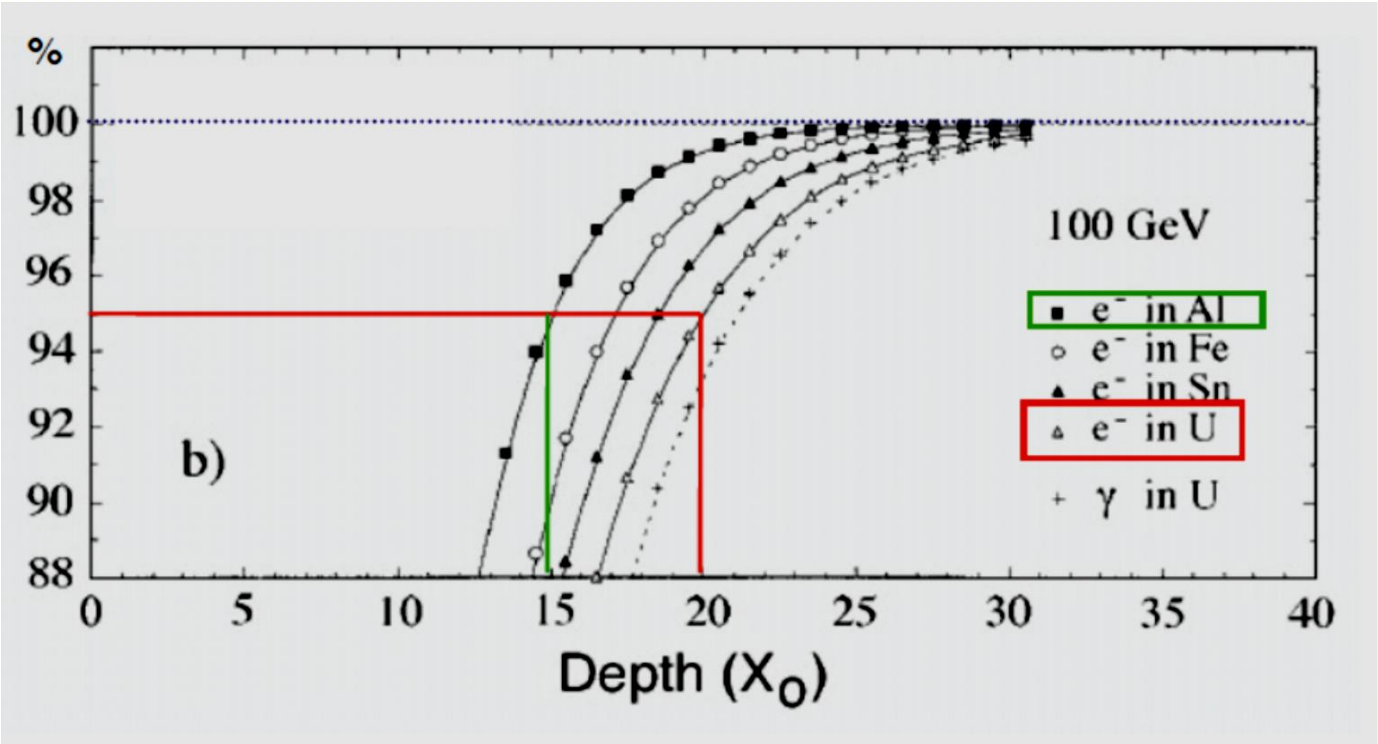

100 GeV electron contained in **15** X_0 of Al and **20** X_0 of U
but remind that X_0(Al) = **89** mm and X_0(U) = **3.2** mm, i.e. **130** vs **6** cm !

Useful parameterisation of containment $L(95\%) = t_{\max} + 0.08Z + 9.6\ [X_0]$

***

Multiple scattering

Charge particle interaction with nuclei
→ Momentum transfer (p)
→ Particle deflexion (θ) (Rutherford scattering formula $1/\sin^4(\theta)$)
→ If thick material (absorber) multiple scattering. On average null effect on position but see as a fluctuation (θ_0) / r.m.s.

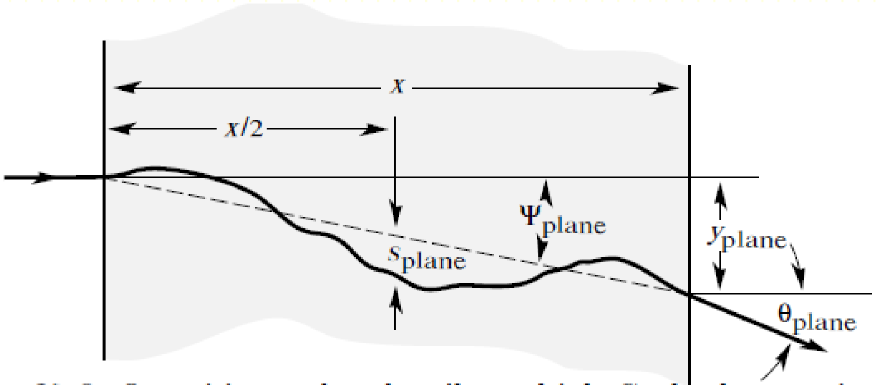

$$\theta_0 = \frac{13.6\ MeV}{\beta c p} z \sqrt{\frac{L}{X_0}} \left\{ 1 + 0.038 \ln\left(\frac{L}{X_0}\right) \right\}$$

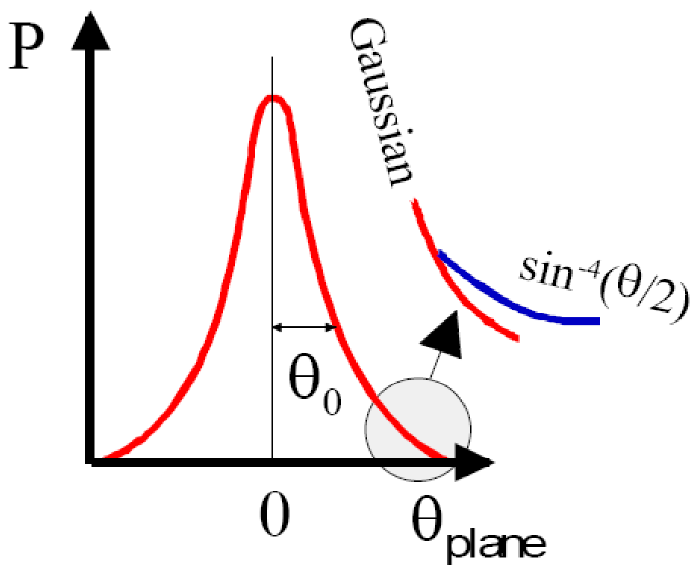

θ_0
-smaller for high energy (p)
-smaller if small material thickness (L)
- smaller if large radiation length

***

Lateral shower development (1)

Pair creation and multiple scattering :
At shower start, dominated by electron/positron scattering along shower axis. Mostly Gaussian

Compton and photo-electric effect at small energy
Process are isotropic. Large penetration length of low energy photon Compton and by photo-electrons

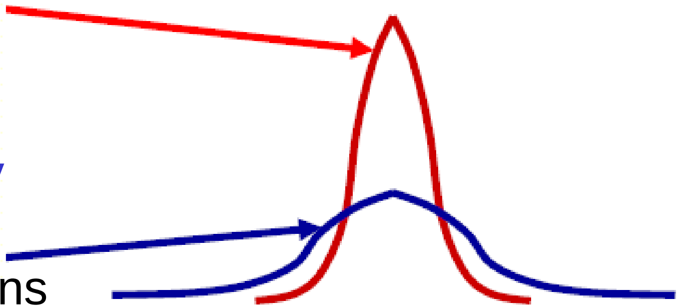

$$\langle\theta\rangle = \frac{21.2\ \mathrm{MeV}}{E_e}\sqrt{\frac{x}{X_0}}$$

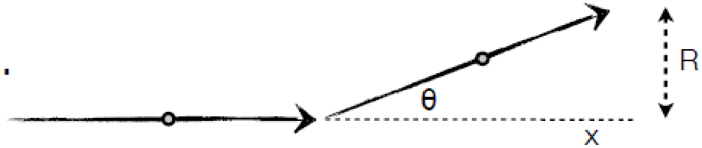

Lateral extension: R = x·tanθ ≈ x·θ, if θ small ...

Main contribution comes from low energy electron, E_c

If one assume that the approximate range of electrons is about 1 X_0,

→ $<\theta> = 21$ MeV/ E_c and lateral extension $R = X_0 <\theta>$

Molière Radius is defined as $R_m = 21\ \mathrm{MeV} / E_c \cdot X_0$

Convenient parameter to estimate lateral shower containment

87 % (96%) of the energy of a electron shower are contained in 1 (2) R_m

Molière Radius governed by material density

***

Lateral shower development (2)

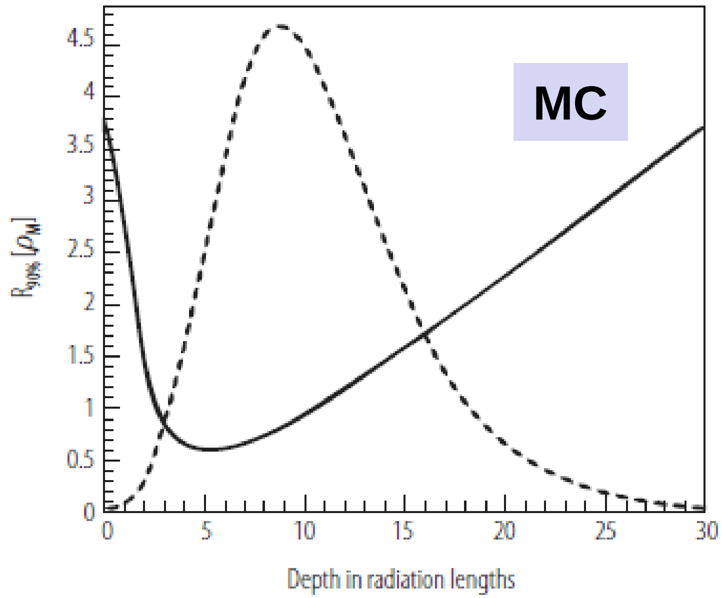

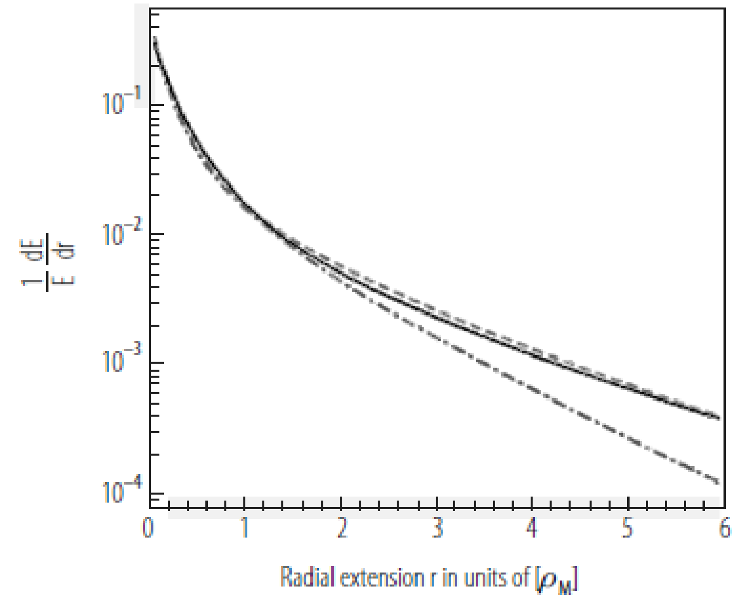

	R_m
Cu	15.2mm
Al	44 mm
Pb	16 mm

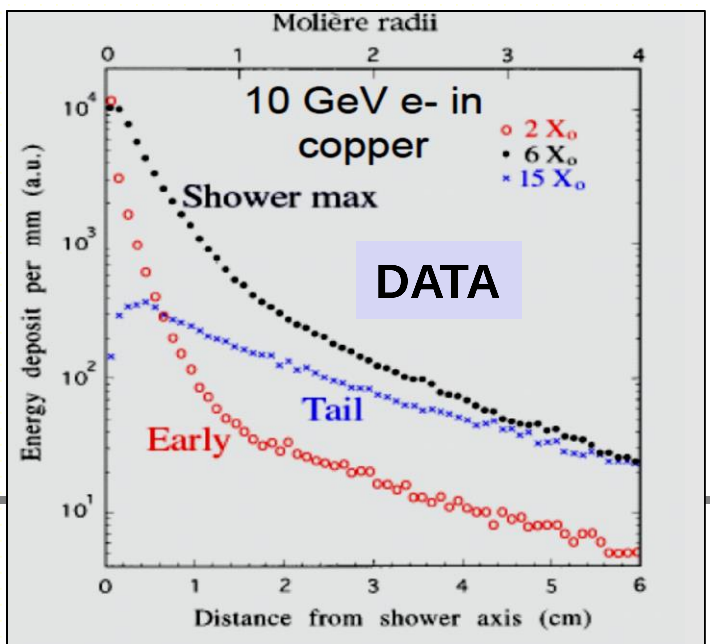

- Core of shower well described with R_m independently of the material (as X_0 in depth)
- Same lateral shower in Cu and Pb while longer depth by 2.5
- Tails at large distance. Z^5 dependence of photo electric cross section

***

Material properties

Material	Z	Density [g cm^{-3}]	ε_c [MeV]	X_0 [mm]	ρ_M [mm]	dE/dx mip [MeV cm^{-1}]	λ_{int} [mm]
C	6	2.27	8.3	188	48	3.95	381
Al	13	2.70	43	89	44	4.36	390
Fe	26	7.87	22	17.6	16.9	11.4	168
Cu	29	8.96	20	14.3	15.2	12.6	151
Sn	50	7.31	12	12.1	21.6	9.24	223
W	74	19.30	8.0	3.5	9.3	22.1	96
Pb	82	11.30	7.4	5.6	16	12.7	170
U 238	92	18.95	6.8	3.2	10	20.5	105
Concrete		2.50	55	107	41	4.28	400
Glass		2.23	51	127	53	3.78	438
Marble		2.93	56	96	36	4.77	362
Si	14	2.33	41	93.6	48	3.88	455
Ar (liquid)	18	1.40	37	140	80	2.13	837
Kr (liquid)	36	2.41	18	47	55	3.23	607
Xe (liquid)	54	2.95	12	24	42	3.71	572
Polystyrene		1.032	94	424	96	2.00	795
Plexiglas		1.18	86	344	85	2.28	708
Quarz		2.32	51	117	49	3.94	428
Pb glass		4.06	15	25.1	35	5.45	330
Air (2C,1atm)		0.0012	87	304m	74m	0.0022	747m
H_2O		1.00	83	361	92	1.99	849
$PbWO_4$		8.3		8.9	20	10.2	207
CeF_3		6.16		16.8	26	7.9	259
LYSO		740		11.4	20.7	9.6	209

Formulae for compound material : $1/X_0 = \Sigma\, w_j / X_j$

*

Summary of useful definition

Energy loss by radiation : $< E(x) > = E_0 \, e^{-\frac{x}{X_0}}$

γ absorption (e+e-) $< I(x) > = I_0 \, e^{-\frac{7}{9}\frac{x}{X_0}}$

Radiation length: $$X_0 = \frac{180A}{Z^2} \frac{\mathrm{g}}{\mathrm{cm}^2}$$

Critical energy:
[Attention: Definition of Rossi used]
$$E_c = \frac{550\ \mathrm{MeV}}{Z}$$

Shower maximum: $$t_{\max} = \ln \frac{E}{E_c} - \begin{cases} 1.0 & e^- \text{ induced shower} \\ 0.5 & \gamma \text{ induced shower} \end{cases}$$

Longitudinal
energy containment: $$L(95\%) = t_{\max} + 0.08Z + 9.6\ [X_0]$$

Transverse
Energy containment: $$R(90\%) = R_M$$ $$R(95\%) = 2R_M$$

R_m = (21 MeV/ E_c). X_0
~ 1/Z * Z (Z/A)
Small dependence with Z

***

Energy resolution

Detectable visible energy subject to fluctuation
→ Finite energy resolution

$$\sigma(E) = \sqrt{\sigma_1^2 + \sigma_2^2 + \sigma_3^2} = \sigma_1 \oplus \sigma_2 \oplus \sigma_3$$

Most of the sources of fluctuation can be considered uncorrelated :

- Shower fluctuations
- Sampling fluctuations in sampling calorimeter
- Signal quantum fluctuations (photo detectors..)
- Leakage
- Noise in the readout
- Specific technology effects (recombination, light attenuation, gas saturation….)
- Specific to detector construction (mechanics tolerance, electronics response…)

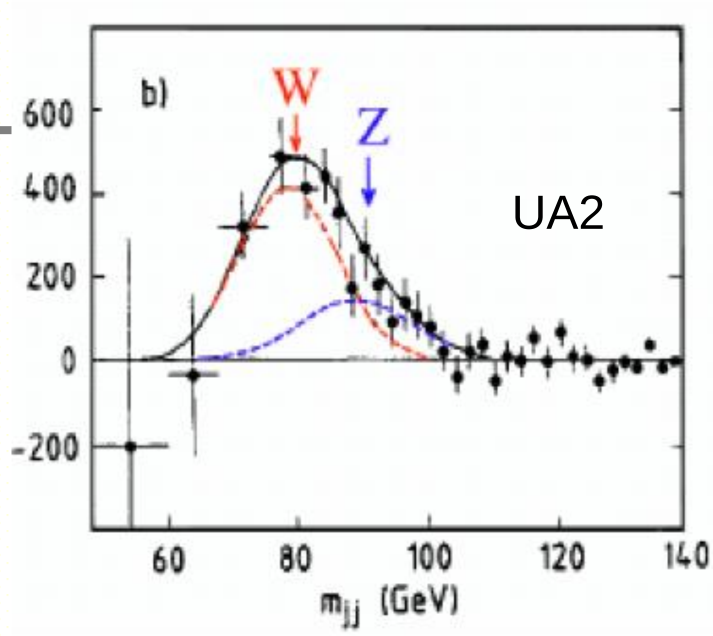

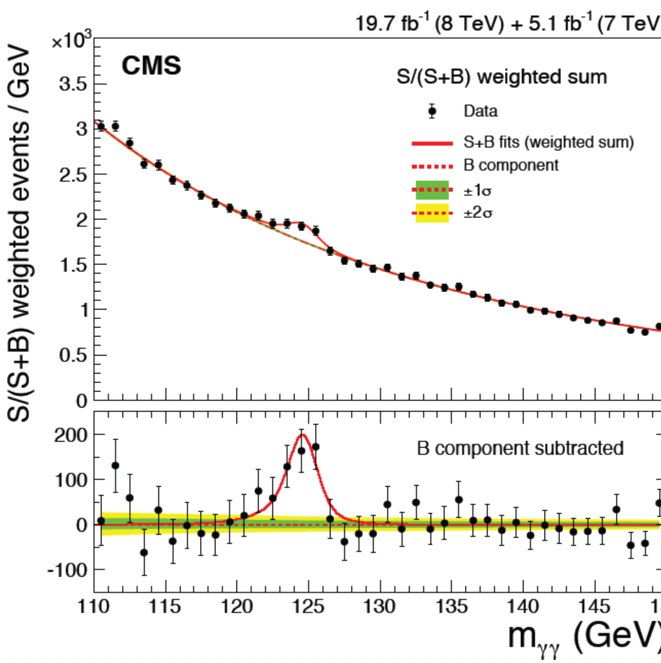

**

Energy resolution

Usually parameterized as

$$\frac{\sigma}{E} = \frac{a}{\sqrt{E}} \oplus \frac{b}{E} \oplus c$$

- **a** stochastic term:
  - intrinsic statistical shower fluctuations
  - sampling fluctuations
  - signal quantum fluctuations (e.g. photo-electron statistics)
- **b** is the noise term:
  - electronic readout noise
  - pileup noise in high luminosity environment: fluctuations of energy from sources other than the primary particle (e.g. particles from other collisions in the same or in previous bunch crossings)
- **c** is the constant term that incorporates all other systematics:
  - detector response non-uniformity (hardware or calibration)
  - imperfections in calorimeter construction and geometry (e.g. not fully hermetic, cracks…)
  - longitudianl leakage
  - energy lost in dead material upfront…
  - dominant contribution at high energies

**

Energy resolution

Usually parameterized as

$$\frac{\sigma}{E} = \frac{a}{\sqrt{E}} \oplus \frac{b}{E} \oplus c$$

Quadratic sum !

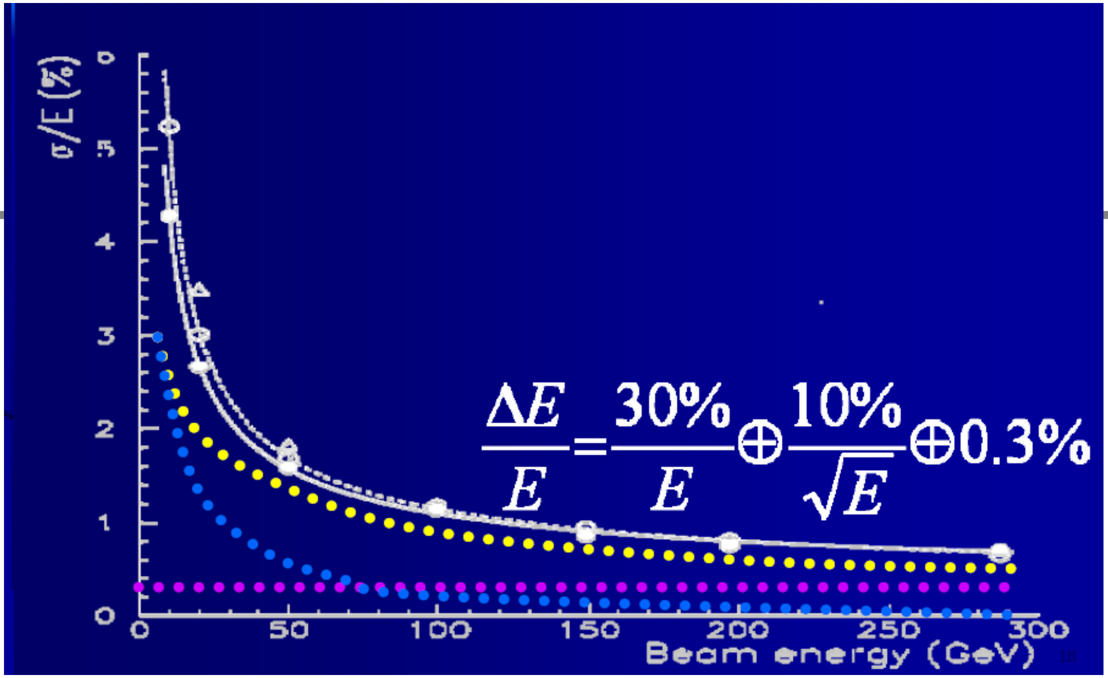

Questions: which term is affected by:

- **fluctuations in the # of particles in the shower?** — **$1/\sqrt{E}$ (a)**
- **global scale (gain) shift?** — **1 (c)**
- **electronics noise?** — **1/E (b)**
- **global offset (pedestal) shift?** — **1/E (b)**
- **shower particles escaping the calorimeter?** — **1* also $1/\sqrt{E}$ if upstream**
- **fluctuations in the # of photo-electrons detected ?** — **$1/\sqrt{E}$ (a)**
- **pile-up (remnants of earlier events)?** — **1/E (b)**
- **radioactivity ?** — **1/E (b)**
- **presence of dead material?** — **1 (c)**
- **statistical uncertainty of scale (gain) constants?** — **1 (c)**
- **statistical uncertainty on offset (pedestal) constants?** — **1/E (b)**

***

Electromagnetic calorimeter technologies :

Homogeneous calorimeters

Sampling calorimeters

Homogeneous calorimeters

- Combine both the role of absorber and signal generation.
- Total volume sensitive to the deposited energy. (Large fraction of visible energy)

Advantage

- Best energy resolution ($1/\sqrt{E}$ term) limited by physical factors as number of photo-electrons if ideal calo (no leakage)
- Intrinsically linear in principle
- Well suited for low energy application (nuclear spectroscopy, medical application…)

Disadvantage

- Limited segmentation (especially in depth)
- Can not be used for hadronic shower to keep "reasonable" detector size.
- Cost (Pb or Cu less expensive than crystals, Silicon or noble liquid)

***

Sampling calorimeters

- Shower is sampled in active layers interleaved with absorbers

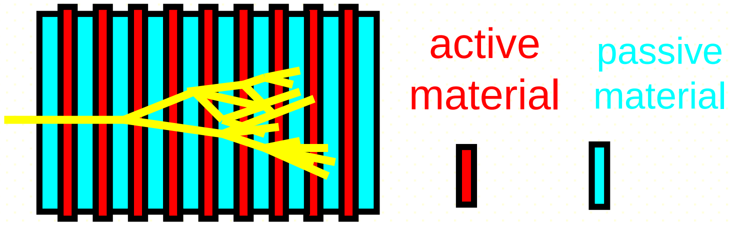

Advantage
- Can achieve easily lateral and longitudinal segmentation
→ Angular measurement and particle Identification
- cheaper calorimeter (in principle !) as absorber not too expensive
- Only possibility for Hadron calorimeters

Disadvantage
- Small fraction of energy seen
→ Stochastic term degraded

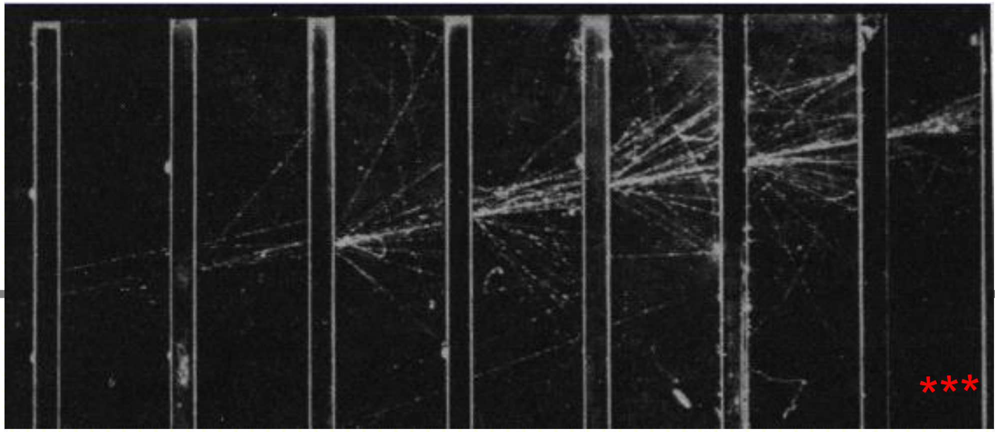

Homogeneous calorimeter technology

Should be dense enough to contain EM shower, give enough signal

- **Semiconductor Si, Ge** : very low threshold to create electron-hole pair (2.9 eV in Ge)

  → *Use in nuclear spectroscopy, medical application*

- **Cerenkov :** high refractive index induces cerenkov light with relativistic charged particle

  → *Lead glass, OPAL@LEP*

- **Scintillators :** ionisation tracks converted in light in crystals (fluorescence)

  → *NaI(Tl) (Crystal Ball), L3 (BGO), Babar, Belle, KTeV (CsI), $PbWO_4$ (CMS)*

- **Noble Liquids :** cryogenics detectors. Ionisation produces charge and light (scintillation)

  → *Kr (NA48, KEDR)*

**

Si/Ge low energy homogeneous calorimeters

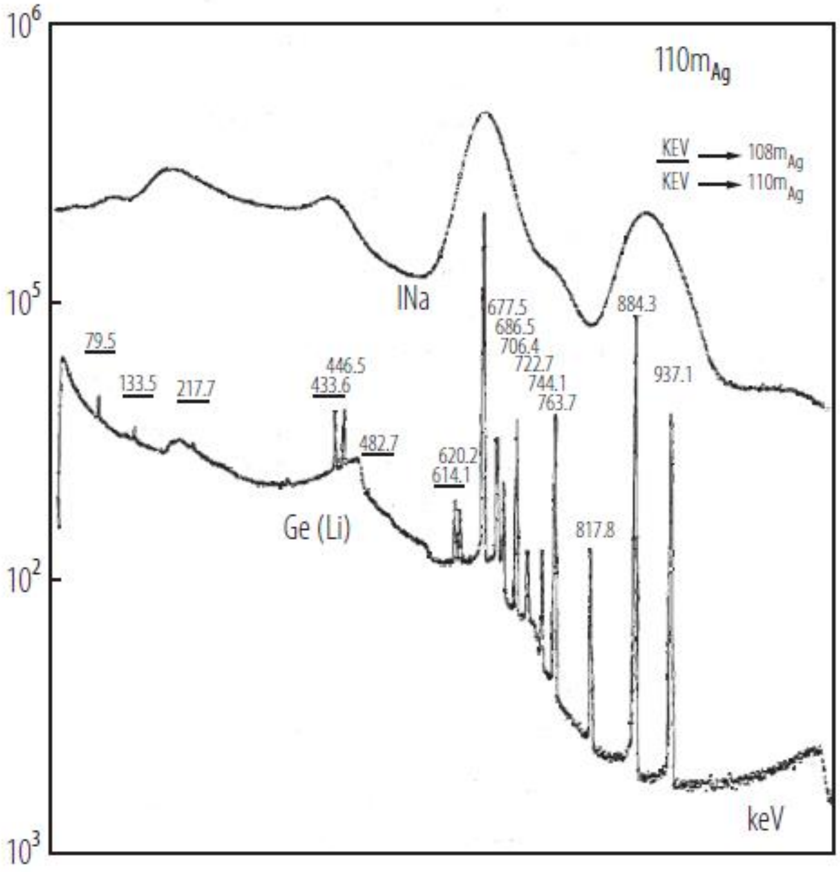

Ge : energy to create an electron-hole pair at 77 K : 2.9 eV

1 MeV → N= 3.4 10^5 pairs

$\sigma_E/E \sim 1/\sqrt{N} = 0.17\%$

Even better due to Fano factor (pairs created not statistically independent, constrained by total energy of incident particle, similar to binomial variance) F = 0.13 in Ge

$\sigma_E/E \sim \sqrt{(F/N)} = 0.06\ \%$

Popular detectors in Nuclear physics (AGATA for instance)

**

Noble liquid homogeneous calorimeters

NA48 : Fixed target experiment for CP violation, and now NA62 rare Kaon decays

1 MeV resolution needed on π^0 mass

Liquid Krypton @120 K

LKr CALORIMETER ELECTRODE STRUCTURE

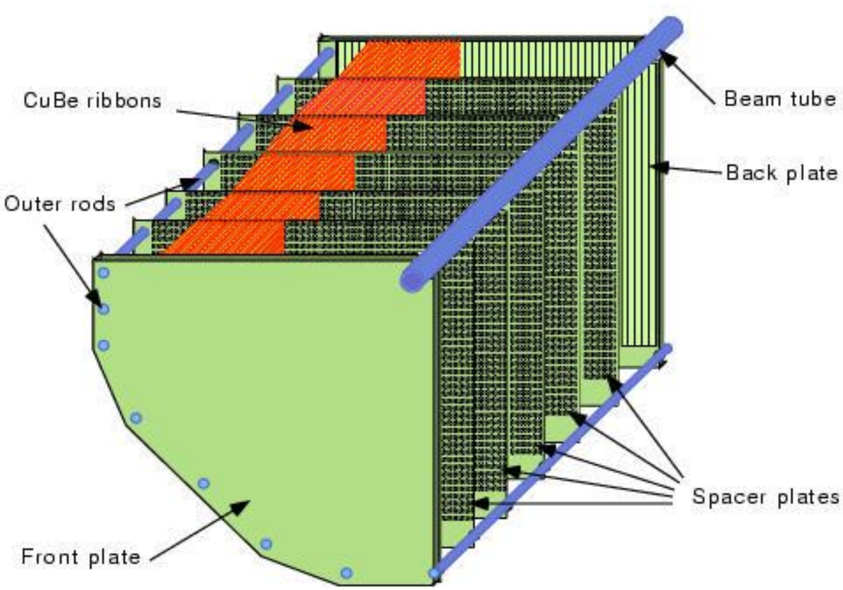

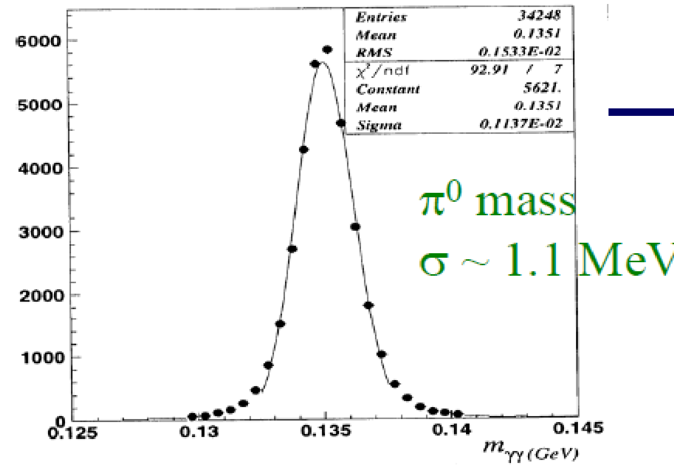

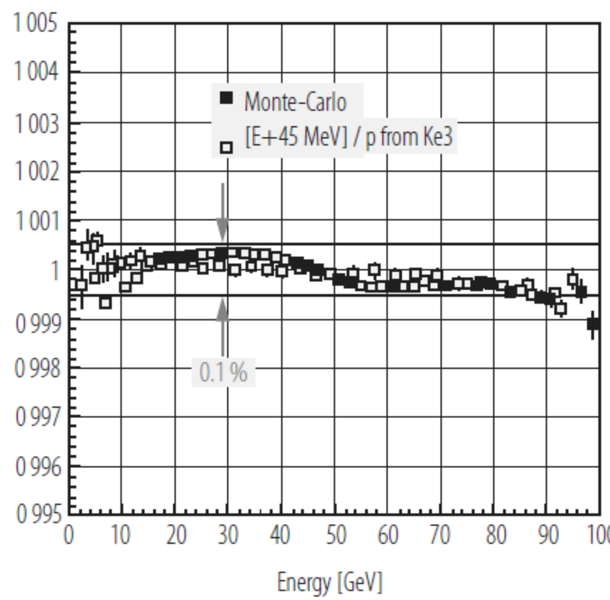

Linearity as important as resolution

Need a careful control of upstream dead material

*

Homogeneous crystals calorimeters

Crystal	light	ρ [g/cm³]	X_0 [cm]	τ [ns]	λ [nm]	Output	Damage (Gy)
NaI	Scint	3.67	2.59	250	410	1 (40000 ph/MeV)	10
BGO	Scint	7.13	1.12	300	410	0.15	10 *
BaF_2	Scint	4.89	2.05	600	310	0.20	10^5 *
CsI **(Tl)**	Scint	4.53	1.85	35 (1000)	420	0.05 **(0.45)**	10^3
$PbWO_4$	Scint	8.28	0.89	5-15	430	0.01	10^4 *
CeF_3	Scint	6.16	1.68	10-30	325	0.10	
Pbglas5	Cer	4.08	2.54	fast	< 350	0.00015	
Pbglas6	Cer	5.20	1.69	fast	< 350	0.00023	

*** Hygroscopy ~2%/°c** *

Homogeneous crystals calorimeters

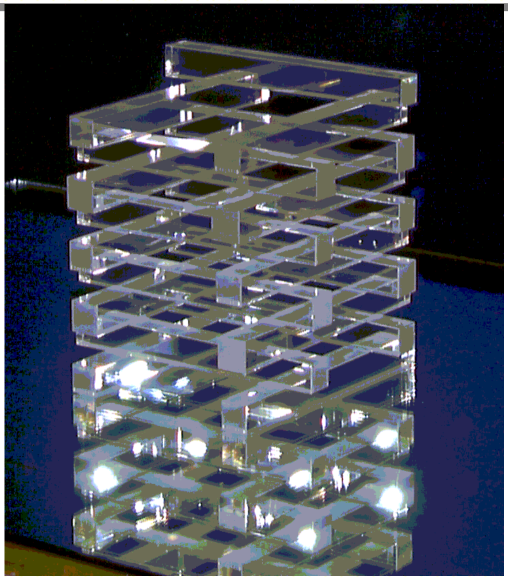

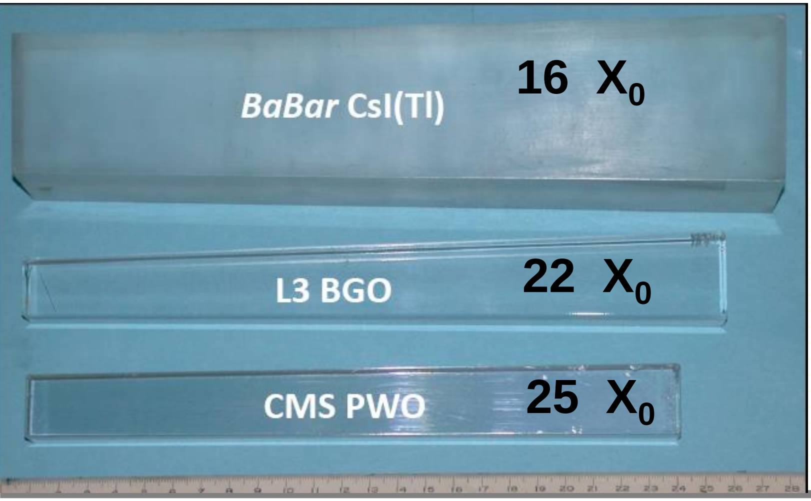

25 cm

Growing crystals not always easy task
By construction non uniform response from one crystal to another (up to 10-20%), different transparency

*

Homogeneous crystals calorimeters

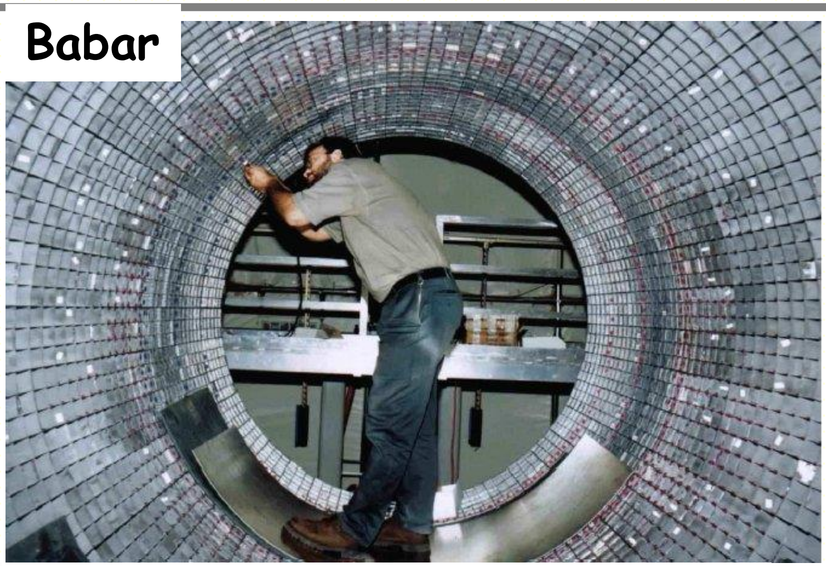

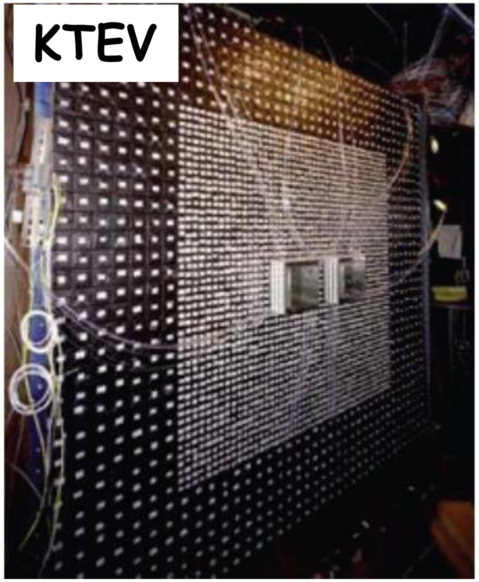

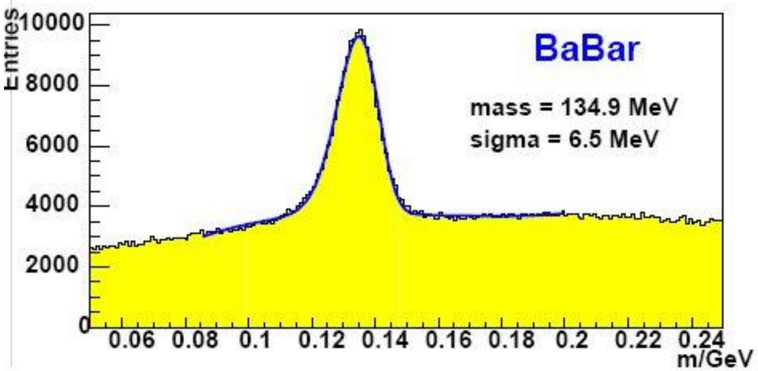

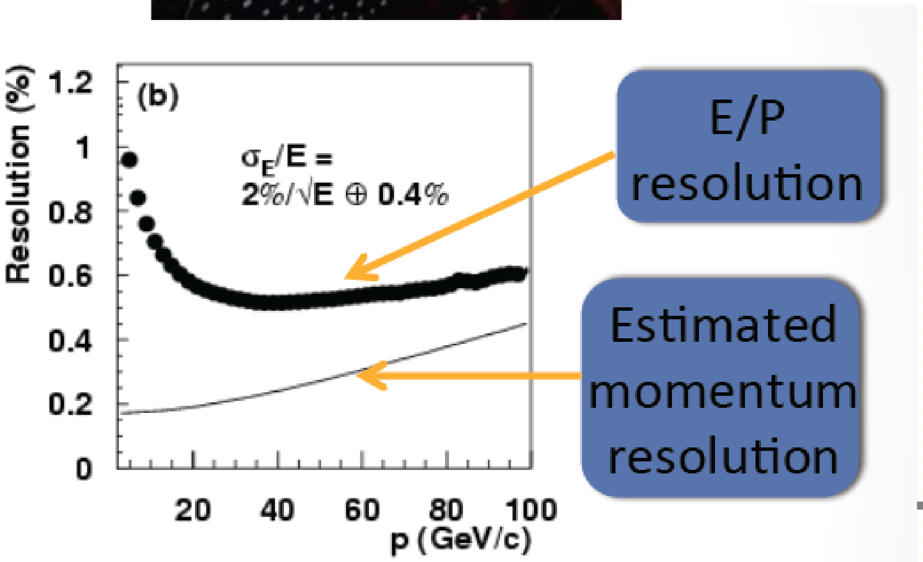

$$\frac{\sigma_E}{E} = \sqrt{\left(\frac{0.066\%}{E_n}\right)^2 + \left(\frac{0.81\%}{\sqrt[4]{E_n}}\right)^2 + (1.34\%)^2}\,, \quad E_n = E/\mathrm{GeV}\,,$$

CMS calorimeter

Scintillator : PBW0$_4$ [Lead Tungsten]
Photosensor : APDs [Avalanche Photodiodes]

Number of crystals: ~ 70000
Light output: 4.5 photons/MeV

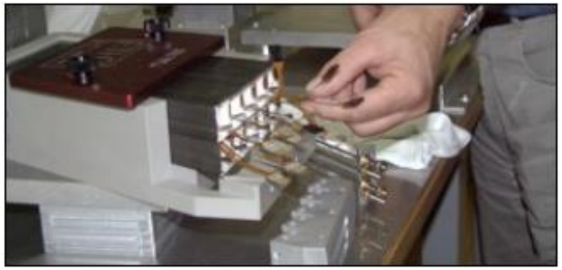

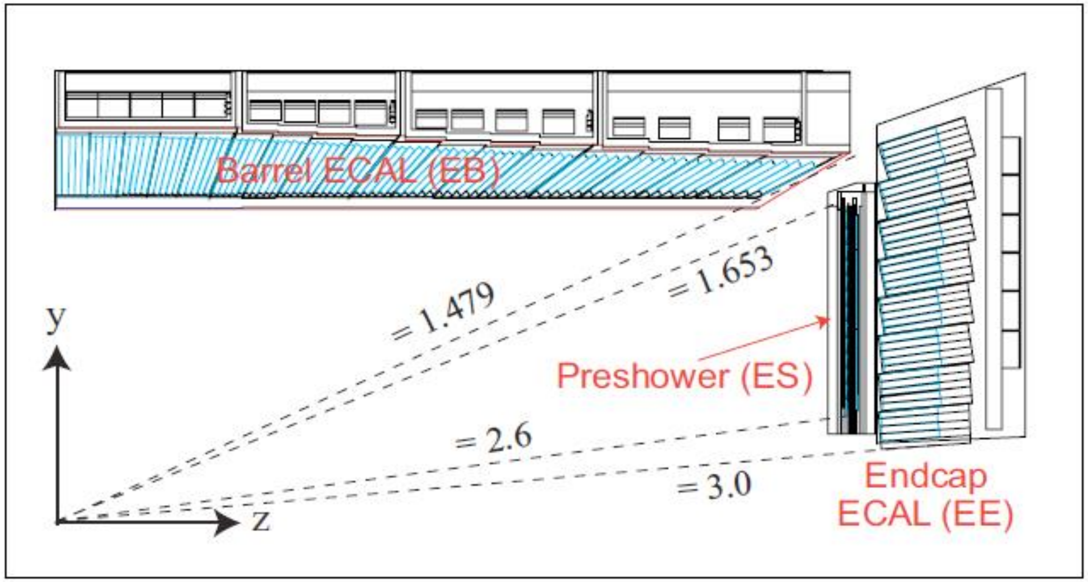

**

Impact of radiation on CMS calo

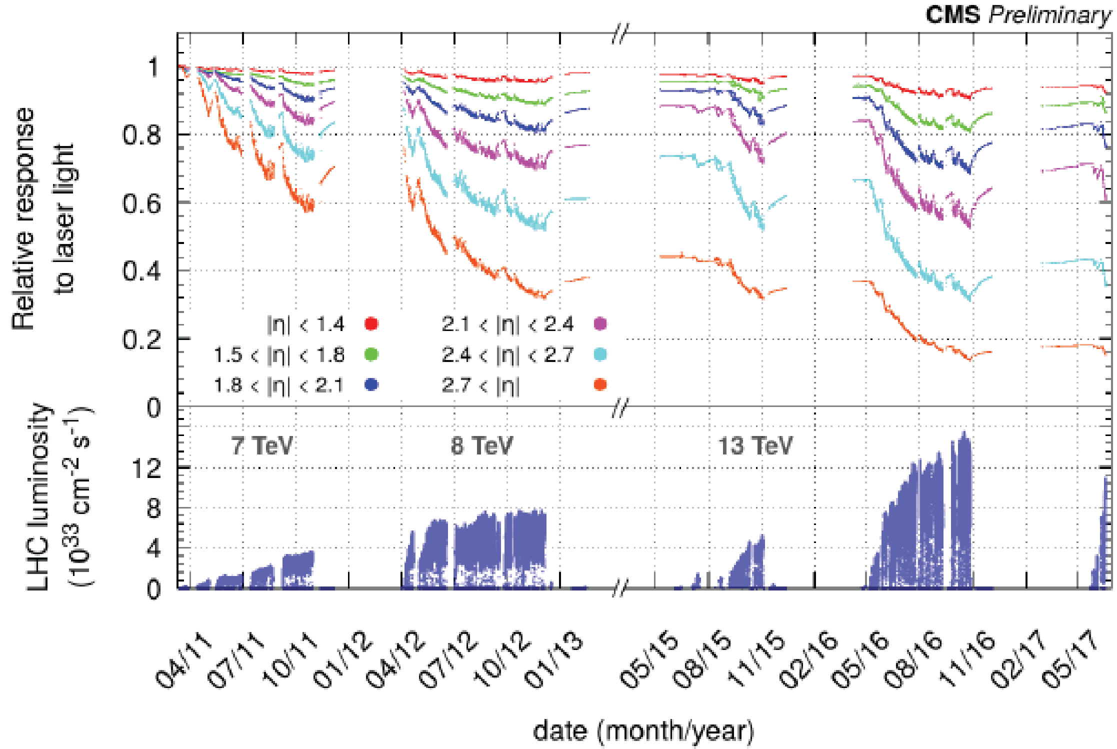

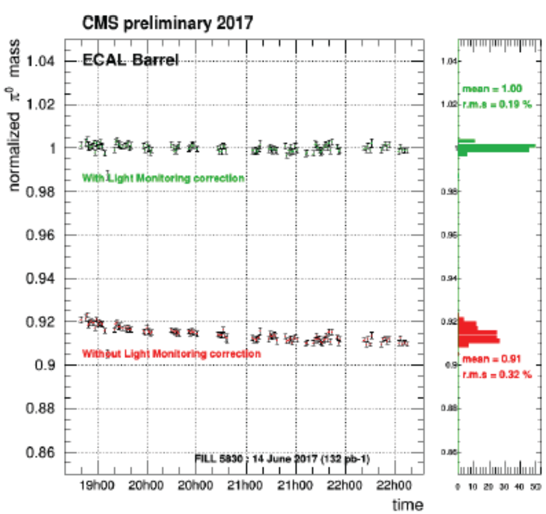

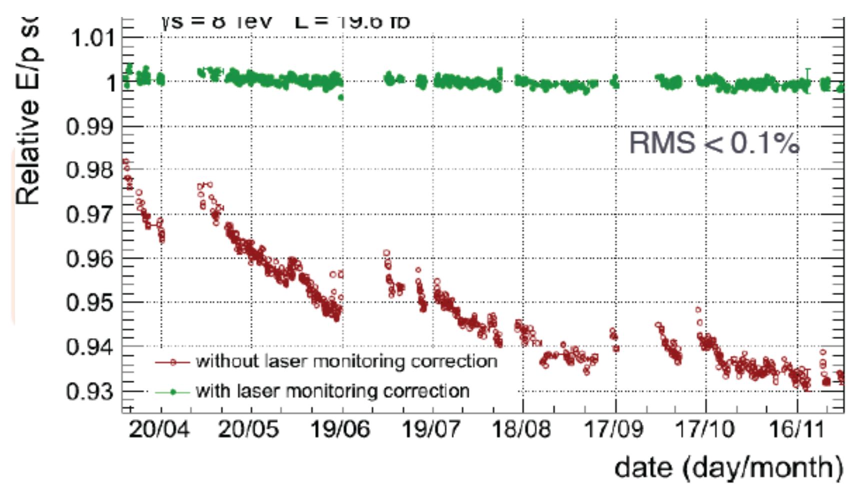

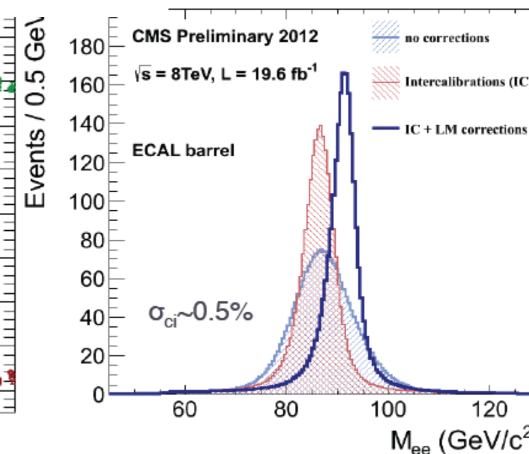

Performance of homogeneous calorimeters

Technology (Experiment)	Depth	Energy resolution	Date
NaI(Tl) (Crystal Ball)	$20X_0$	$2.7\%/\mathrm{E}^{1/4}$	1983
$Bi_4Ge_3O_{12}$ (BGO) (L3)	$22X_0$	$2\%/\sqrt{E} \oplus 0.7\%$	1993
CsI (KTeV)	$27X_0$	$2\%/\sqrt{E} \oplus 0.45\%$	1996
CsI(Tl) (BaBar)	16–$18X_0$	$2.3\%/E^{1/4} \oplus 1.4\%$	1999
CsI(Tl) (BELLE)	$16X_0$	1.7% for $E_\gamma > 3.5$ GeV	1998
$PbWO_4$ (PWO) (CMS)	$25X_0$	$3\%/\sqrt{E} \oplus 0.5\% \oplus 0.2/E$	1997
Lead glass (OPAL)	$20.5X_0$	$5\%/\sqrt{E}$	1990
Liquid Kr (NA48)	$27X_0$	$3.2\%/\sqrt{E} \oplus 0.42\% \oplus 0.09/E$	1998

Homogeneous

For crystals/Cerenkov stochastic term contains both shower fluctuation and photo-electron statistics (converting photons in electrical signal).

Example : Lead Glass : Cerenkov only if e+/- with E > 0.7 MeV and
photon-detector provides 1000 photo-electrons/GeV
Expected resolution for 1 GeV ? → stochastic term ?

**

Sampling calorimeters

- Shower is sampled in active layers interleaved with absorbers

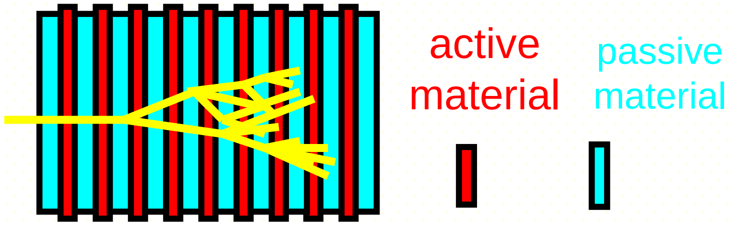

Advantage

- Can achieve easily lateral and longitudinal segmentation
→ Angular measurement and particle Identification
- cheaper calorimeter (in principle !) as absorber not too expensive
- Only possibility for Hadron calorimeters

Disadvantage

- Small fraction of energy seen
→ Stochastic term degraded

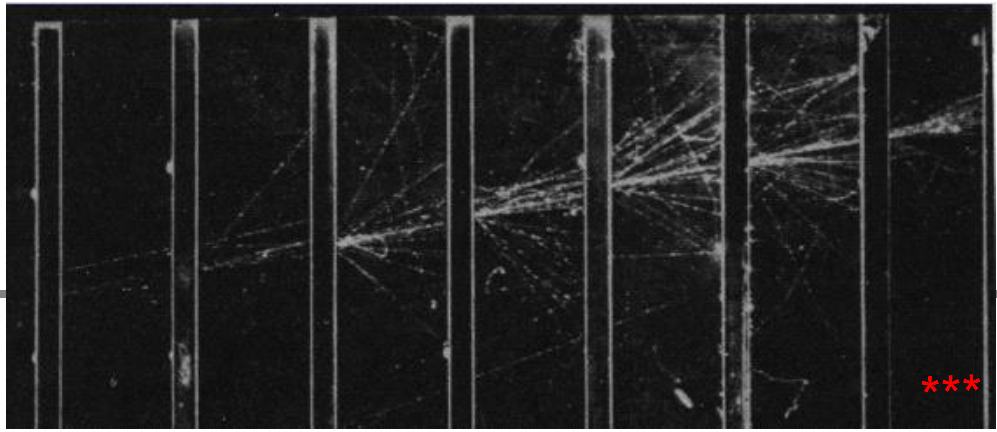

EM sampling calorimeter technology

Absorber with dense material with low critical energy (high Z) for shower development (U, Pb, W…). All technologies possible for active layers :

- **Scintillators**
  →U + scint (Zeus@Hera) , Pb + scint (CDF@Tevatron)

- **Gazeous detectors**
  → Pb + wire chambers (ALEPH@LEP)

- **Liquid Argon :**
  → LAr + Pb (Cello , NA31, SLD, H1@Hera, ATLAS@LHC)
  → LAr + U (D0@Tevatron)
  Kr considered as option at SSC & LHC

- **Semiconductors**
  → Si+W (Pamela, Calice@ILC, CMS HGCAL@HL-LHC)

**

Sampling calorimeter

Simplified model of previous :
Active medium : counts only charged particle produced in absorber shower development.
$N_{max} = E/E_c$, 2/3 are charged particles

→

Pb : E_c = 7.4 MeV
For 1 GeV shower, Nch~90
$\sigma(Nch)/Nch = 1/\sqrt{Nch} = 10\%$
Typical best stochastic term of sampling EM calorimeter

Key parameters :

Sampling frequency : Number of times a high energy electron/γ is sampled. Linked to absorber thickness (t).
Thinner is t, higher is the sampling frequency, better is the resolution, but if too small correlated signals in two active layers

Sampling fraction : Fraction of energy deposited by a mip in active layer

$$f_{samp} = \frac{E_{mip}(actif)}{E_{mip}(actif) + E_{mip}(absorbeur)}$$

E_{mip} = (dE/dx)*distance
t for passive material, s for active

Fractional energy response $f_R = (E_{active}) / (E_{active} + E_{passive})$ (includes showering process)

***

Sampling Calorimeter

Blue absorber (t) , red active medium (s)

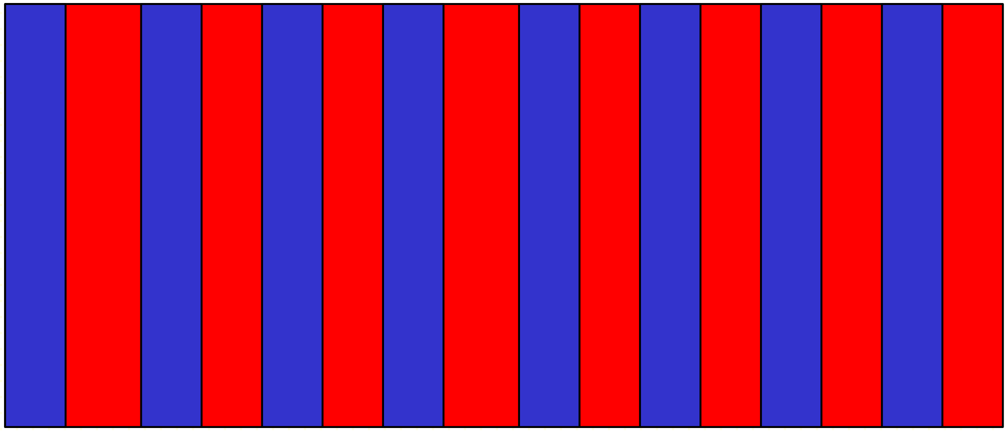

Sampling Calorimeter

Blue absorber (t) , red active medium (s)

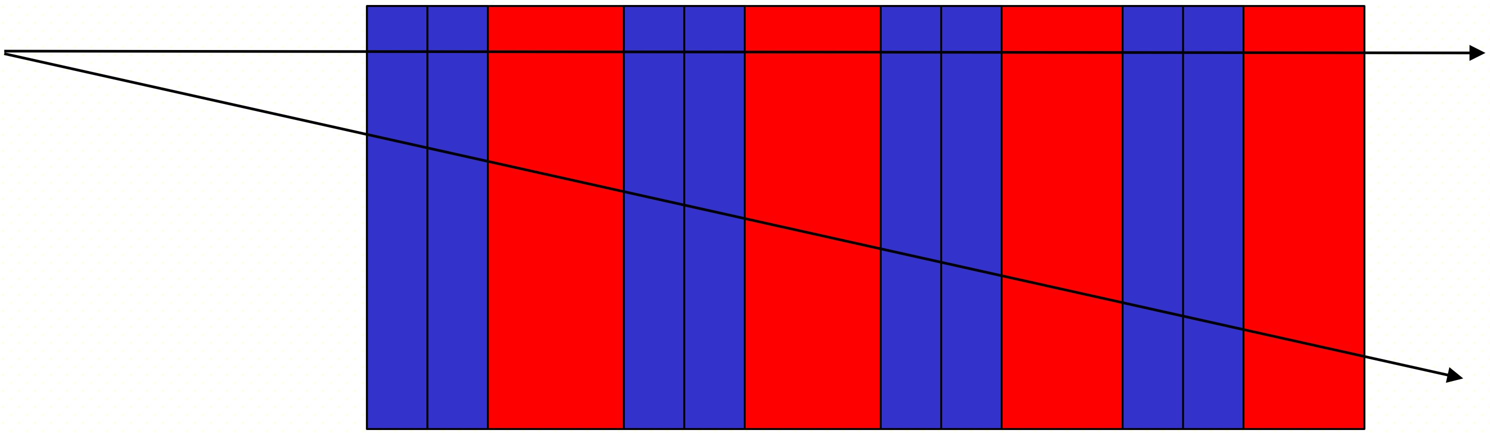

Same sampling fraction but smaller sampling frequency
(4 / 8) → worse stochastic term
Angular effect : constant sampling fraction but smaller frequency

EM sampling calorimeter E resolution

Total track length detectable → $T_d = f_{samp} * T$

→ expect energy resolution as $1/\sqrt{T_d} \sim 1/\sqrt{f_{samp}}$

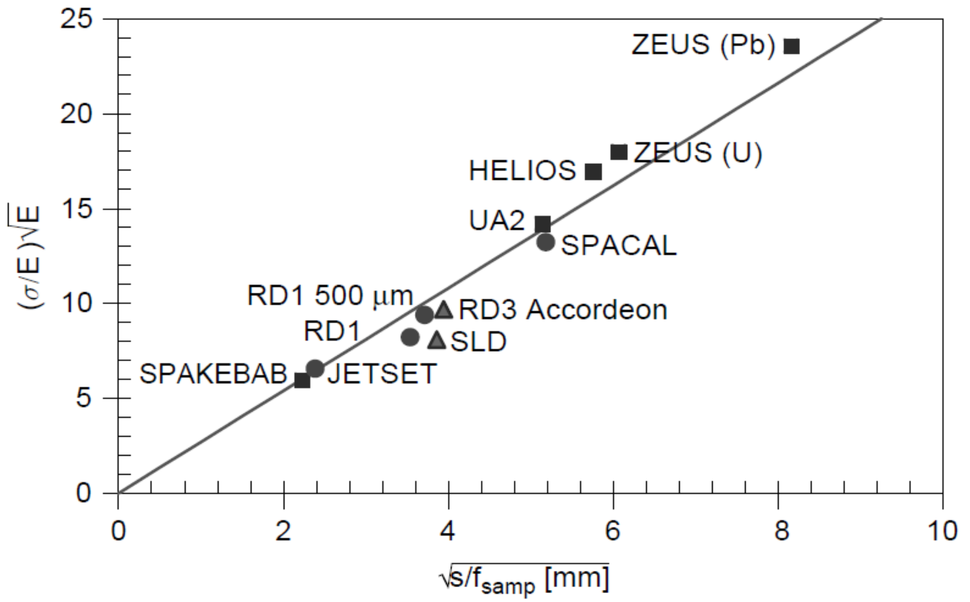

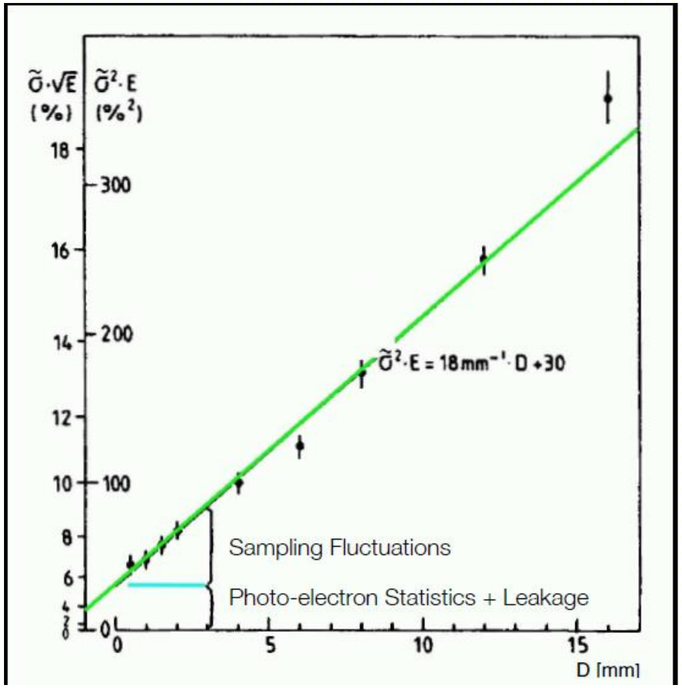

$$\frac{\sigma_{samp}}{E} = \frac{2.7\%}{\sqrt{E\ [\mathrm{GeV}]}}\sqrt{\frac{s\ [\mathrm{mm}]}{f_{samp}}}$$

$$\frac{\sigma_E}{E} = 3.2\%\sqrt{\frac{E_c\ [\mathrm{MeV}]\cdot t_{abs}}{F\cdot E\ [\mathrm{GeV}]}}$$

**

EM sampling calorimeter examples

Possible setups

Scintillators as active layer;
signal readout via photo multipliers

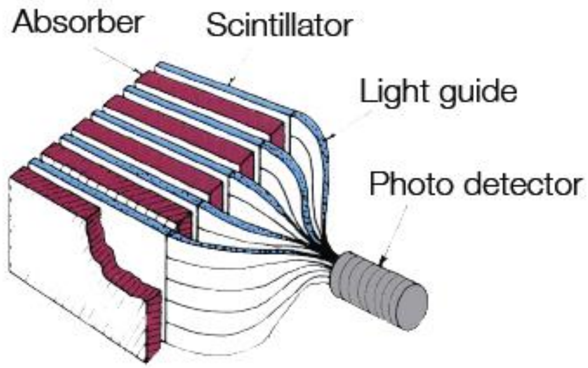

Scintillators as active layer; wave length shifter to convert light

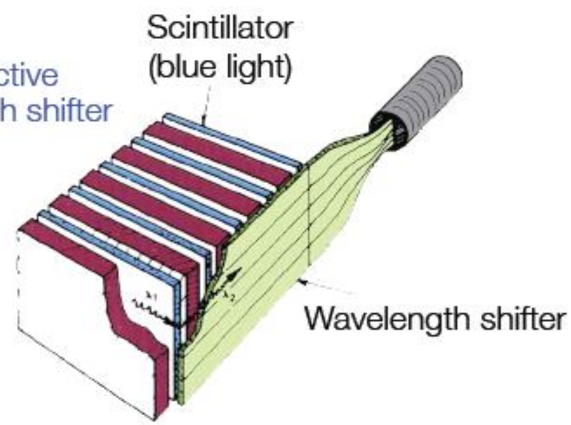

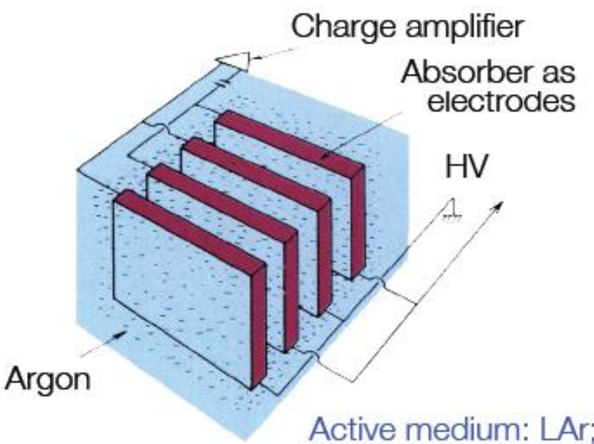

Active medium: LAr; absorber embedded in liquid serve as electrods

Ionization chambers between absorber plates

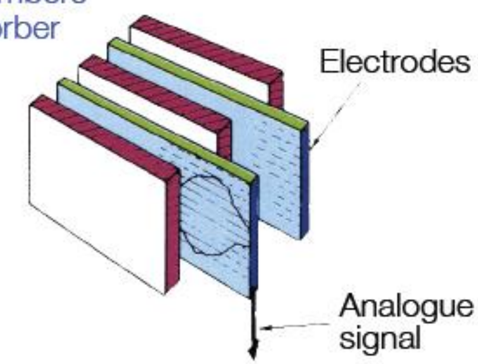

*

ATLAS Lar EM Calorimeter

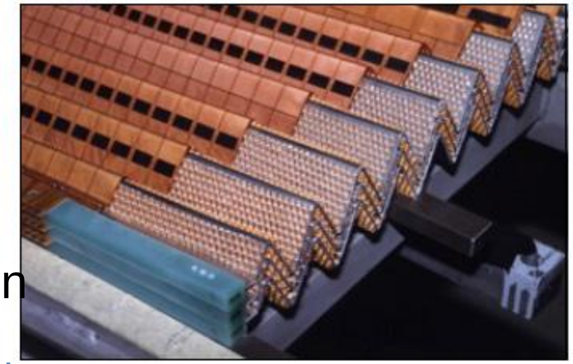

Example:
ATLAS Liquid Argon Calorimeter

Main optimisation : constant term and γ/π^0 separation

f_{samp} ~30 %

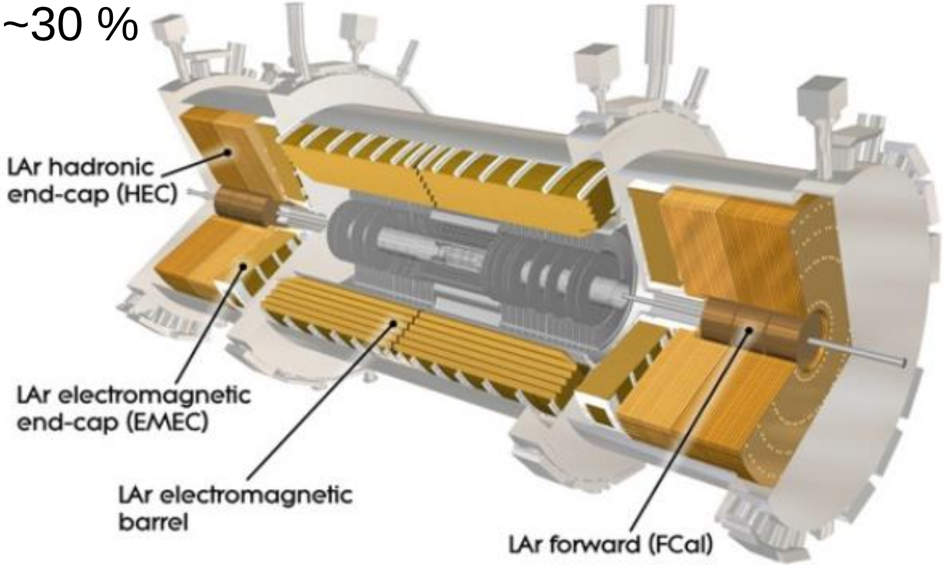

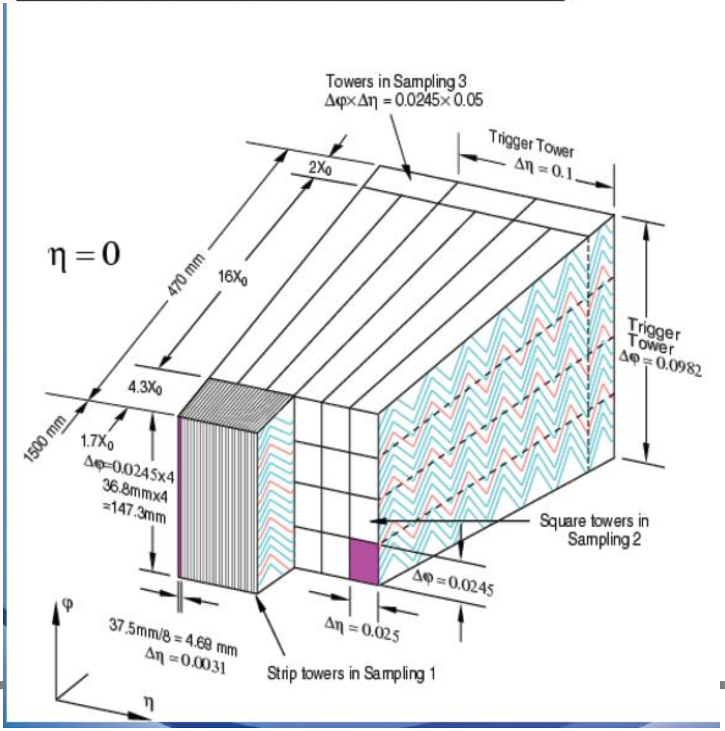

**

Trigger parenthesis

Si/W calorimeter : Calice & Pamela

Pamela calorimeter (satellite cosmic rays experiment)

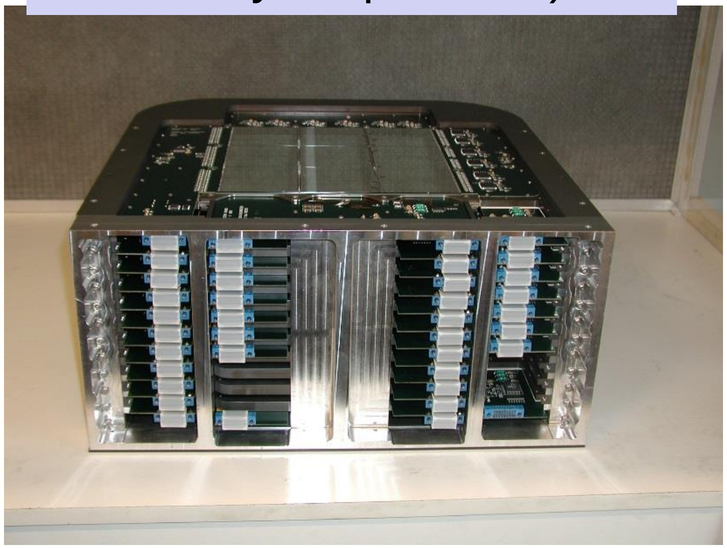

Compact calorimeter :
- 24x24cm transversal
- 16.3 X_0 depth, > 20layers

Topological reconstruction of shower
e/π separation and position measurement, poor energy resolution

Calice : prototype for ILC detectors

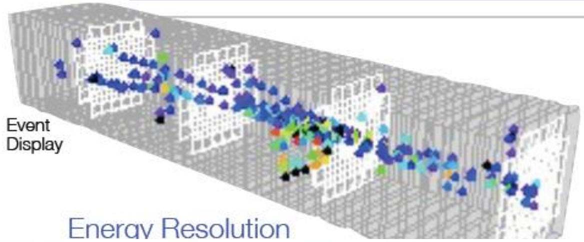

ECAL 'Physics' Prototype
[CALICE]

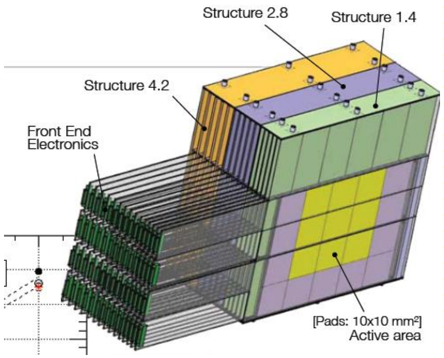

Optimized for shower separation (lateral and Longitudinal) especially for jets and Particle Flow Analysis

*

e/γ
Reconstruction

Calibration

Performance

From signal cell to cell energy (1)

Detector output

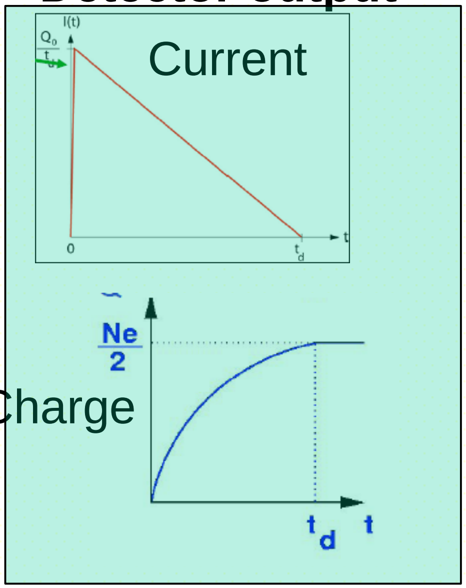

Filtering
Shaping

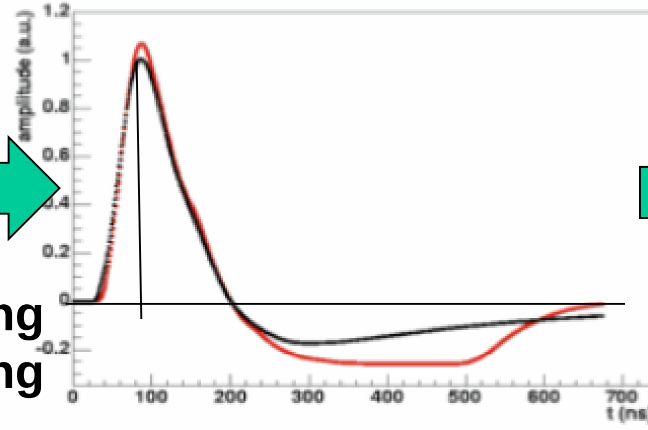

Digitisation

Amplitude digitised on
n bits : adc counts
12 bits : 0-4096
(when no signal, measure pedestal)

$$E_{cell} = F(\mu A \rightarrow MeV) \times F(adc \rightarrow \mu A) \times (adc - ped)$$

F(adc→μA) : take into account electronics chain gain.

Calibration system can be laser signal in a crystal or inject charge at detector output as similar as possible to signal (but residual bias !)

Measure or correction for linearity. To be done for all channels !

Stability measurement with time / temperature …..

**

From signal cell to cell energy (2)

Detector output

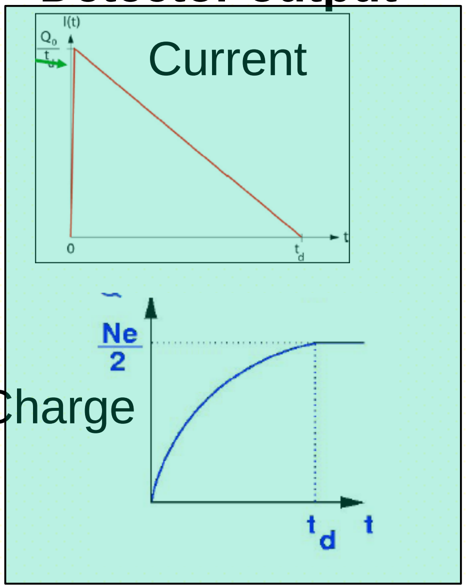

Filtering Shaping

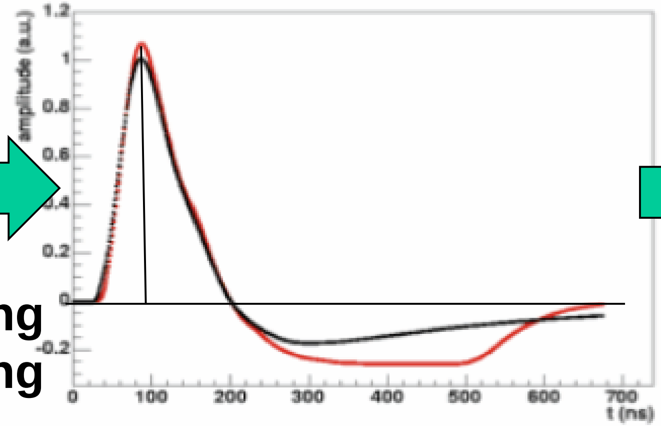

Digitisation

Amplitude Coding on n bits : adc (when no signal, Measure pedestal

$$E_{cell} = F(\mu A \rightarrow MeV) \times F(adc \rightarrow \mu A) \times (adc - ped)$$

F(μA→MeV) : Can be computed from first principles to 5-10% but not enough accurate (for sampling calorimeters includes sampling fraction)
Usually extracted from beam test with prototype by shooting and reconstructing particles of well know energy
Still not accurate ultimately……

**

μ (mip) signal in calorimeter

Muons will not produce showers in calorimeter but deposit Minimum Ionizing Particle energy (dE/dx at minimum)

→ Can be used for rough calibration / Inter calibration / time dependence

→ Difficult to extract absolute EM energy scale as e/μ for mip ≠ 1

→ Landau spectrum with high energy tail, characterized by Most Probable Value

→ Useful quantify is S/N =MPV/σ to qualify electronics readout/noise

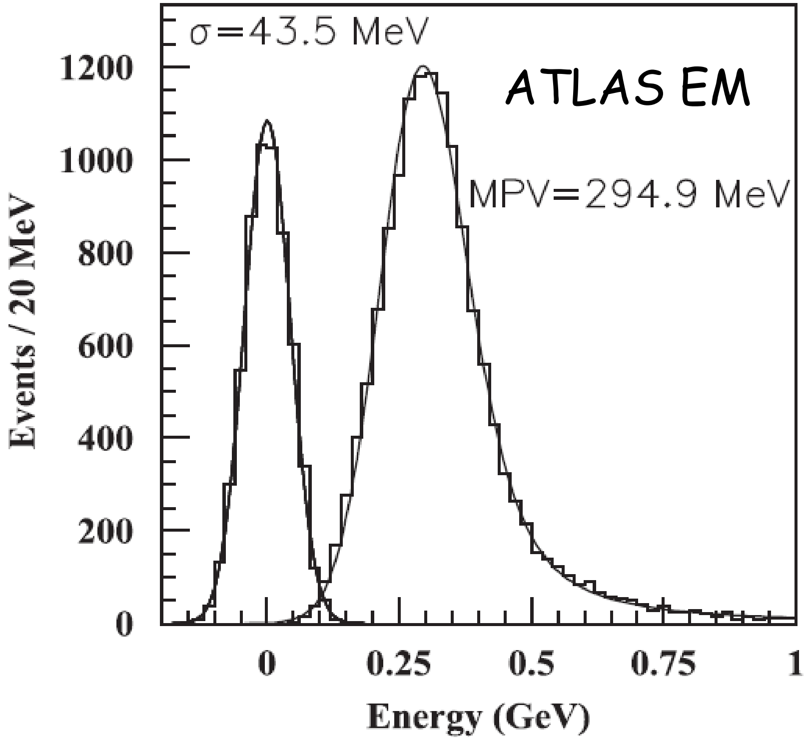

***

Shower energy reconstruction

Em shower + noise (or other particle)

Fixed cluster size :

- Large enough to contains >95 % of EM shower energy
- Small enough to minimize noise and shower separation

($\sigma_{noise}= \sqrt{N_{cells}}\,\sigma_{inco} \oplus N^2_{cells}\ \sigma_{coh}$)

Fast and easy algorithm

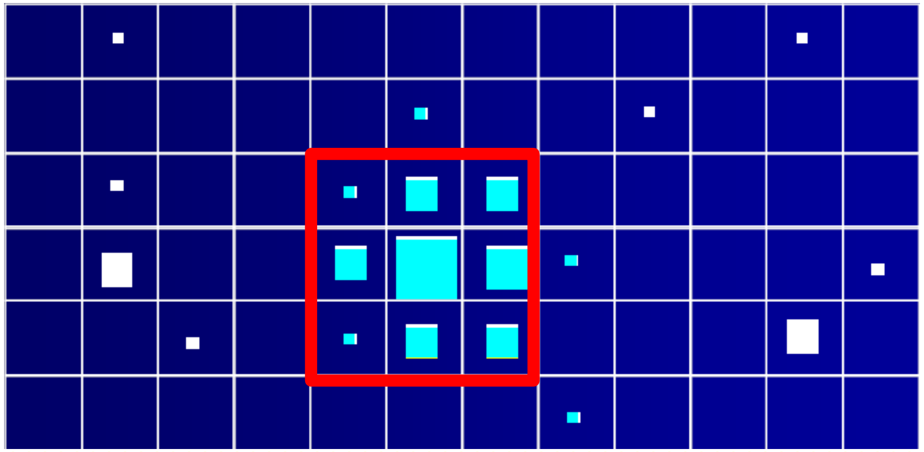

Topological algorithm :

- Consider all cells with $E > E_{cut}$ (3 σ noise)
- Start from a seed (max)
- Add neighbour cell if $E > E_{cut}$

Iterative process. Can achieve same energy resolution but more difficult for linearity (calibration) and noise contribution (different from one shower to another)

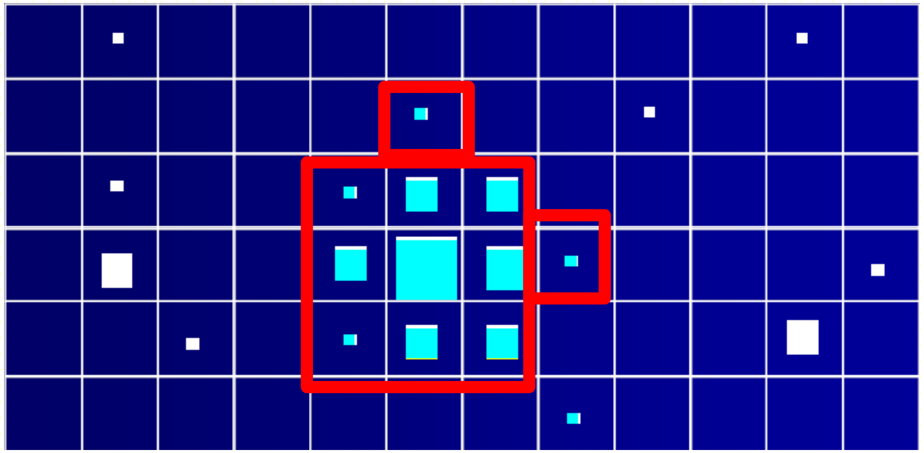

**

From cluster to particle energy

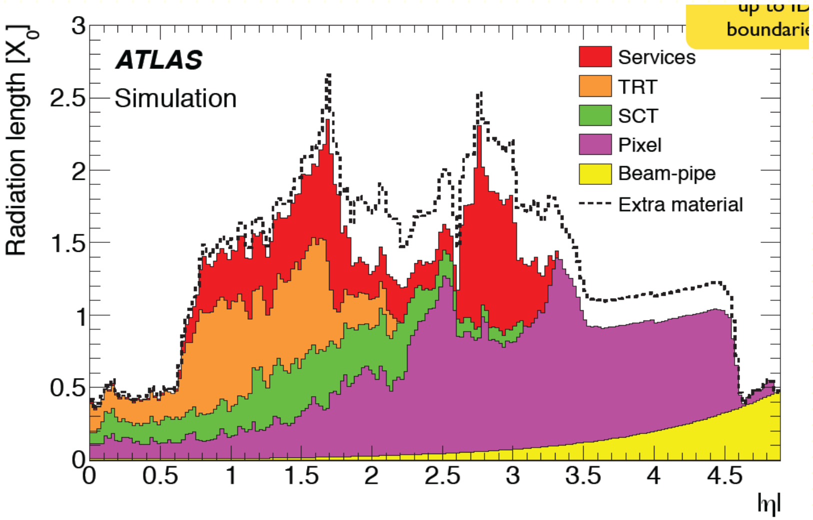

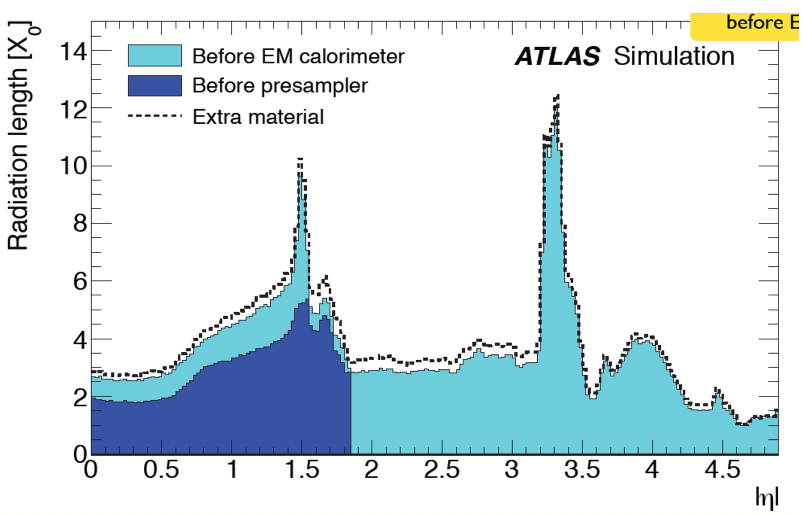

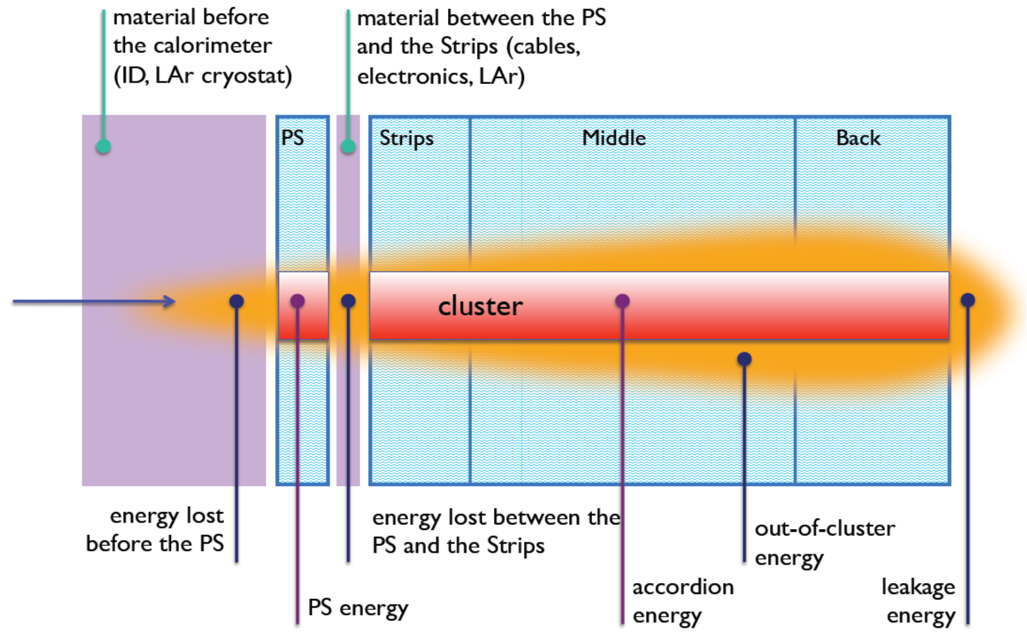

Energy lost upstream, laterally and longitudinally for any calorimeter
+presampler for ATLAS

**

In situ particle energy calibration

- Can use E(cal)/p(tracker) if material upstream uniform and not large

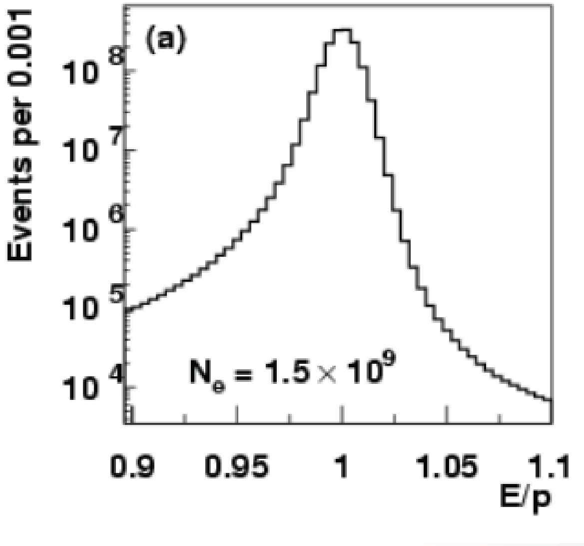

Example of KTeV CsI calorimeter :

use electrons from $K_L \rightarrow \pi e \nu$

Set absolute energy scale

Crystal to crystal calibration

Time dependence of signals

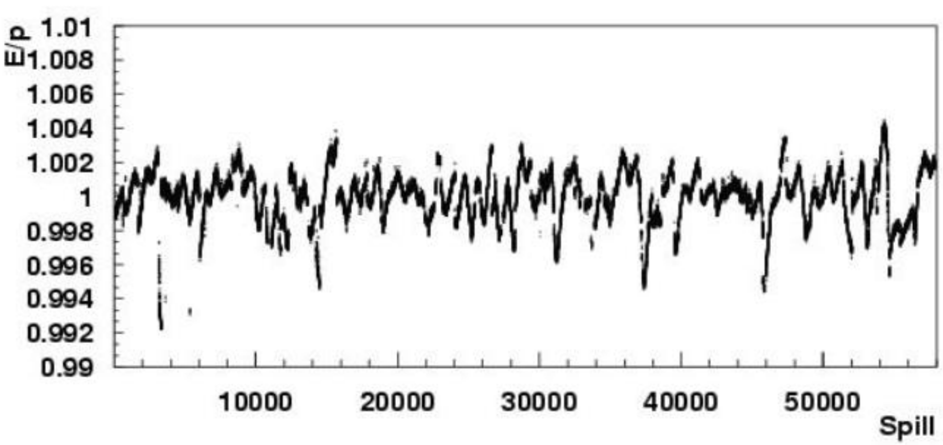

Quite difficult at LHC with material variation along $\eta \rightarrow$ E/p distribution with too many tails

**

In situ particle energy calibration (3)

- Use mass constraint on well known particle : Z→ e+e- @ LHC

$$m = \sqrt{2E_1E_2\left(1-\cos(\theta_{12})\right)}$$

$$E^{\mathrm{corr}} = E\left(1+\alpha_i\right)$$

$$m_{ij}^{\mathrm{corr}} \simeq m_{ij}\left(1+\frac{\alpha_i+\alpha_j}{2}\right)$$

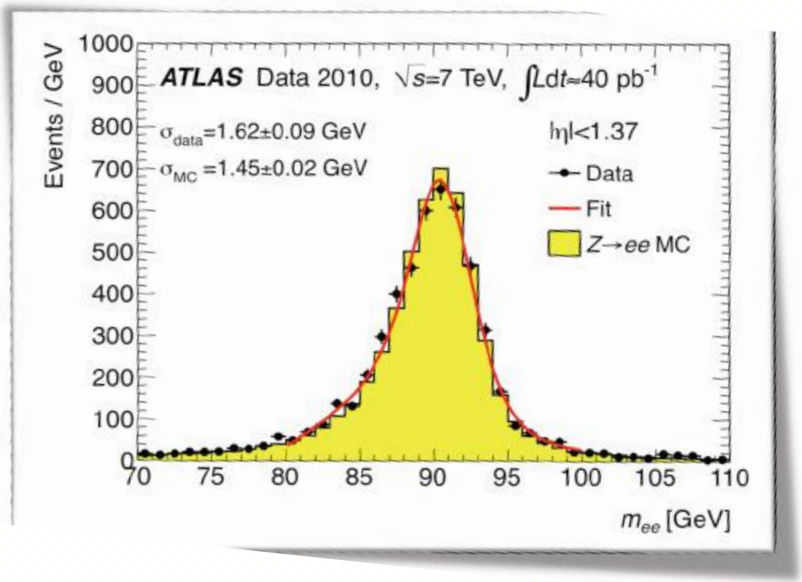

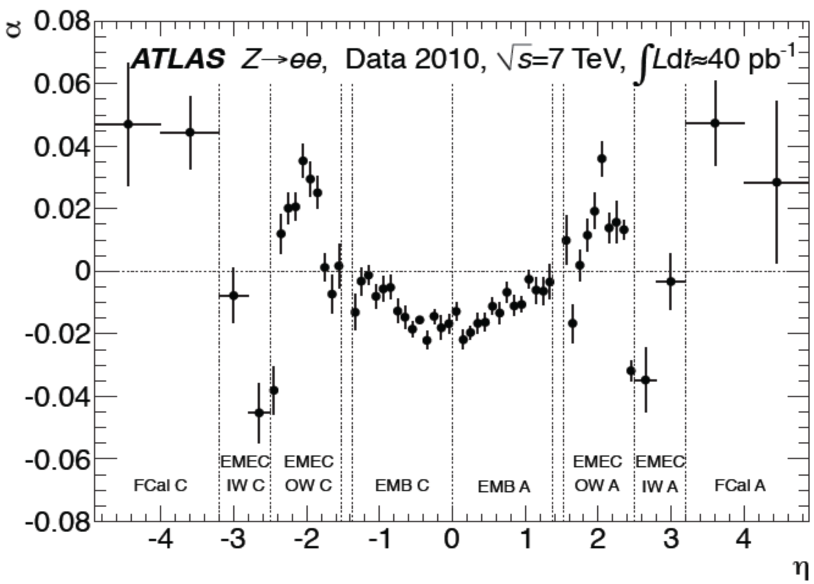

With more stat :

- Reduce region for each α + along φ
- Can use J/psi→e+e- for low energy (linearity)
- Needs to extrapolate γ from simulation or Z→eeγ/$\mu\mu\gamma$

**

e+e- resonances

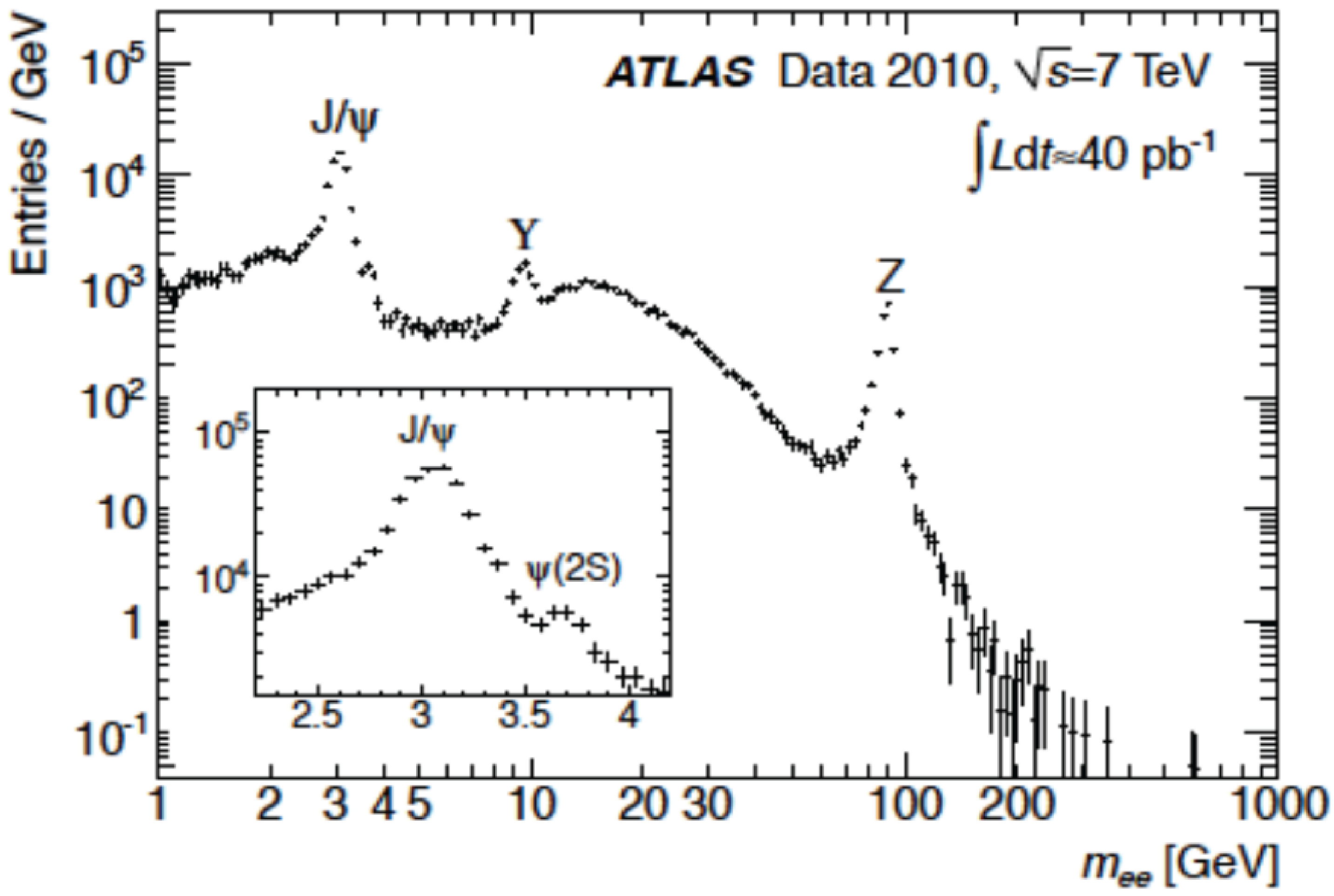

*

Photon pointing in ATLAS

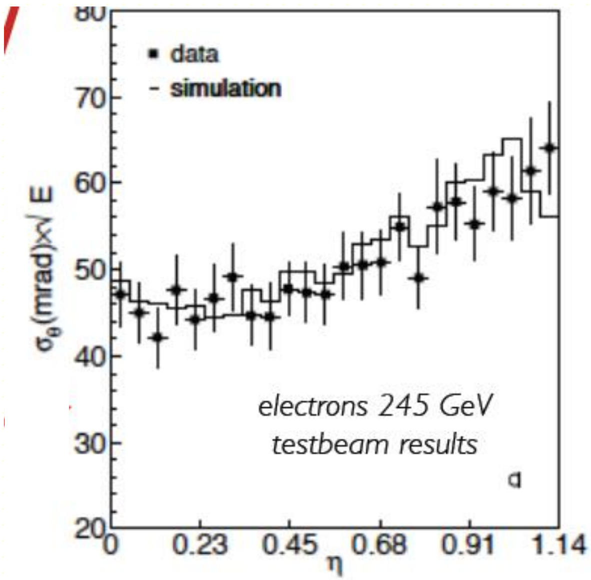

Barycentre in strips
and middle section
→ Angular measurement

$$\sigma_\theta = 60 \text{ mrad}/\sqrt{E}\,[\text{GeV}]$$

Z vertex position measurement

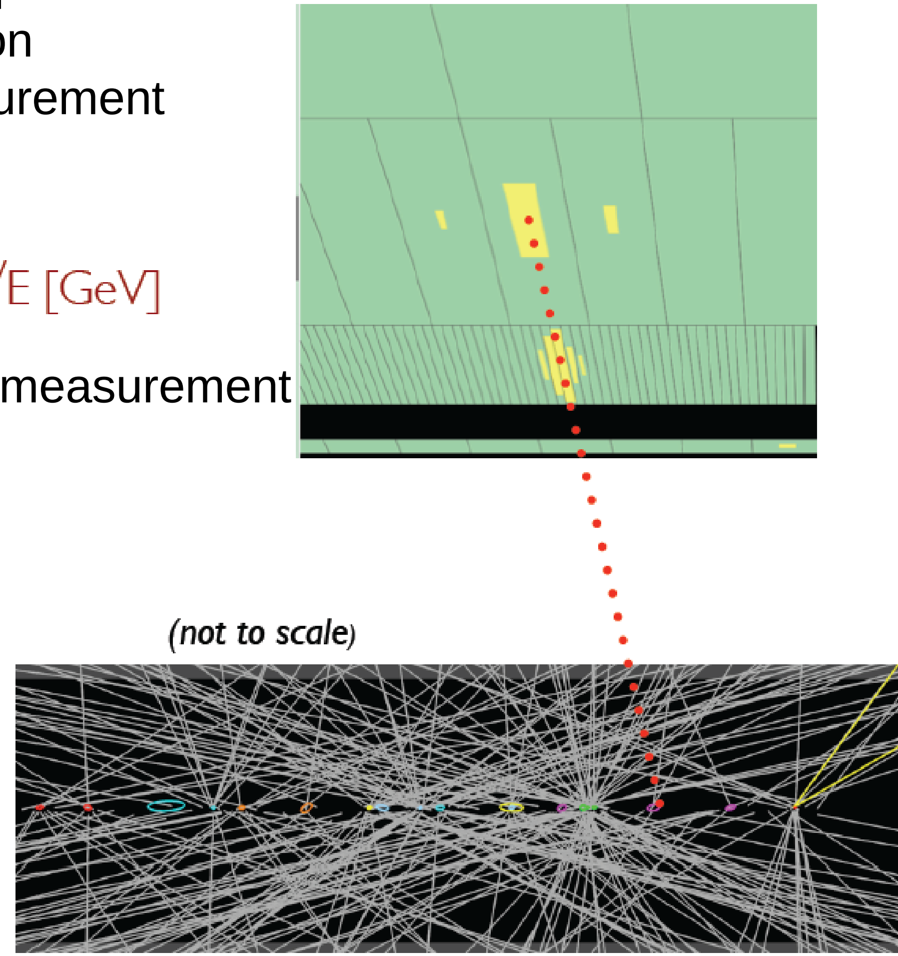

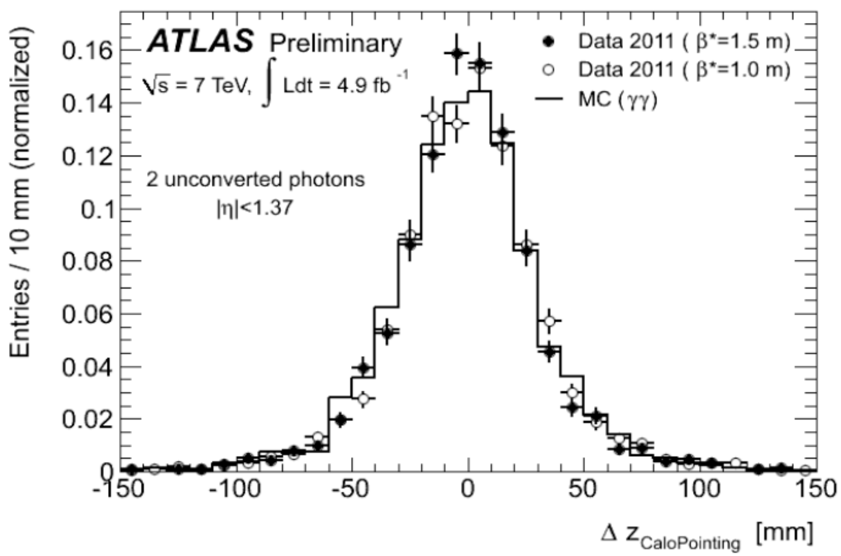

Zoom on collision interaction

*

Timing resolution

Shower (electron/photon) time measurement can also be achieved, can be useful to reject out of time events (accidentals) with respect to collision

KLOE calorimeter

Fine sampling lead/scintillating fibers calorimeter

- Volume Ratio Fiber:Lead 50:50
- Energy sampling fraction 13 %
- X_0 = 1.6 cm ρ=5.3 g/cm^3

Triangular shape: high sampling frequency & flat response in θ

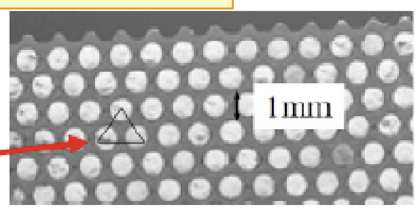

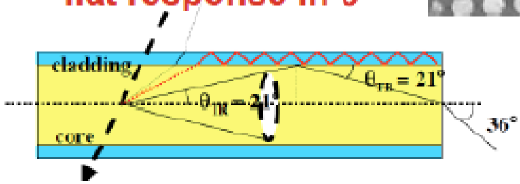

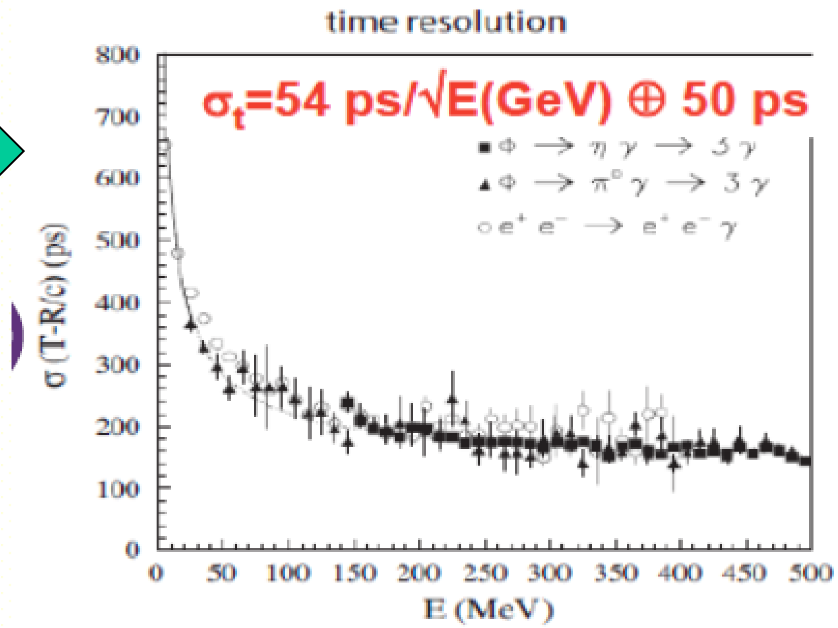

Time measurement in calorimeter, promising way to mitigate ”in time” pile-up at LHC

*

neutrons

Table 12-1. Average number of collisions required to reduce a neutron's energy from 2 MeV to 0.025 eV by elastic scattering

Element	Atomic Weight	Number of Collisions
Hydrogen	1	27
Deuterium	2	31
Helium	4	48
Beryllium	9	92
Carbon	12	119
Uranium	238	2175

Neutron Cross Sections

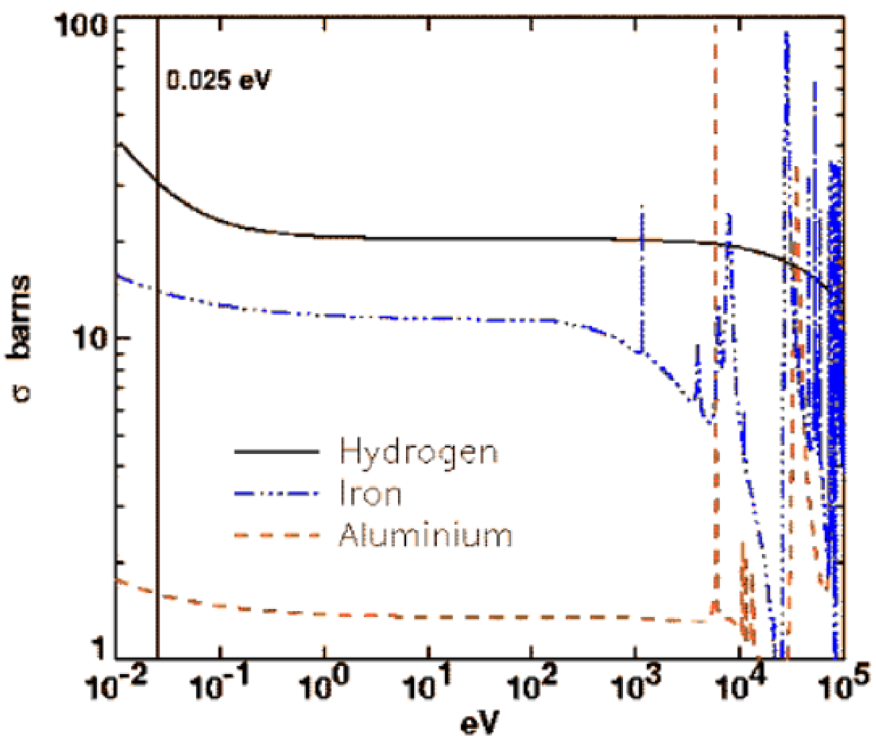

Capture may be increased at some energy due to resonnance effect in the total cross section…

T (K)	E_o (eV)	v_o (m s^{-1})	$\bar{E}_{th}$ (eV)
300	0,0253	2200	0,038
400	0,034	2600	0,051
600	0,052	3100	0,075
800	0,069	3600	0,103
1000	0,086	4000	0,129

Cross section on Th-232

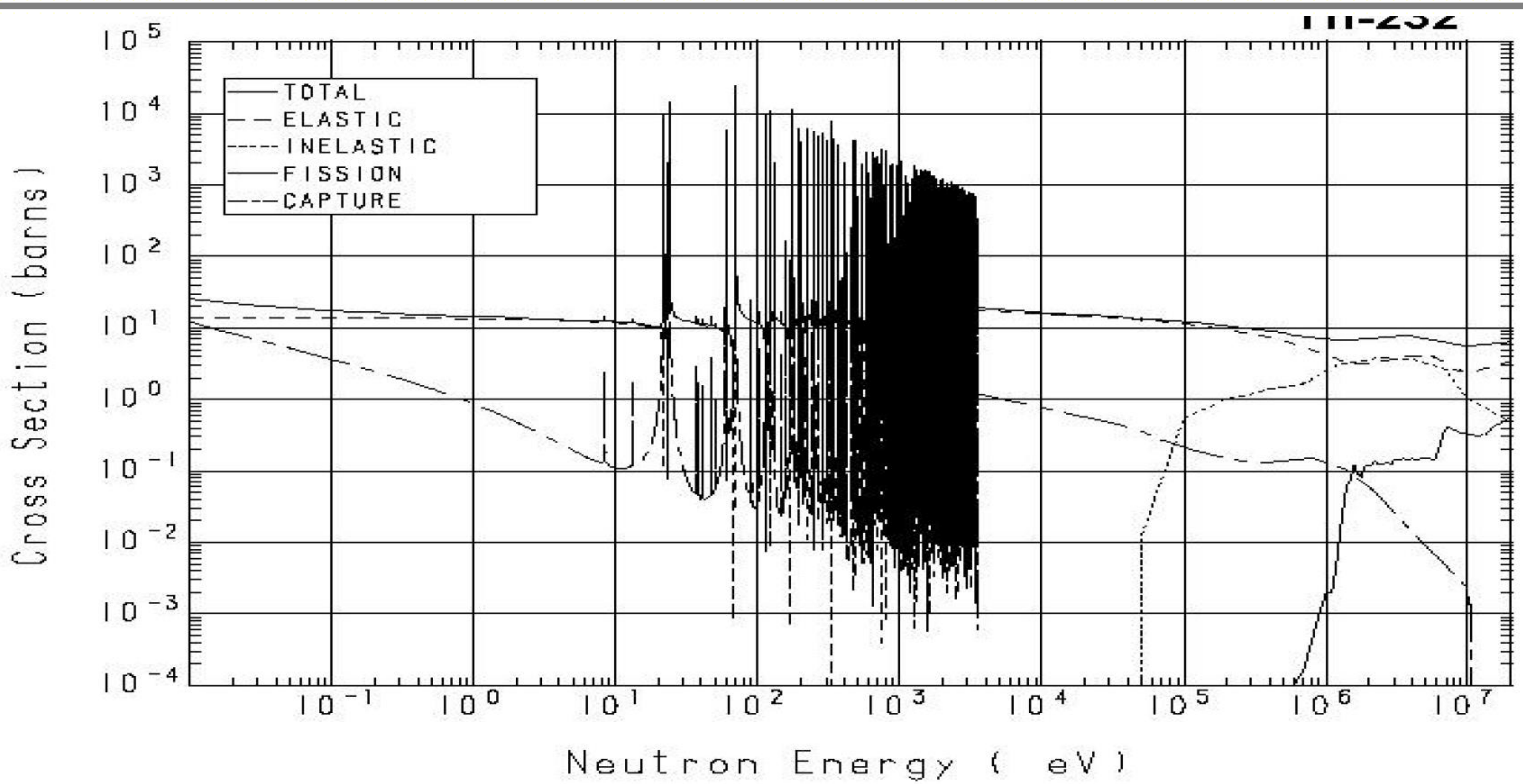

Consequences on LHC experiment hall

Background in Atlas cavern

<u>Background comes from residues of p-p interactions</u>
<u>(through spallation process) :</u>

- Huge production of *neutrons*, thus creating γ, thus creating *e,* etc…
- Also at higher energy, *n* and γ create ionizing particle (mainly: p, e+, e-)
- Direct background: μ and punchthrough (smaller)

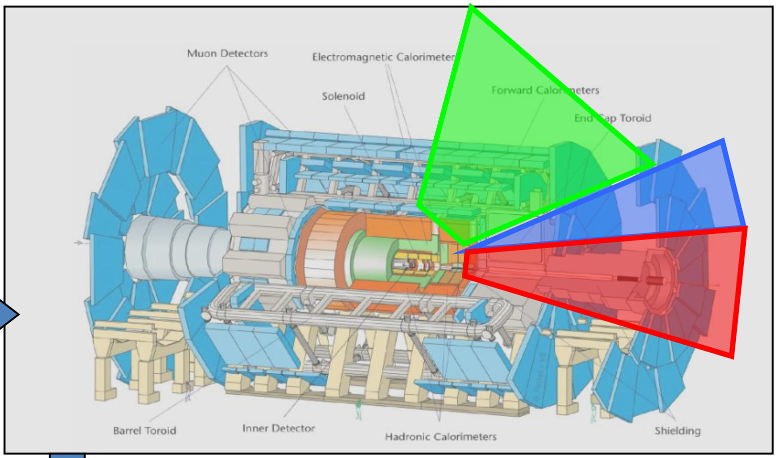

Neutron “gas” in the cavern
(-> therm. of neutrons)

E_{cin}=10 MeV : v_n ~ 15% c (23 ns pour 1m)
10 keV : ~ 5.10^{-3} c (0.7 μs pour 1m), out of time

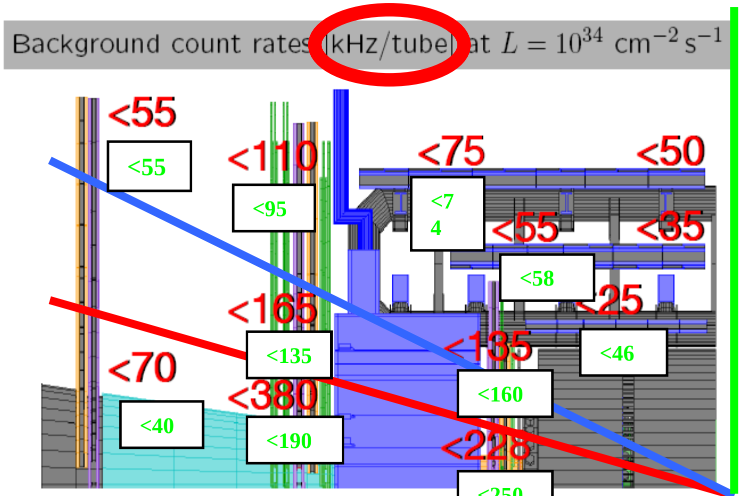

(Numbers include a safety factor of 5.)

- pp x section for part. prod. (~1.2)
- …d. propagation in calo. and shielding (~2.9)
- …ficiency in chambers (~1.4)

10 kHz/cm²

ε_n^{hit} ~10^{-4} à 10^{-3}

ε_γ^{hit} ~$4\text{-}8.10^{-3}$

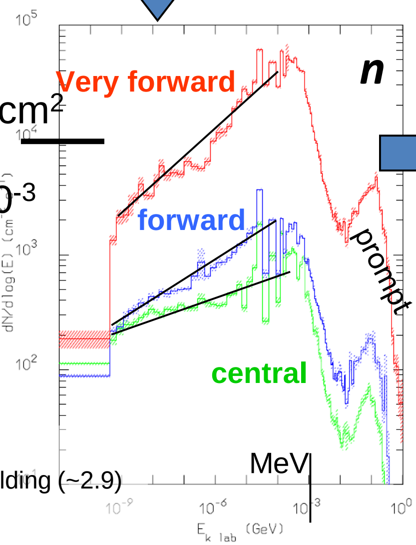

Figure 5-67 The expected <u>neutron flux</u> as a function of neutron energy in different rapidity regions of the muon spectrometer (top curve: $2.3 < \eta < 2.7$, middle curve: $1.4 < \eta < 2.3$ and bottom curve: $\eta < 1.4$).

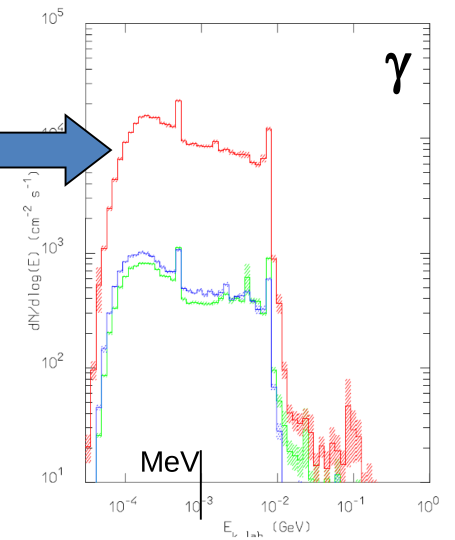

Figure 5-66 The expected <u>photon flux</u> as a function of photon energy in different rapidity regions of the muon spectrometer (top curve: $2.3 < \eta < 2.7$, middle curve: $1.4 < \eta < 2.3$ and bottom curve: $\eta < 1.4$).

Atlas needs to measure ca…n bac…round …sing muon spectrometer) in order to re…uce un…rtaintie… on background for s-LHC.

Background in Atlas cavern

<u>Background comes from residues of p-p interactions</u>
<u>(through spallation process) :</u>

- Huge production of *neutrons*, thus creating γ, thus creating *e*, etc…
- Also at higher energy, *n* and γ create ionizing particle (mainly: p, e+, e-)
- Direct background: μ and punchthrough (smaller)

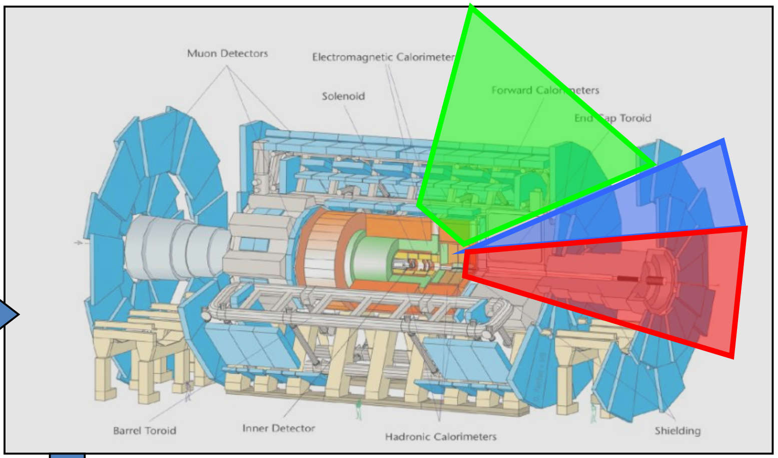

Neutron “gas” in the cavern
(-> therm. of neutrons)

E_{cin}=10 MeV : v_n ~ 15% c (23 ns pour 1m)
10 keV : ~ 5.10^{-3} c (0.7 μs pour 1m), out of time

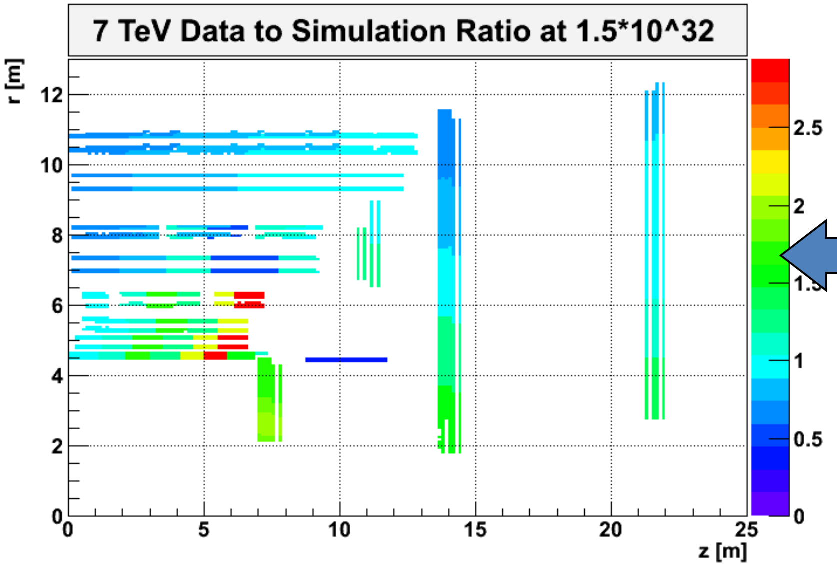

10 kHz/cm^2

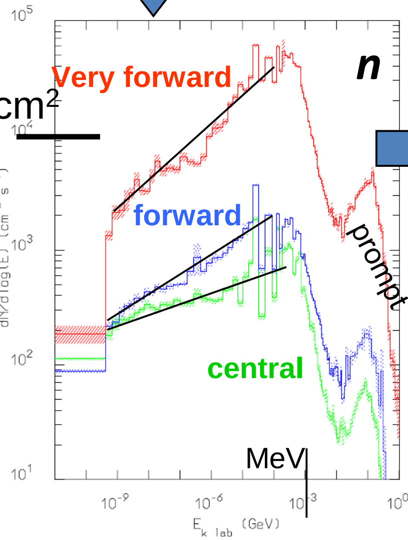

Figure 5-67 The expected <u>neutron flux</u> as a function of neutron energy in different rapidity regions of the muon spectrometer (top curve: 2.3 < η < 2.7, middle curve: 1.4 < η < 2.3 and bottom curve: η < 1.4).

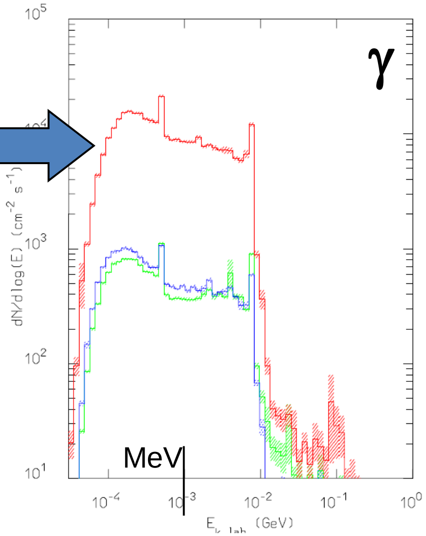

Figure 5-66 The expected <u>photon flux</u> as a function of photon energy in different rapidity regions of the muon spectrometer (top curve: 2.3 < η < 2.7, middle curve: 1.4 < η < 2.3 and bottom curve: η < 1.4).

(dernière simulation : facteur de sécurité ~ x2)

Magnets

Charge track momentum measurement in a magnetic field

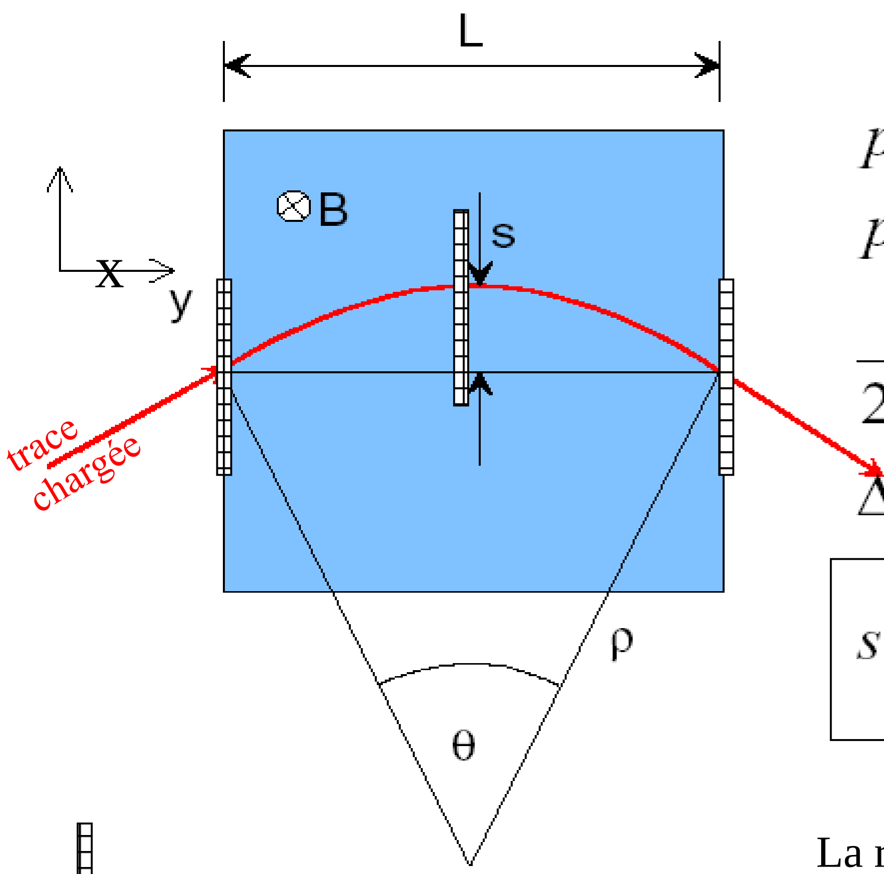

$$p_T = qB\rho$$

$$p_T\ (\mathrm{GeV/c}) = 0.3B\rho \quad (\mathrm{T\cdot m})$$

$$\frac{L}{2\rho} = \sin\theta/2 \approx \theta/2 \quad \rightarrow \quad \theta \approx \frac{0.3L\cdot B}{p_T}$$

$$\Delta p_T = p_T \sin\theta \approx 0.3L\cdot B$$

$$s = \rho(1-\cos\theta/2) \approx \rho\frac{\theta^2}{8} \approx \frac{0.3}{8}\frac{L^2 B}{p_T}$$

= détecteur de traces
(ex. : TPC, ch. à dérives)

La résolution est dégradée par :

diffusion multiple (matière au milieu)

ET désalignement

Examples of magnetic field configuration

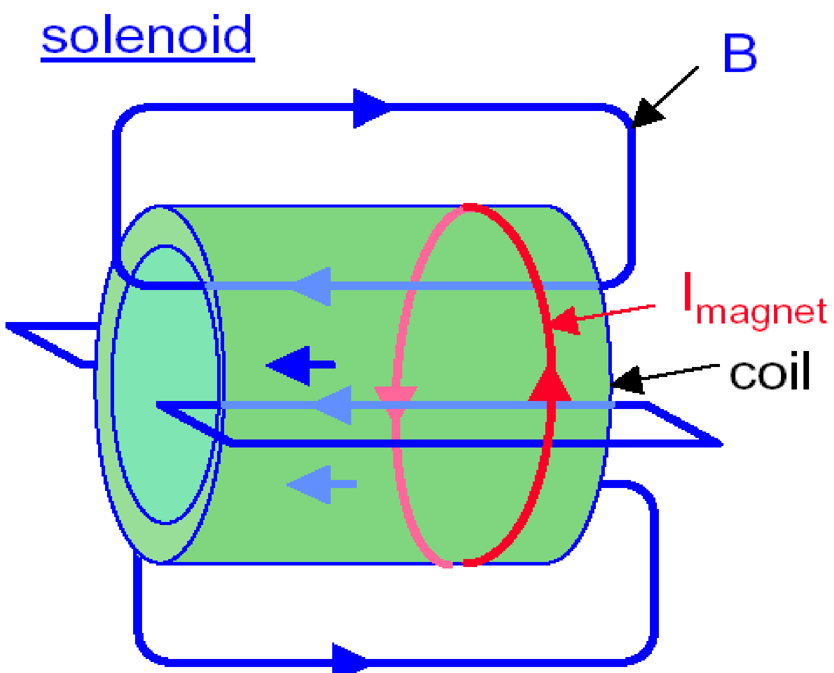

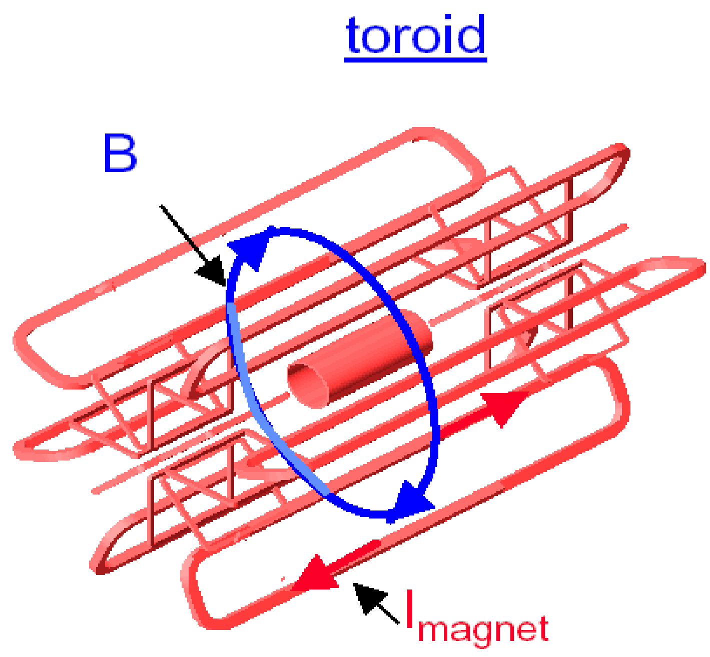

+ Vertex information usefull
+ Large homogenous field inside coil
- weak opposite field in return yoke
- Size limited (cost)
- rel. high material budget

+ independant muon system (redondancy)
+ Rel. large fields over large volume
+ Rel. low material budget
- non-uniform field
- complex structure
- Vertex non-usable

Superconducting devices in LHC

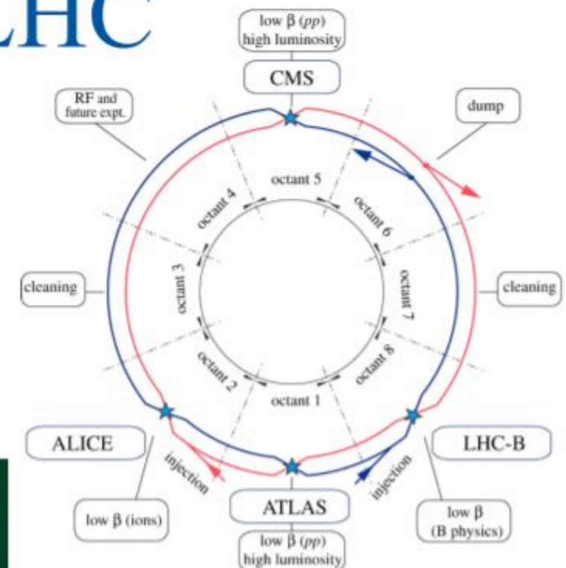

Magnets

- **LHC ring magnets (Nb-Ti): Rutherford cables**
  - **1232** main dipoles: **8.3 T** x **15 m**
  - **392** Main quadrupoles **223 T/m (7 T)** x **4 m**
  - **7600 other SC magnets (cable or wire)**

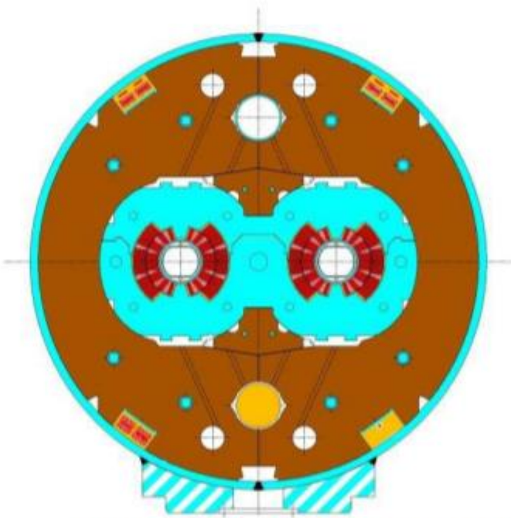

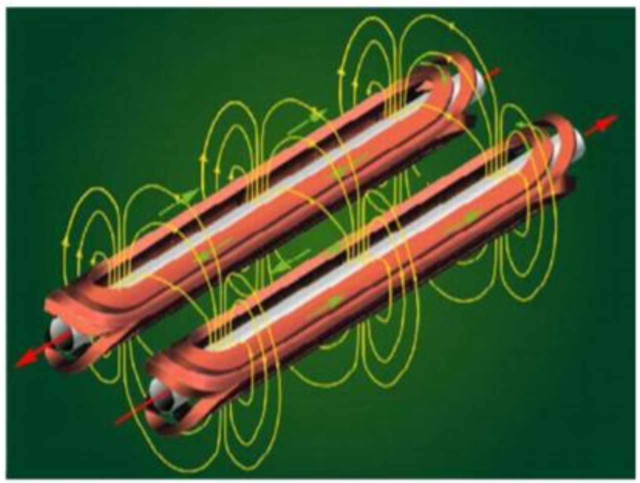

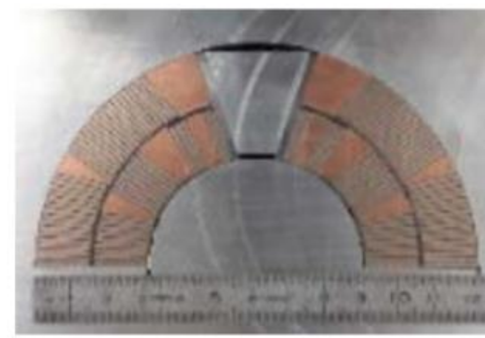

- **RF cavities (N_b coating)**

➢ **Rutherford Nb-Ti cable: a key technology for LHC**

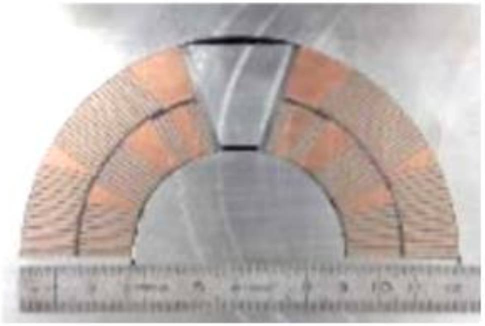

o

	Tevatron	HERA	RHIC	LHC
Dipole field	4.4 T	5.3 T	3.5 T	8.3 T
Number of strands	23	24	30	28-36
Cable current	4 kA	5.5 kA	5 kA	11.8 kA

cables

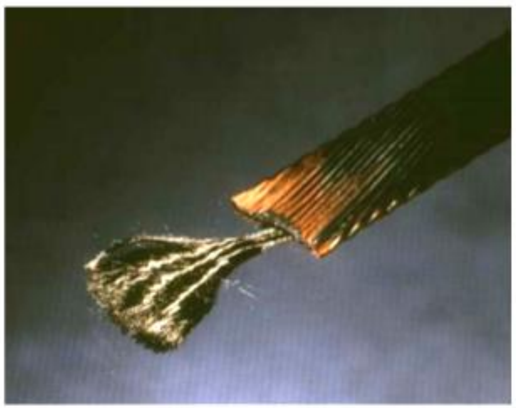

ess)

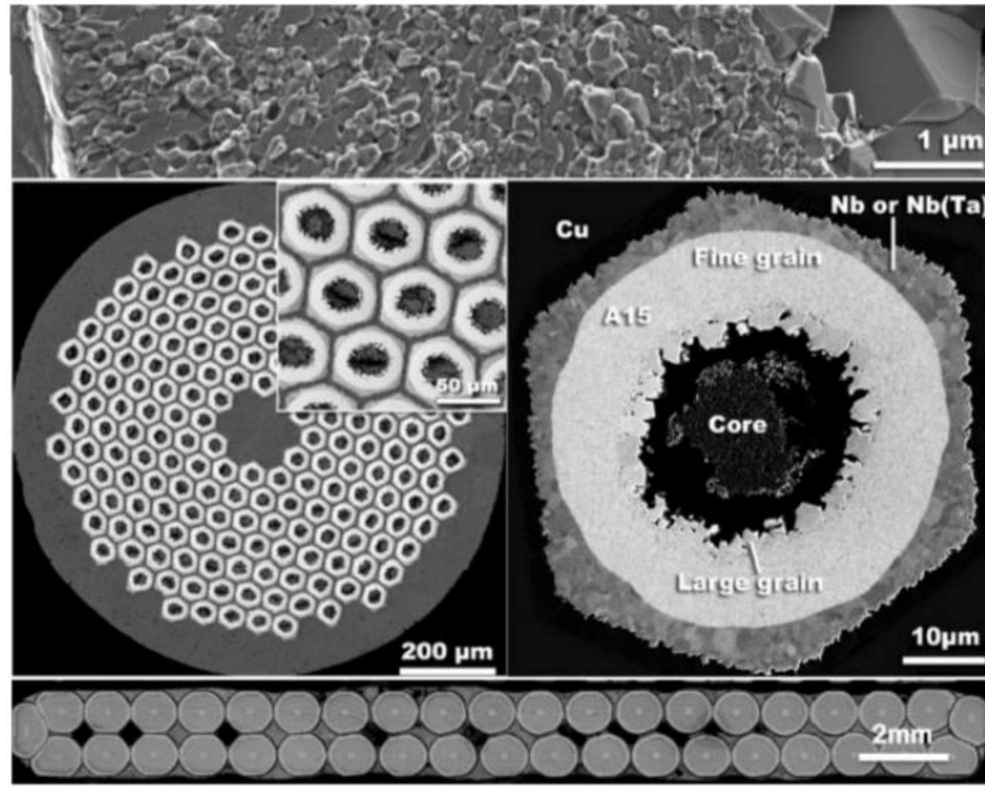

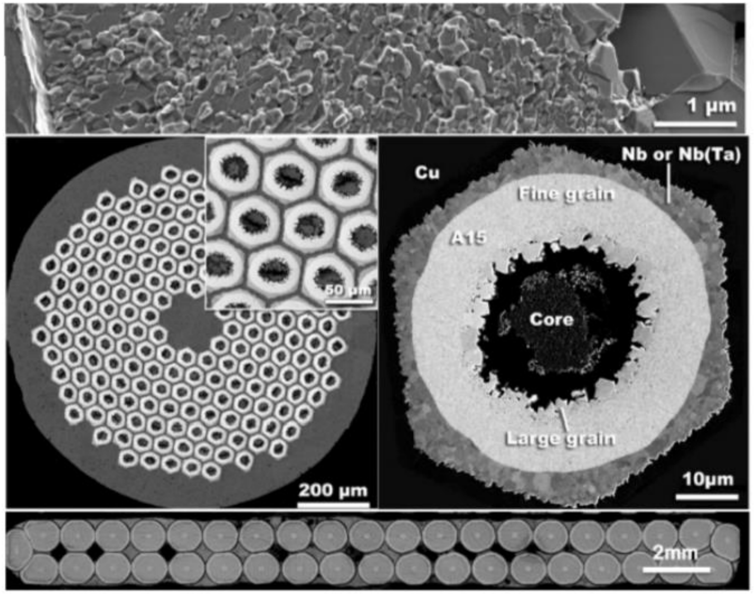

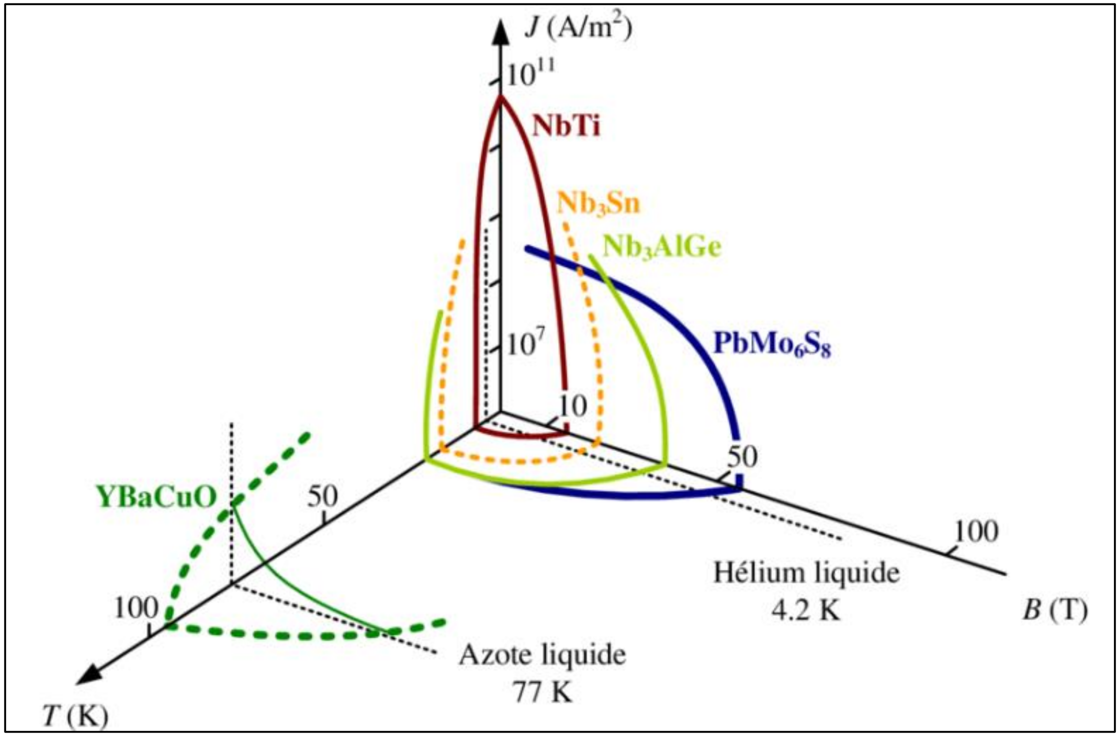

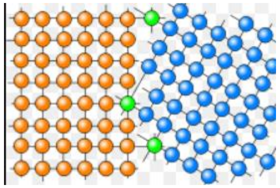

Critical current limited by density of cable defects
(grain boundery / *joint de grain*)

Magnetic fields : supraconducting magnets of ATLAS

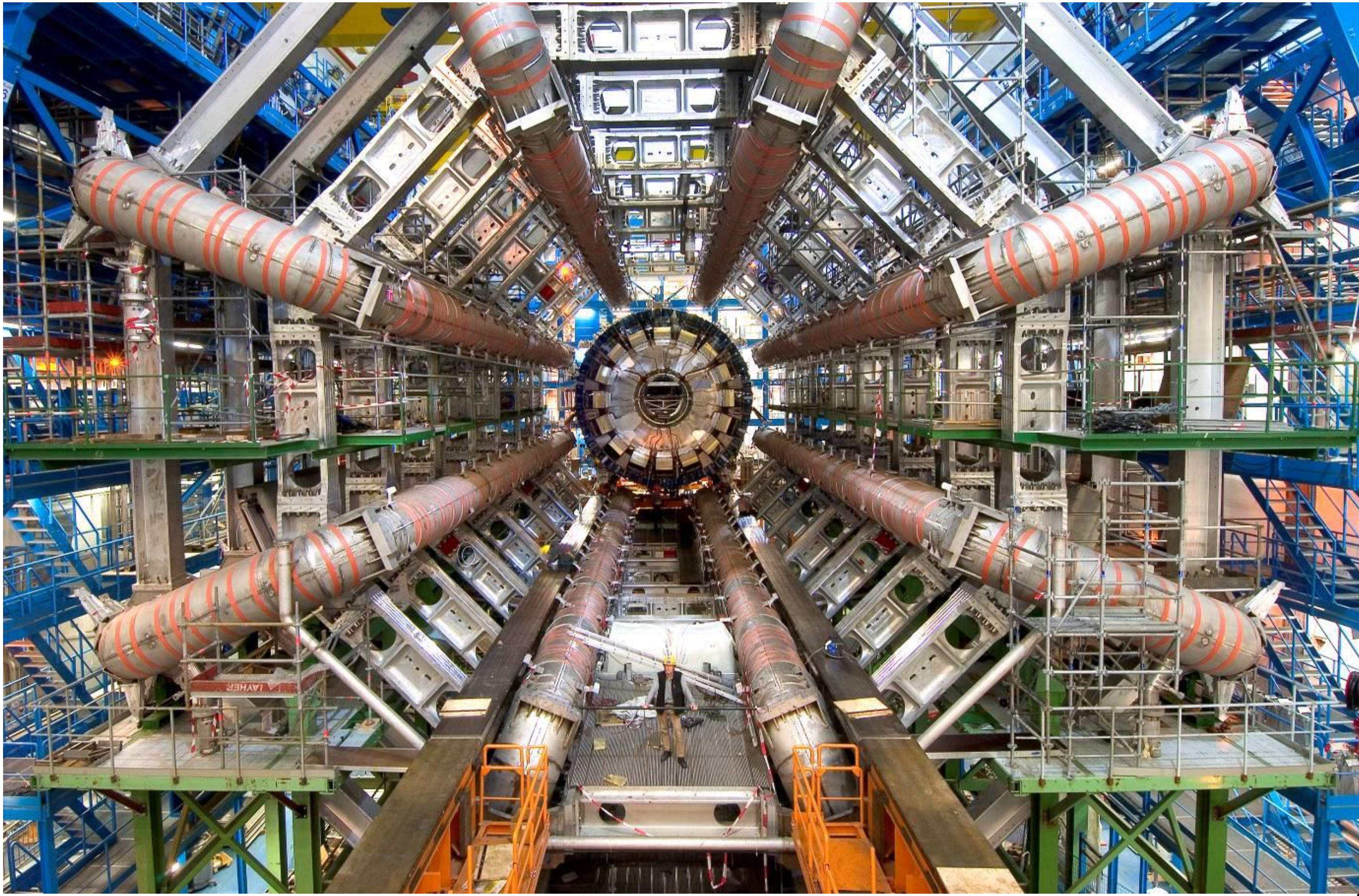

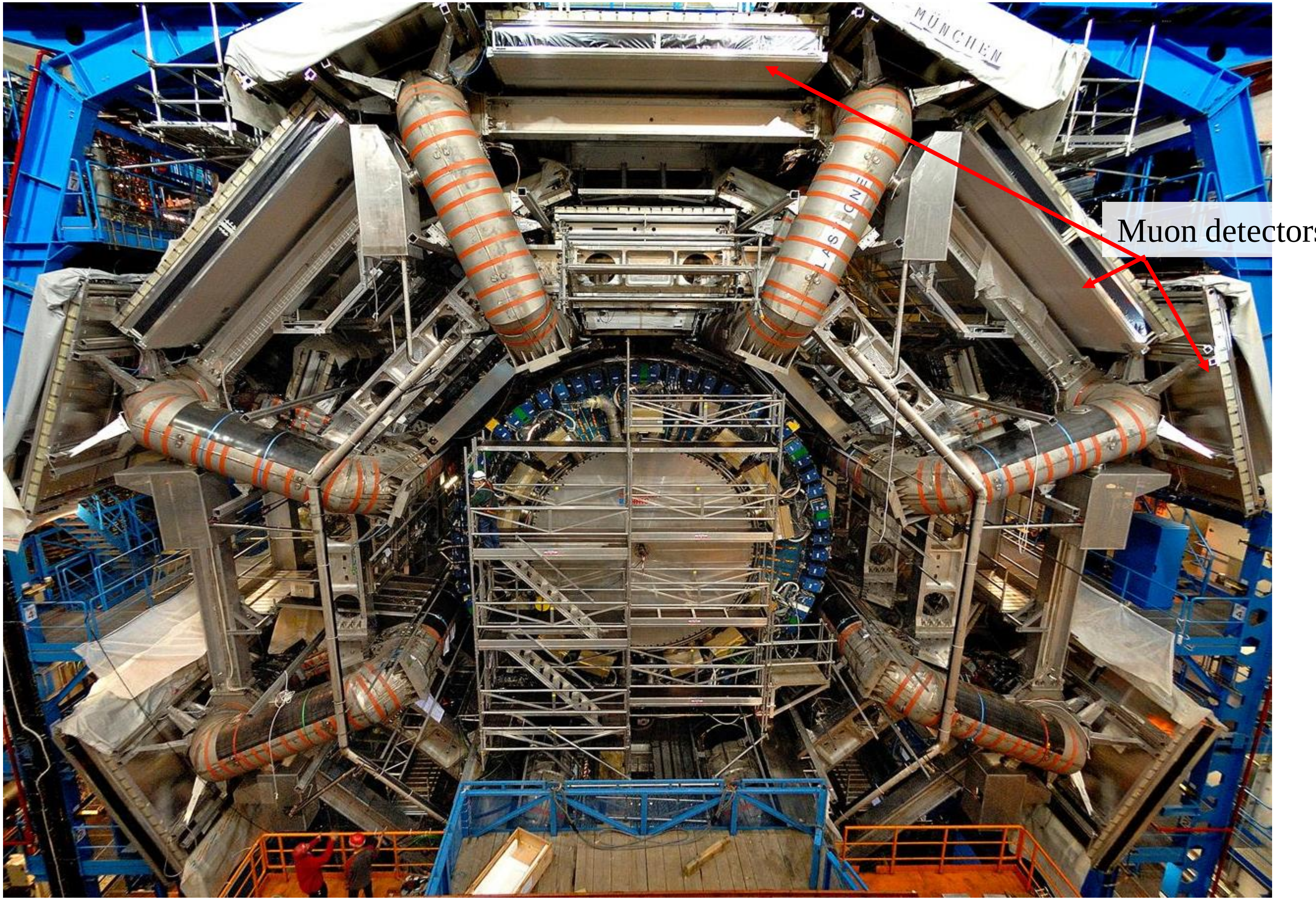
MÜNCHEN
Muon detectors

Champs magnétiques possibles :
aimant solénoïdale de CMS

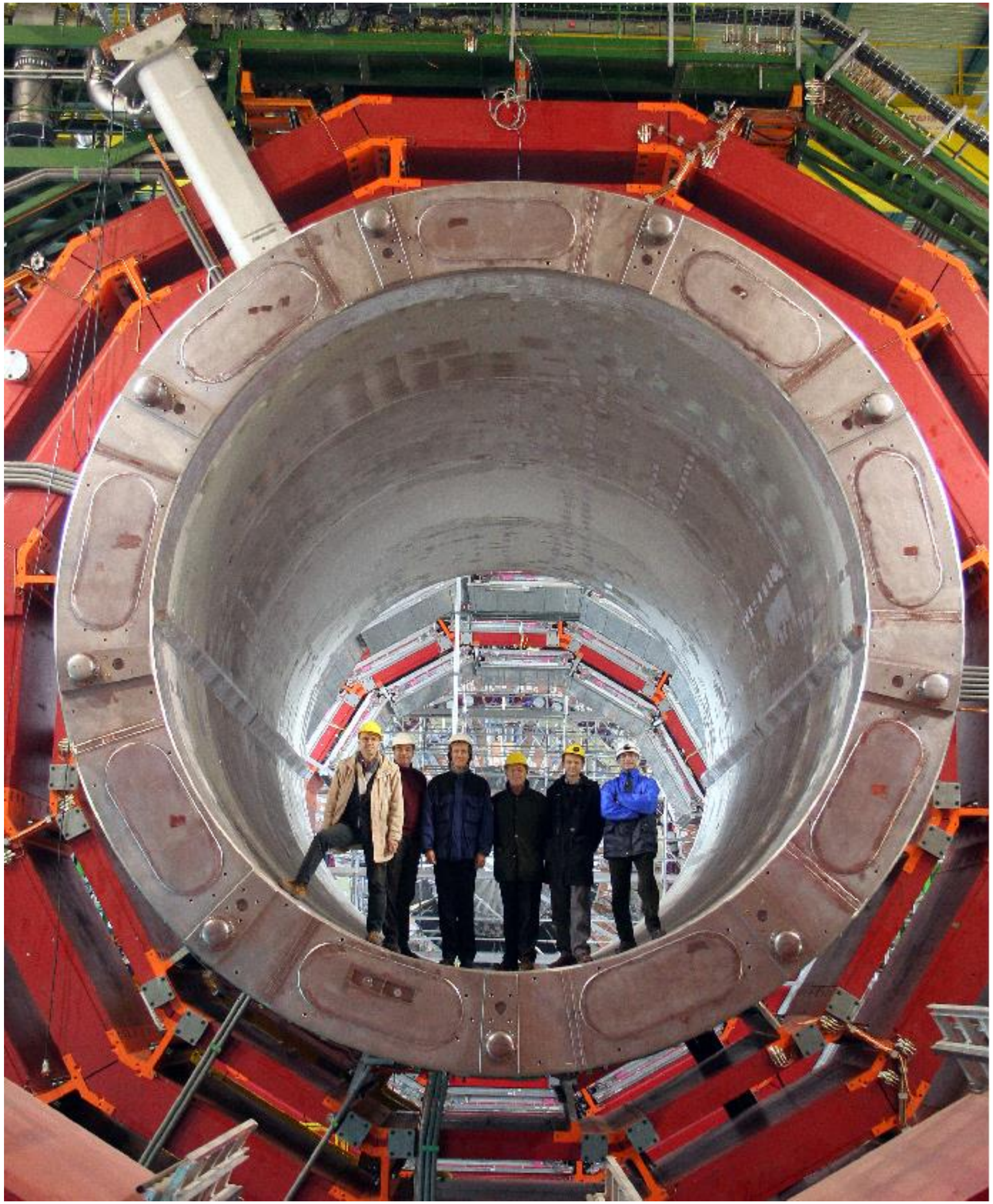

Muon detectors

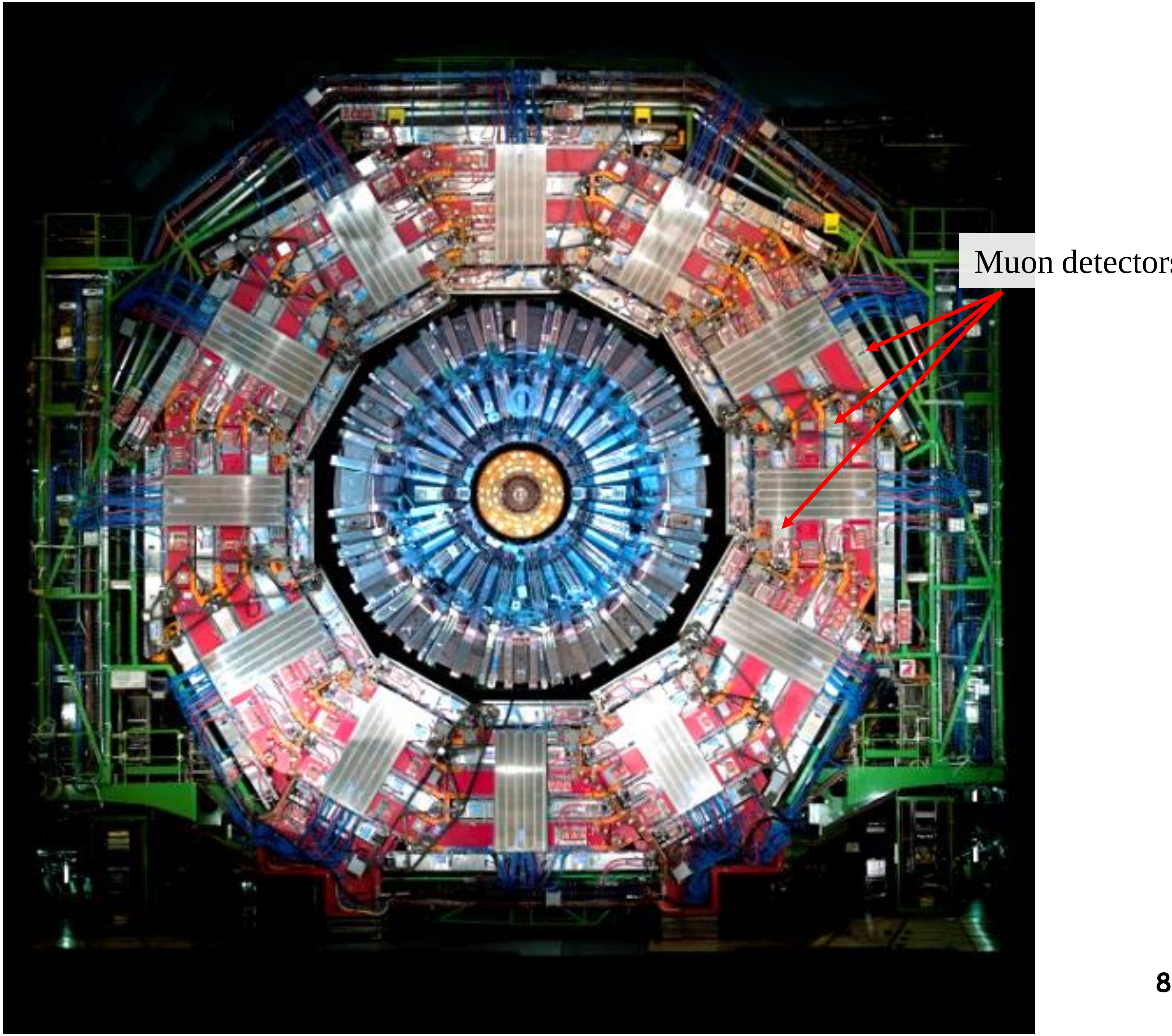
Muon detectors

backup

Example of calorimeters

Collider calorimeters : Geometry is usually more complex, need to cover almost 4π solid angle (Missing energy) but also to extract signals. Usually central part with cylindrical geometry (barrel) and small angle part at each end (endcap/forward)

SPS experiments UA1 and UA2

UA2 calorimeter

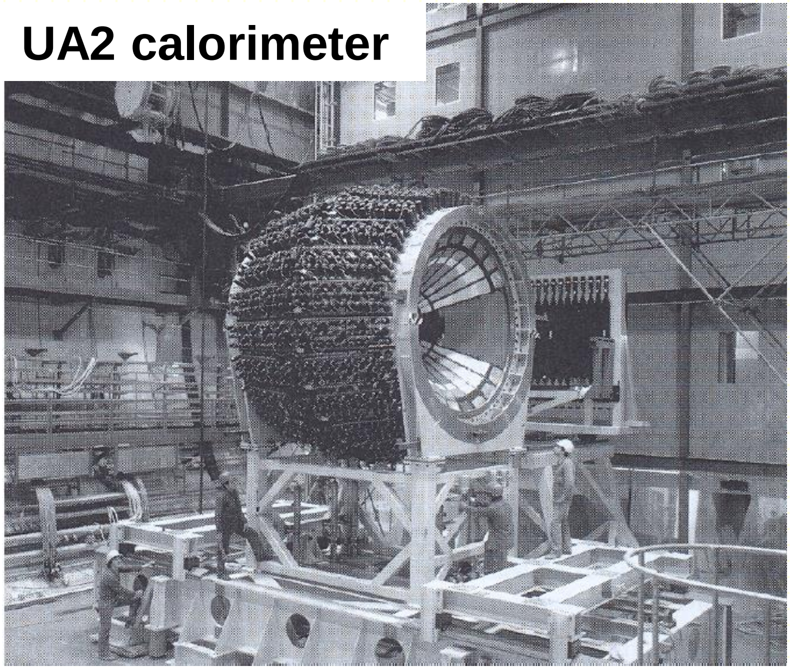

Calorimeter had a crucial role in W/Z discoveries :next slides

LEP experiments :

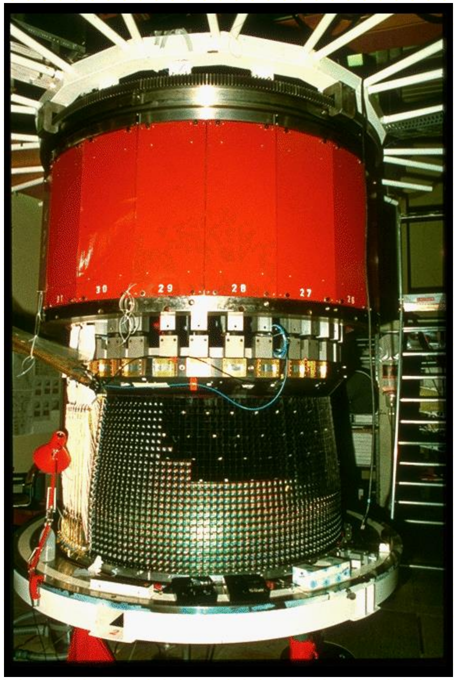

L3 had a EM calo with excellent energy resolution (γ) :
11 000 BGO crystals

But no real impact on main physics topics at LEP

Other experiments (ALEPH, DELPHI and OPALE) put more emphasis on TPC, and Calorimeter granularity

*

Electromagnetic shower

e^+ / e^-

- Ionisation

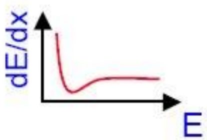

- Bremsstrahlung

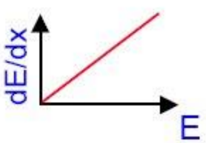

γ

- Photoelectric effect

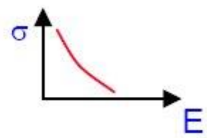

- Compton effect

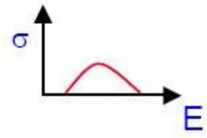

- Pair production

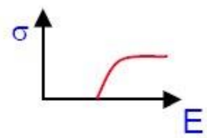

20 GeV e^-

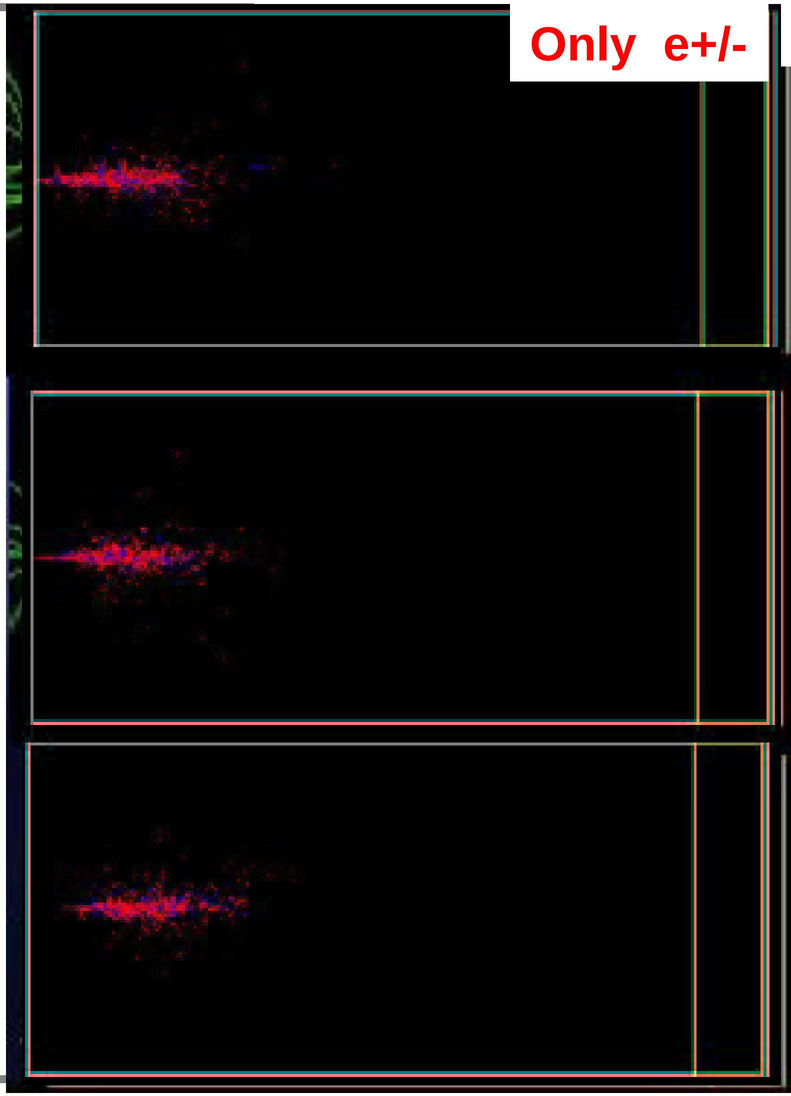

***

Impact of leakage

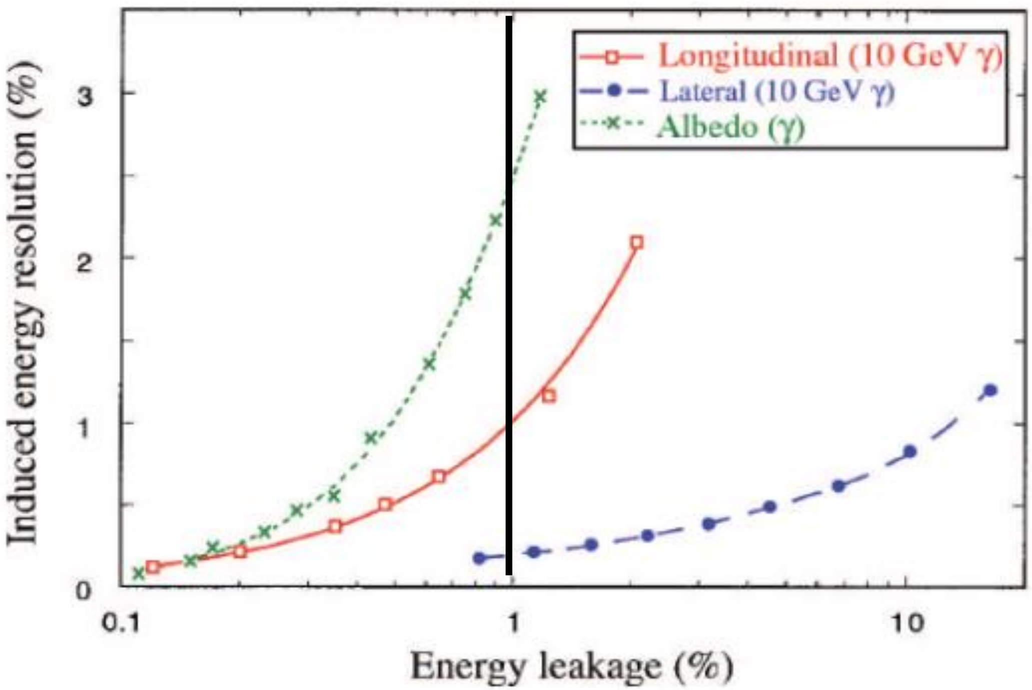

Leakage fluctuation usually not poissonian → induces low energy tails
Longitudinal leakage worsens more the resolution than lateral leakage at fixed value.
Albedo (back scattering photon) usually dominated by dead material energy loss
in front of calorimeter

***

Sampling calorimeter with gas

Gas low density medium
Usually poor energy resolution:
- Small sampling fraction (so need larger gap)
+ Track length fluctuation : low electron can travel much in gap
Resolution increases with √s

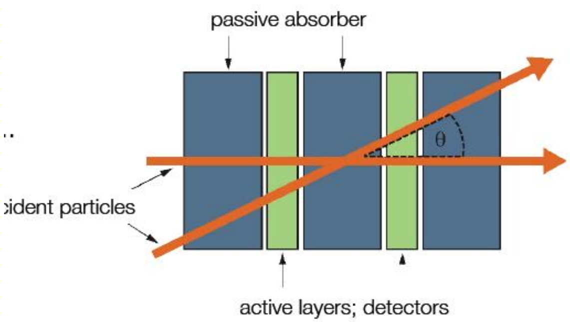

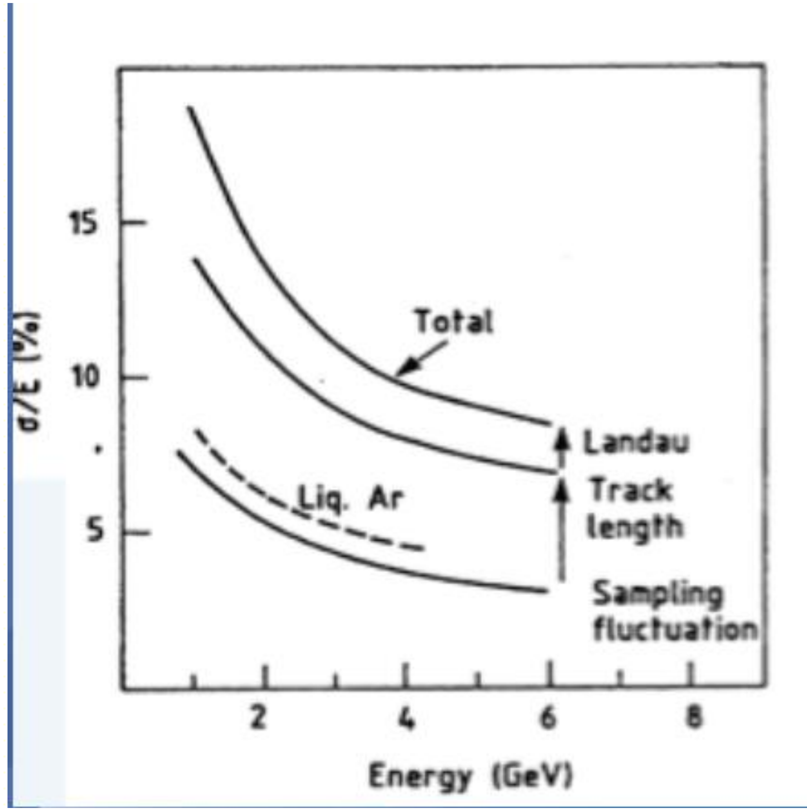

+ Landau fluctuation
Asymmetric energy deposit in thin active layer (non Gaussian energy measurement)

Calorimeter with gas detector not optimal for good resolution

$$\left[\frac{\sigma(E)}{E}\right]_{\text{Landau fluctuations}} \propto \frac{1}{\sqrt{N}\ln(k\cdot\delta)}$$

δ proportional to density

**

From cluster to particle energy (2)

$$E^{cal}_{reco} = a(E^{acc}_{reco},|\eta|) + b(E^{acc}_{reco},|\eta|)E^{cl\,LAr}_{ps} + c(E^{acc}_{reco},|\eta|)(E^{cl\,LAr}_{ps})^2$$

(upstream)

$$+ f_{acc}(X,|\eta|) \times (1 + f_{out}(X,|\eta|)) \times \left(\sum_{i=1}^{3} E_i^{cl\,LAr}\right)\left(1 + f_{leak}(X,|\eta|)\right) \times F(\eta,\varphi)$$

geometry

lateral

longitudinal

Energy position correction

Parameters/function determined on simulation events, different for electron/photon

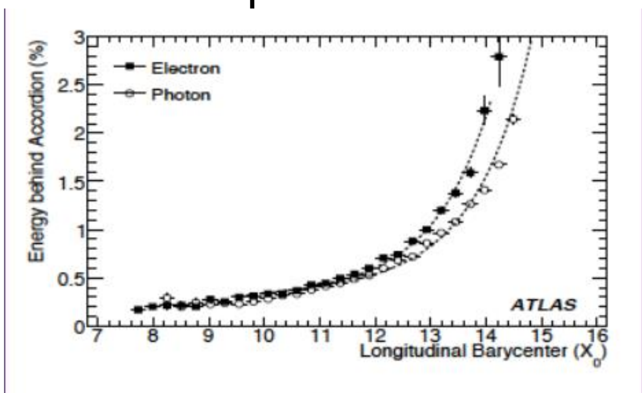

(a) $|\eta| = 0.3.$

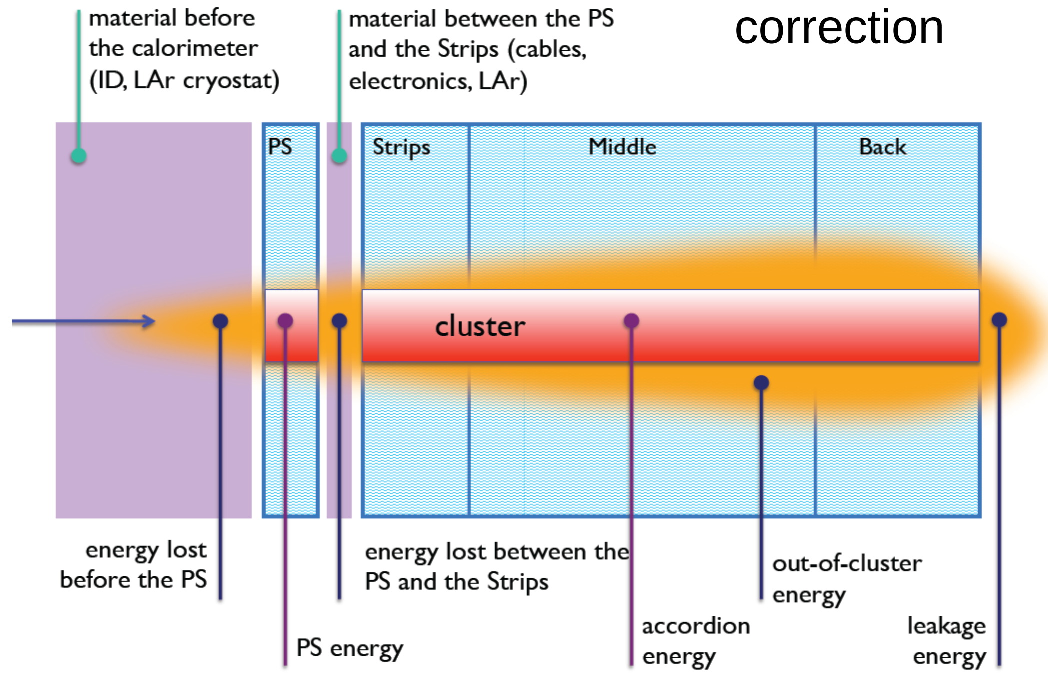

But still not ultimate correlation as detector description/simulation not perfect

**

Time stability of ATLAS Calo

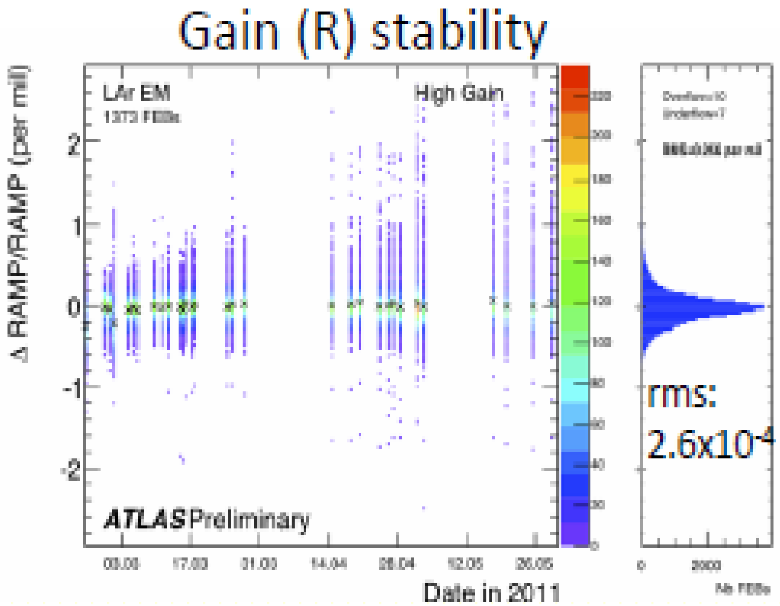

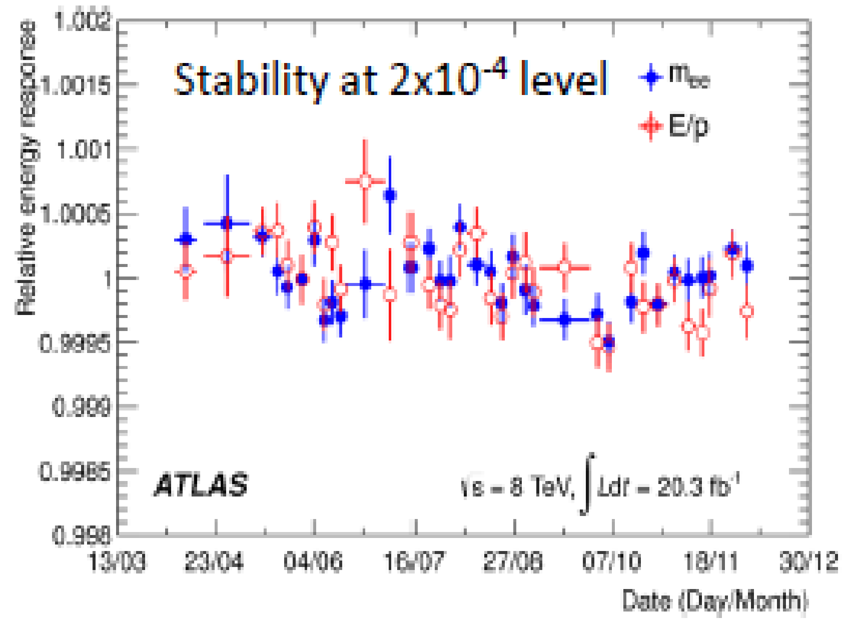

*

Calibration not easier in CMS !

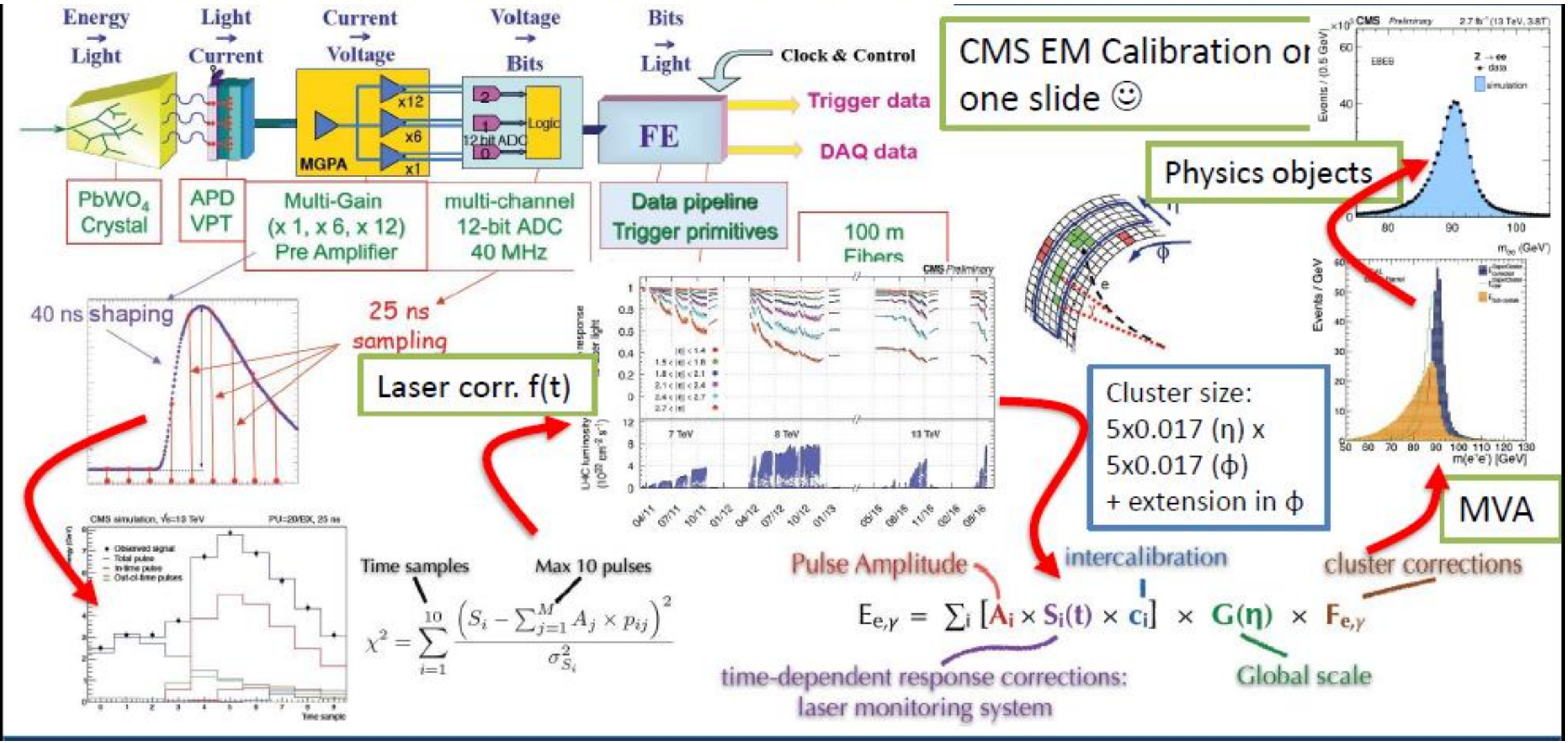

*

Shower position reconstruction

Energy weighted barycentre

$$E_{rec} = \sum_{i,j} E_{ij}$$

$$x = \frac{1}{E_{rec}} \sum_i x_i \cdot E_i$$

$$y = \frac{1}{E_{rec}} \sum_j y_j \cdot E_j$$

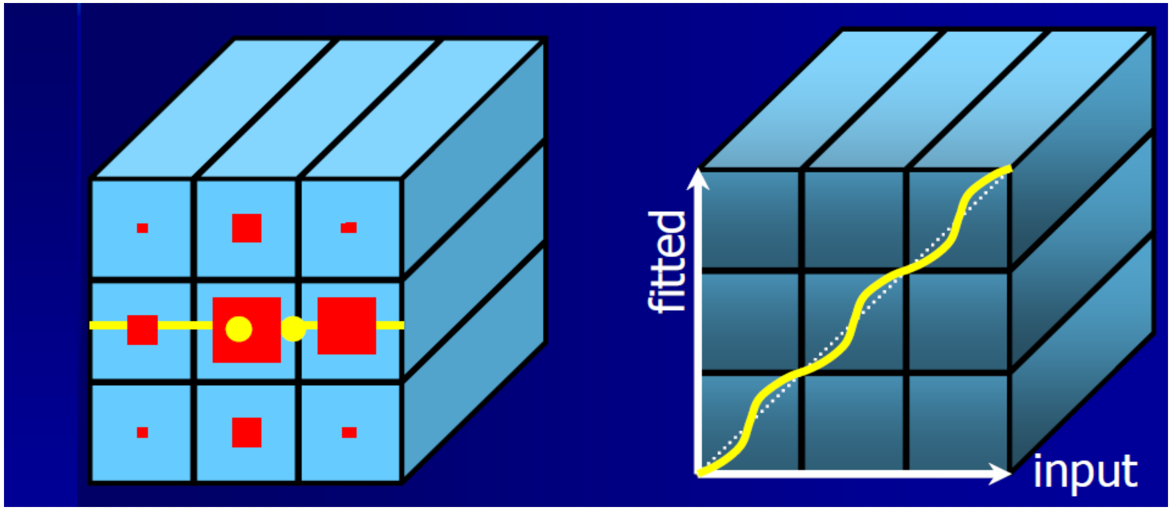

Bias due to finite cell size : S shape → correction to apply
If longitudinal segmentation can also estimate shower depth from
$X = \Sigma X^o_i E_i / E_{rec}$

From barycentre per layer → Shower direction

***